I. THE EMISSION AND ABSORPTION SPECTRA OF SOME SIMPLE

MOLECULES TRAPPED IN SOLID RARE GASES

II. THEORY OF ELECTRONIC RELAXATION IN THE SOLID PHASE

Thesis by

Robert Peter Frosch

In Partial Fulfillment of the Requirements

For the Degree of

Doctor of Philosophy

California Institute of Technology

Pasadena, California

1965

(Submitted September 16, 1964)

ACKNOWLEDGMENTS

It is a pleasure to thank Professor G. W. Robinson for much assistance and guidance during my stay at Caltech.

I am also grateful to the people in the shops who patiently listened to research problems and then proceeded to do a fine job in making apparatus. One man among them has been particularly helpful in solving difficult problems, namely, Mr. W. W. Schuelke.

I. THE EMISSION AND ABSORPTION SPECTRA OF SOME SIMPLE

MOLECULES TRAPPED IN SOLID RARE GASES

II. THEORY OF ELECTRONIC RELAXATION IN THE SOLID PHASE

Thesis by

Robert Peter Frosch

ABSTRACT

This thesis consists of two parts. The first part describes a study of the spectral properties of simple molecules trapped in liquid helium-cooled rare gas matrices and the equipment used in these studies. Measurements have been made of the phosphorescence lifetimes of C_6H_6, C_6D_6, $C_{10}H_8$, and $C_{10}D_8$ in at least one of the following solids: Ar, Kr, and Xe. The $a^4\Pi \rightarrow X^2\Pi$ and the $B^2\Pi \rightarrow X^2\Pi$ transitions of NO have been excited in Ar and Kr using x rays, and the resulting spectra measured and interpreted. The radiative lifetime of the NO quartet state has been measured in Ne, Ar, and Kr and found to be 156, 93, and 35 msec, respectively, in these solvents.

C_2H_2 and C_2D_2 have been deposited in Ar, Kr, and Xe and submitted to x-ray damage. The well-known Swan bands of C_2 have been observed in both emission and absorption. Both the upper and lower states of the Swan system have ΔG values in the solid more than 10% greater than the gas phase values. In addition two new C_2 band systems with 0-0 bands in Ar at 22973 and 19619 cm^{-1}, respectively, and with a common lower state have been tentatively identified. These systems apparently have not been reported in the gas phase. A transient

system has been seen in the emission of a deposit of C_2H_2 in Kr that may be due to HC_2. Another series observed when C_2H_2 is deposited in either Kr or Xe is apparently diacetylene phosphorescence.

The second part of this thesis presents a theory of electronic relaxation in solid media. The theory indicates that rates of electronic relaxation in solids depend in an important way on the electronic coupling between initial and final states and on the vibrational overlap between initial and final states. The theory has been successful in explaining the effect of deuterium substitution and the heavy atom effect on relaxation rates. Only a small temperature effect is predicted.

v

TABLE OF CONTENTS

PAGE

I. The Emission and Absorption Spectra of Some Simple

Molecules Trapped in Solid Rare Gases

A. Introduction

The use of inert lattices for trapping molecules and observing

their spectra has a long history. Among the first to use this technique

was Vegard (1) who froze nitrogen and nitrogen-argon mixtures using

liquid hydrogen as a coolant. He used a beam of electrons or positive

ions to excite emission from these systems. More recently Pimentel

and co-workers (2) and Robinson and co-workers (3) have made ex-

tensive use of rare gas solids for trapping both free radicals and

stable molecules. They then observe either the infrared or the visi-

ble and ultraviolet spectra of these solids. Briefly the method con-

sists of mixing the rare gas "solvent" and the "solute" in the desired

proportions and freezing the mixture out on a liquid helium (or liquid

hydrogen) cooled window. The exciting light passes through this

window during the photographing of spectra. Free radicals can be

prepared in the system either by passing the gaseous mixture through

an electric discharge just prior to freezing or by photolyzing the solid.

The systems described in this thesis were studied by the matrix

isolation technique. The first part of this section describes the appa-

ratus used in the studies and the subsequent parts report the findings.

The β band emission of NO and a series of emission bands believed to

be due to the transition between the lowest quartet state and the ground

state of NO were studied. The lifetime of the lowest NO quartet state

was measured.

The x irradiation products of acetylene trapped in rare gases were also studied. The most important product is C_2 for which three band systems have been identified. Among these systems were the Swan bands (in both absorption and emission) and two series of C_2 emission bands that could not be correlated with previously observed gas phase transitions. The $^3\Pi_u$ state was found to be the ground state in the solid contrary to the situation in the gas phase (4). Emission was observed from the two lowest vibrational levels of the upper state of the Swan system indicating that the vibrational relaxation of C_2 in the solid is slow. Besides emission from C_2, emissions were observed in several instances which may be due to HC_2 and diacetylene. Further study is needed to confirm these last two identifications.

The x irradiation of CO_2 deposited in solid Kr or Xe produced emission tentatively attributed to CO. The CO was identified by the appearance of the Herzberg bands $(C^1\Sigma^+ \rightarrow A^1\Pi)$ in emission. The appearance of the Herzberg bands is surprising because the transition is between two highly excited states of CO.

Finally the phosphorescence lifetimes of C_6H_6, C_6D_6, $C_{10}H_8$, and $C_{10}D_8$ were studied in rare gas solids. The lifetime of the perdeuterated compounds was observed to be much longer than that of the perprotonated compounds. Also the lifetime of both ordinary and perdeuterobenzene in Ar is an order of magnitude longer than in Kr and two orders of magnitude longer than in Xe. A similar heavy atom effect holds with the napthalenes.

3

References

1. L. Vegard, Ann. Physik 79, 377 (1926).

2. H. W. Brown and G. C. Pimentel, J. Chem. Phys. 29, 883 (1958); D. E. Milligan and G. C. Pimentel, J. Chem. Phys. 29, 1405 (1958).

3. M. McCarty and G. W. Robinson, J. Chem. Phys. 28, 349 (1958); ibid., 350 (1958).

4. E. A. Ballik and D. A. Ramsay, Astrophys. J. 137, 61 (1963).

B. The Experimental Apparatus

The experimental apparatus used in deposition experiments is very simple in principle but can be quite complicated in practice. Basically the apparatus consists of two parts: a manifold in which the solvent and solute are mixed and a high vacuum chamber where the mixture is frozen on a liquid helium-cooled window. The solvent-solute mixture is passed from the manifold through a few inches of one millimeter capillary tubing and directed from the capillary at the surface of the cold window. The apparatus used for the benzene and napthalene experiments reported in this thesis was designed and built by Robinson and McCarty (1) and has been adequately described by them. The other experiments reported in this thesis were done with apparatus designed by the author with the assistance of Mr. William Schuelke. A rather detailed description of this apparatus which will hereafter be referred to as "the system" follows.

The system (except for the x-ray power supply) is contained on a single table of welded steel construction (see Fig. 1). The table rests on castors which can be rotated a full 360° for easy positioning of the table. When the castors rest on the floor, the table top stands 35 inches high, but the system can be raised eight additional inches on three threaded legs.* A socket wrench with a ratchet action is used to raise and lower the table.

---

*This method of raising and lowering the table has proved time consuming. It would be better to raise and lower the castors themselves and to have stops on them to prevent movement of the system when it is in use.
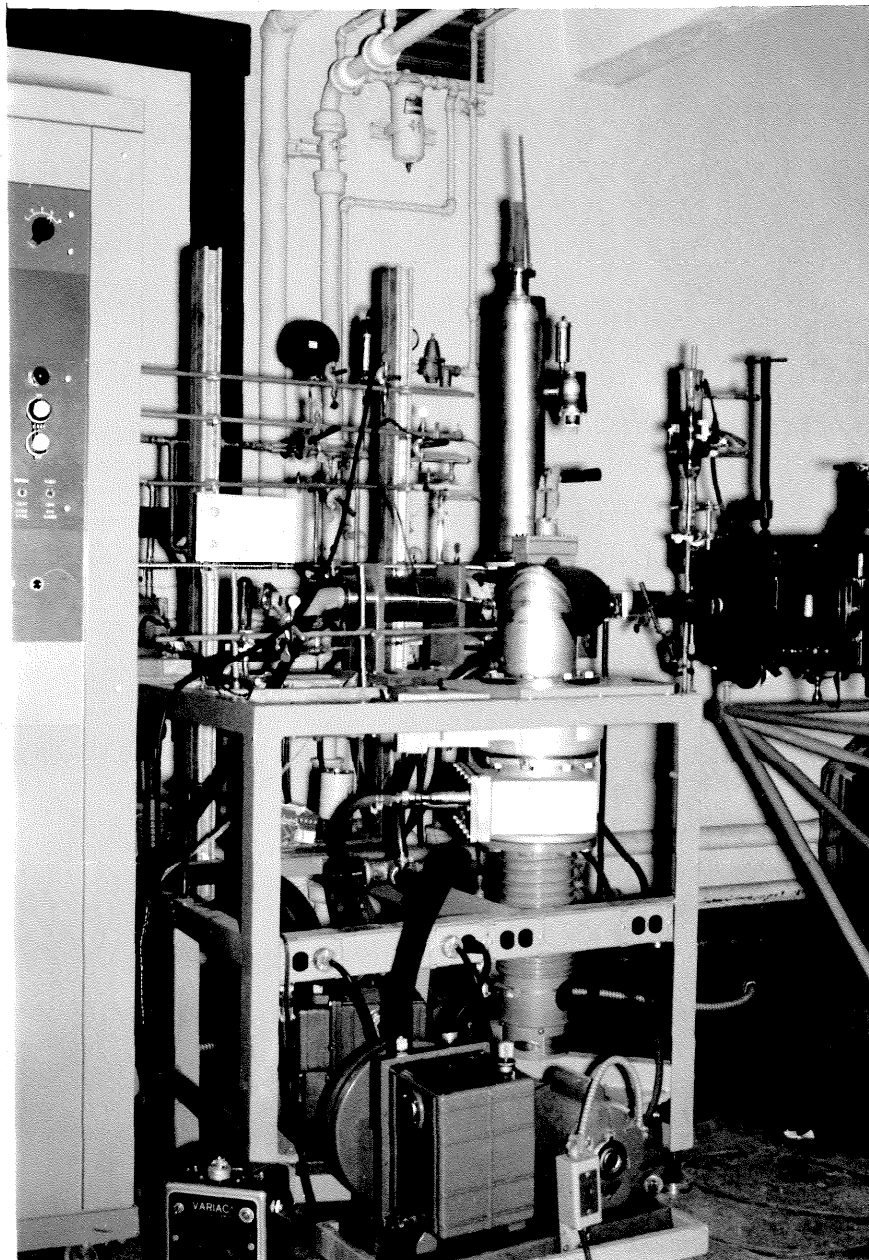
Fig. 1. The system.

On one side of the table there are two vertical unistrut studs which extend from eighteen to seventy-two inches off the floor. A vacuum rack (to be described later) is attached to these studs. On the opposite side of the table there is a horizontal panel with eight 115 volt outlets in three separate circuits. These circuits are powered by cables connected to twist-lock wall outlets.

The high vacuum system is built in the table. The block diagram in Fig. 2 shows the essential parts. The forepump is a 140 l/min Welch Duo-Seal pump which rests on the floor beneath the system. The forepump is connected by means of heavy-walled rubber tubing to a tee joint as shown in Fig. 2. During an experiment, valve G is open and valve H is closed. The oil diffusion pump is a model PMC-720 made by Consolidated Vacuum Corporation. It has a pumping speed of 720 l/sec and an ultimate pressure of 2×10^{-7} mm at the pump. The pump is suspended from the table top. The baffle which is bolted directly to the pump inlet is also made by CVC. It is four inches in diameter and consists of a number of water-cooled[*] chevrons. The first gate valve is a four inch CVC product, and the second is a similar two inch model. The four inch valve is mounted horizontally in the table top. The two inch gate valve is separated from the first gate valve by a twenty inch section of four inch diameter

---

[*]The chevrons may, at the discretion of the user, be liquid nitrogen cooled rather than water cooled. Liquid nitrogen cooling should improve both the pumping speed and the ultimate obtainable vacuum but proved unnecessary for the experiments described in this thesis.
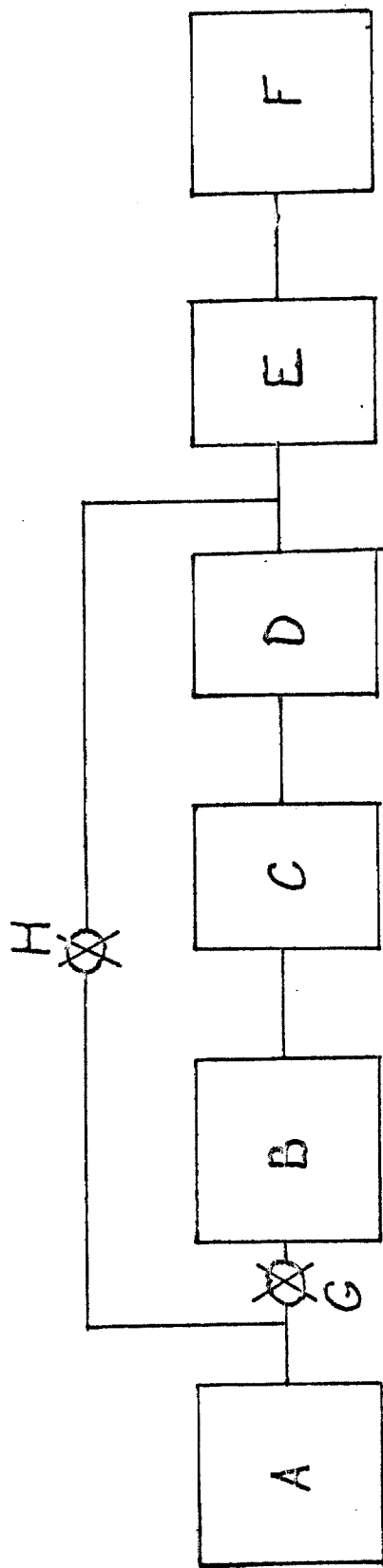
A. Forepump

B. 4" Diffusion Pump

C. 4" Chevron Baffle

D. 4" Gate Valve

E. 2" Gate Valve

F. High Vacuum Chamber

G. Valve

H. Diffusion Pump Bypass Valve

Fig. 2. Block diagram of the high vacuum system.

stainless steel tubing. The two inch valve permits isolation of the high vacuum chamber from the pumping system. The high vacuum chamber will be described later in this section.

Valve G (Fig. 2) and the four inch gate valve permit isolation of the diffusion pump. When these two valves are closed, the high vacuum chamber can be pumped through valve H. The use of the bypass means that it is never necessary to introduce air at atmospheric pressure into the diffusion pump.

The "working" or high vacuum system is in two parts, a liquid helium dewar and a base. The liquid helium dewar is of welded stainless steel construction. It has a central helium dewar which is surrounded by a liquid nitrogen dewar acting as a heat shield. A thermocouple gauge and an ionization gauge for monitoring the pressure are mounted near the top of the dewar. The cold finger which is soldered to the bottom of the helium dewar contains liquid helium when in use. The entire dewar system is mounted on the base.

The helium dewar including the nitrogen heat shield and cold finger can be rotated 360° while under vacuum. The vacuum is maintained with an ordinary rubber 0-ring. A teflon gasket embedded in the surface of the base extends about .01 inches above the surface. The purpose of the teflon is to prevent the metal surfaces of the dewar and the base from binding during rotation. The teflon plays no part in maintaining the vacuum.

The base is the central feature of the system in the sense that the deposit is located in the base and exciting light, x rays, etc. enter

and leave through the base. It is constructed of a welded stainless steel tube 8 inches long and 3 inches in diameter in which four port holes have been made for various purposes. A cross-sectional drawing of the base and cold finger is shown in Fig. 3. The cold finger, as shown, is in position for an absorption spectrum. The base is attached at B in Fig. 3 to the two inch gate valve shown in Fig. 2. Pumping is through this valve. The inlet for the deposition mixture is at C in Fig. 3. This inlet is made from 1/4 inch stainless steel tubing. The last 1/4 inch has a one millimeter inside diameter. The narrow tip acts as a nozzle which directs the deposition gases at the helium-cooled window.

Three other ports (D, E, F) shown in Fig. 3 can be used as windows or as alternate inlets for the solvent and solute. During an x-ray experiment, for example, the x rays enter through E, the light for absorption spectra enters through D, and the unabsorbed (or emitted) light exits through F.

A copper heat shield H is screwed tightly to the bottom of the nitrogen reservoir in the helium dewar. To insure good thermal contact a piece of indium wire inserted between the nitrogen reservoir and the heat shield is crushed between the two when the shield is screwed on. The 3/8 inch diameter holes in the heat shield provide an optical path. There are two sets of holes. As shown, the holes are lined up for taking absorption spectra. Rotation counterclockwise by 45° would line the holes up for an emission spectrum. A further 45° counterclockwise rotation would line the holes up for x-ray damage to the sample.
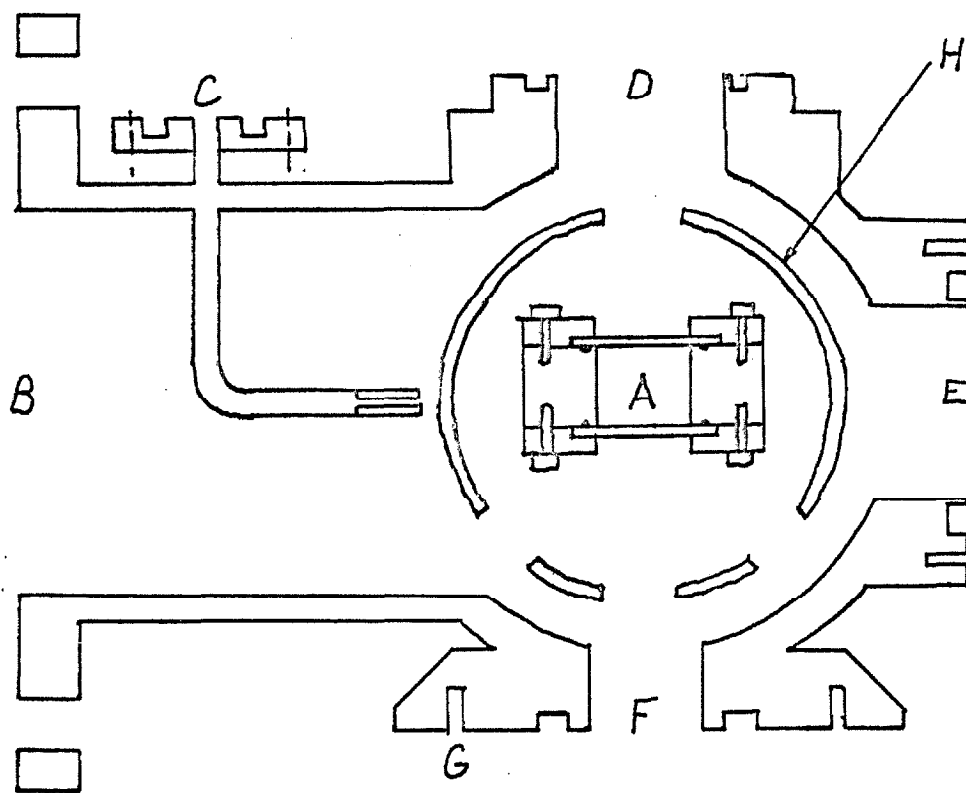
Fig. 3. A cross-sectional view of the base and cold finger. A cold finger; B exit to vacuum pump; C inlet for deposition gases; D window; E window for x rays or entry for deposition gases; F window; G connection to vacuum ultraviolet monochromator; H copper heat shield.

The cold finger is an extension on the helium dewar. The windows on the cold finger are sapphire. Sapphire rather than fused quartz was chosen because of its high thermal conductivity at low temperatures (2). Hydrogen and neon, for instance, can be deposited on a sapphire but not on a fused quartz window. Care must be taken in sealing the windows to the cold finger, since helium will pass through the smallest orifice. The windows and the surface of the cold finger should first be cleaned with acetone or methanol. No special care need be taken in handling the materials after cleaning if the hands have just been washed well with soap and water (except, of course, for optical surfaces). After the cleaning process a piece of indium wire is cut to the exact length needed and laid in the groove in the surface of the cold finger. The groove whose cross section is semicircular should have the same diameter as the indium wire. Normally .026 inch diameter wire is used. The ends of the wire are butted together in the groove, and a cold weld is made by gently pushing the ends together with the fingernail or a knife blade. The window is then centered carefully above the wire and a teflon washer is then placed above the window. For a one millimeter thick window the washers are cut from 1/32 inch thick teflon. A brass cover is then placed over the assembly and screwed down. The recess in the cover should be about 1/64 inch less than the sum of the thickness of the window and the teflon. Screwing down the cover must be done slowly and uniformly to avoid breaking the window. Each screw is tightened about a half turn and then the one opposite is tightened until all are tightened down hard. A torque wrench might be useful in tightening the screws

but none was used by the author. When a seal is made properly it will withstand thermal cyclings down to liquid helium temperatures indefinitely!

A little more should be said about the ports in the base. The system has been designed for use with the McPherson Model 235 0.5 meter vacuum ultraviolet monochromator. The port F shown in Fig. 3 can be sealed to the monochromator by means of a brass plate. The plate is first screwed to the port. An 0-ring in the brass plate forms a vacuum seal to the system. The system is then brought flush with the monochromator exit slit housing, and the brass plate is screwed to the monochromator. An 0-ring in the exit slit housing makes a vacuum tight seal.

If a window with the proper transmission characteristics is available it is desirable to use it at port F to separate the two vacuum systems. The window prevents impurities such as water in the monochromator from condensing on the cold finger.

The McPherson Model 630 vacuum ultraviolet light source can be attached to the port marked D in Fig. 3. As with the monochromator a brass plate is used to seal the light source to the system. Since the rare gases used in the lamp would freeze out on the cold finger it is necessary to use a window between the lamp and the cold finger. If it is not desired to remove the lamp during an experiment, the lithium fluoride window supplied with the lamp is best. However, if it is desired to remove the light source, then it is necessary to use a recessed window which remains attached to the base when the light source is removed.

During experiments requiring x rays both ports D and F in Fig. 3 should be covered with barium fluoride windows at least an eighth of an inch thick. The barium fluoride absorbs the scattered x rays but is transparent in the visible and ultraviolet. For other experiments almost any optically satisfactory window can be used.

X rays enter the system through port E in Fig. 3. A .029 inch thick beryllium window[*] covers this port. The x rays pass through a short hollow brass fitting located between the x-ray tube and the window. The fitting is machined to dovetail with the port and the brass jacket on the x-ray tube. In this way the radiation count outside the system can be held to background. When the x-ray tube is not in use, port E serves as a convenient deposition inlet.

The x-ray tube is a Machlett AEG-50S with a tungsten target. It has a maximum rating of 50-kV and 50 mamp. The x-ray control is a General Electric XRD5.

The manifold for preparing the deposition mixture is shown in Fig. 4. It is constructed of Pyrex, brass, and copper tubing. Kovar glass to metal seals are used to connect the two types of material. The valves are Kerotest two-way line valves with nylon seats. A test of the valves with a helium leak detector showed no leakage.

The vacuum system for the manifold is quite simple. A Welch Duo-Seal forepump and a CVC PMC 115 diffusion pump are used. There is a bypass of the diffusion pump so that, when desired, the

---

[*]Care must be taken in handling beryllium, since the dust is very poisonous.
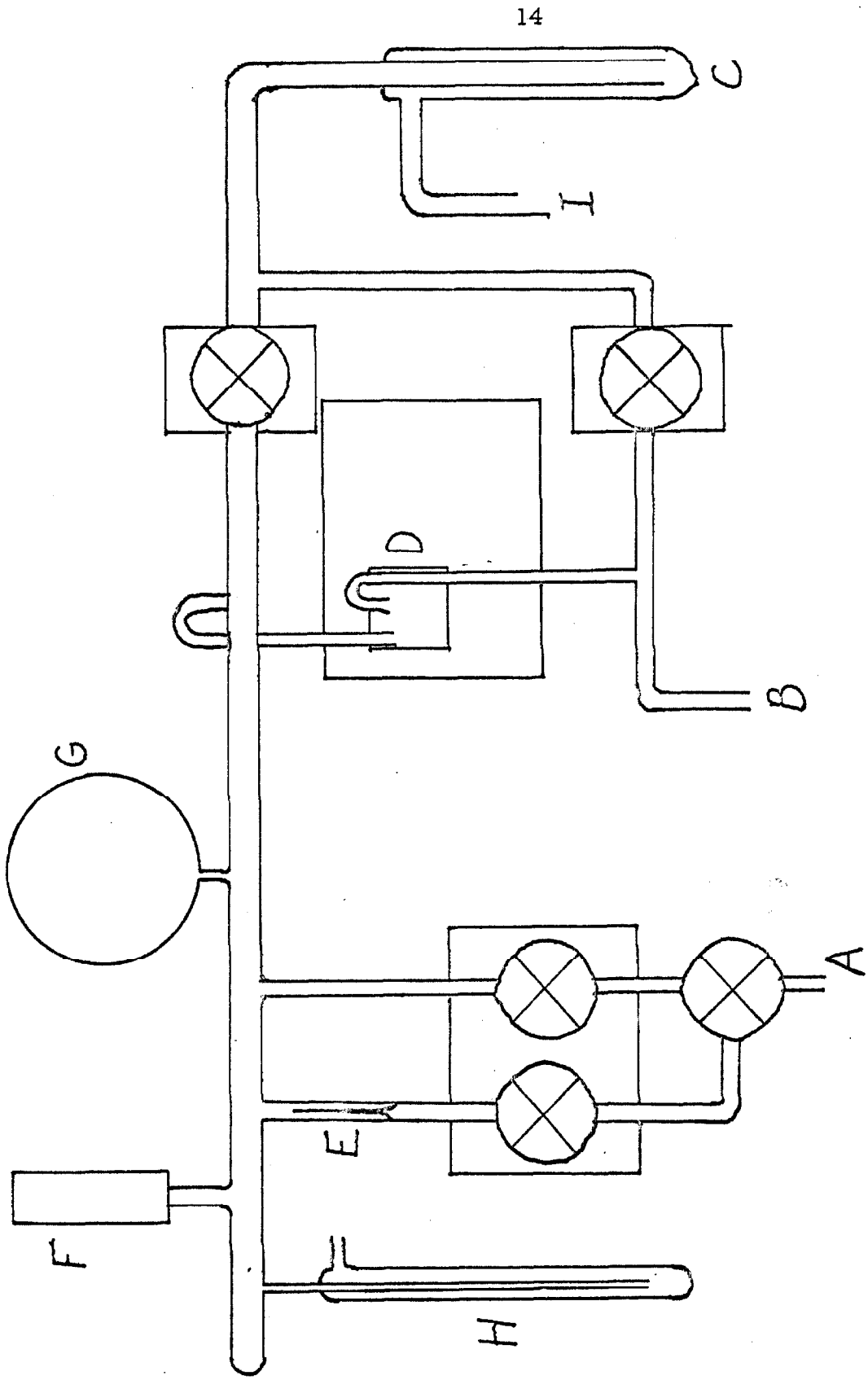
14

Fig. 4. Manifold.

Legend to Fig. 4

A. Gas inlet.

B. Gas inlet.

C. Trap.

D. Variable leak.

E. Fixed leak.

F. Thermocouple gauge.

G. 0 to 20 mm pressure gauge.

H. Trap.

I. To diffusion pump.

system can be pumped down without contaminating the oil. A Pyrex liquid nitrogen trap keeps pump oil out of the system. A Granville-Phillips leak with a continuously variable conductance from 10 to less than 10^{-10} cc/sec is located at D in Fig. 4. A Pyrex, fixed-capillary leak with a flow of about three milliliters per minute is located at E. A thermocouple gauge F and a 0 to 20 millimeter gauge G permit monitoring the pressure. There are two ways of preparing the solvent-solute mixture. If both are gases, the solvent can be introduced into the system through the fixed leak. The variable leak is adjusted so that the ratio of its flow rate to the flow rate through the fixed capillary is equal to the desired solute concentration. Of course the variable leak must be readjusted whenever the solvent or solute is changed since the leak rate depends on the nature of the gas.

If the solute has a vapor pressure of about 20 microns at some temperature between 77°K and 300°K, there is another way in which the solute can be added to the solvent. The trap H in Fig. 4 is used to maintain the solute at the desired temperature, and the solvent is allowed to pass over the cooled solute. It seems reasonable to assume that equilibrium will be maintained if the solvent passage is slow and that the resultant solute concentration will be the ratio of the vapor pressure of the solute to the total pressure in the manifold. Since the pressure in the manifold is of the order of two millimeters during deposition and since solute concentrations of about one mole per cent are usually desirable, a solute vapor pressure of about .02 millimeters is required. Since the solvent and the solute may not freeze out on the cold finger with the same efficiencies, the only sure way of determining

the solute concentration is by analysis. In most experiments only an approximate knowledge of the concentration, say ±50% is needed; the methods described above for concentration control should certainly be reliable within these limits.

A typical experiment proceeds as follows. The forepumps usually run continuously. The night before the experiment the water is turned on in the baffle and in the large diffusion pump. Valve H in Fig. 2 is closed, valve I is opened, and the diffusion pump is turned on. While the diffusion pump is warming up, the pressure in the system may substantially increase because of outgassing of the oil, and therefore the pump should be completely separated from the high vacuum system. After the diffusion pump has warmed up (about 15 minutes), the four inch gate valve is opened (the two inch valve should already be open) and the system allowed to pump overnight. A thermostat on the pump will turn it off if it becomes too hot.

The next morning the pressure should be checked in both the high vacuum system and in the glass manifold. The pressure in the glass manifold should read "zero" on the thermocouple gauge, while the pressure in the high vacuum system should be less than 10^{-4} mm of Hg.

Any condensed water in the nitrogen reservoir of the helium dewar should be pumped out with an aspirator; then about 100 ml of methanol or acetone should be added and also pumped out. Failure to follow this procedure will cause the dewar to rupture. After removing the water and checking the pressure, liquid nitrogen is added simultaneously to the center helium dewar and the nitrogen dewar. About

250 ml of liquid is filtered into the center dewar through cotton to prevent foreign matter from falling into the dewar and blocking the light path. The nitrogen dewar is filled to within about $1\frac{1}{2}$ inches from the top and is refilled when the level falls more than 4 inches from the top.

In the meantime the diffusion pump to the glass manifold is turned on and the system, including the lines to the gas cylinders, pumped out. If a condensable solute is to be used, it can be introduced into trap H at this time. If the solute is to enter the system through the variable leak, the flow rate can be adjusted. After closing the valves between the system and the cylinders (gases pump through ordinary reducing valves even if they are "closed"), one can open the gas tanks and adjust the exit pressure to about 5 lb. gauge.

After about an hour with liquid nitrogen in the reservoir, the pressure in the high vacuum system should be less than 2×10^{-6} mm. Unless neon is to be the solvent the two inch gate valve should now be closed and the system filled with liquid helium. If the solvent is to be neon, the valve should be left open because deposited neon often falls off during an experiment raising the pressure and causing the liquid helium to boil away unless the neon is immediately pumped out.

After the liquid helium has been transferred, the deposition may be started. The solute and solvent are allowed to mix inside the manifold until the total pressure is about 2 mm. The dewar is rotated until the window is opposite the deposition tube, and the valve between the manifold and the high vacuum system is opened. During deposition

the pressure in the manifold should be about 2 mm and the pressure in the high vacuum system 10^{-3} to 10^{-4} mm. Depositing may require from one to four hours.

After deposition the experiment is performed. This may include x-ray damage, the taking of emission or absorption spectra, etc. When the experiment is completed, the gas cylinders are closed and the system is pumped out. After the deposit has sublimed and has been pumped out of the system, the four inch gate valve and valve G in Fig. 2 can be closed and the four inch diffusion pump turned off. The water in the pumps and baffle should be left running until the pumps have cooled.

References

1. G. W. Robinson and M. McCarty, J. Chem. Phys. $\underset{\sim\sim}{30}$, 999 (1959).

2. R. L. Powell and W. A. Blanpied, "Thermal Conductivity of Metals and Alloys at Low Temperatures," U. S. Nat. Bur. of Stds. Circ. No. 556 (1954).

C. The Emission Spectrum of NO in Solid Rare Gases: The

Lifetime of the $a^4\Pi$ State and the Spectrum of the

$a^4\Pi \rightarrow X^2\Pi$ and $B^2\Pi \rightarrow X^2\Pi$ Transitions.[*]

Abstract

The emission spectrum of NO molecules trapped in solid argon

and krypton has been excited with x rays.   Two series of bands have

been observed, the well-known β-bands ($B^2\Pi \rightarrow X^2\Pi$) and a series with

(unobserved) origin near 38000 cm^{-1} believed to be the $a^4\Pi_{5/2} \rightarrow X^2\Pi_{3/2}$

transition.   The lifetime of the assumed quartet state has been

measured in solid Ne, Ar, and Kr and found to be 156, 93, and 35 msec,

respectively, in these solids.   These lifetimes are compatible with the

above assignment of the bands.   A least squares fit has been made of

the spectral data to obtain the 0-0 band positions and the vibrational

constants of the NO molecule in the solid.   The doublet-quartet bands

are believed to arise from a spin-orbit mixing of the $a^4\Pi_{5/2}$ state with

the $B'^2\Delta_{5/2}$ state.   The possibility of observing high resolution spectra

of the $a^4\Pi - X^2\Pi$ transition in either absorption or emission is con-

sidered.   The role of the $a^4\Pi$ state of NO in photochemical reactions

and in auroral and airglow spectra is briefly discussed.

Introduction

Recently Broida and Peyron (1) observed a series of bands emitted from condensed argon containing oxygen and nitrogen as impurities. These bands had been observed earlier by Vegard (2); he attributed them to N_2. However, Broida and Peyron have shown by isotopic substitution that the emitter is NO. They suggest that this band system (referred to by Broida and Peyron as the M-bands) may originate from the NO $^4\Pi$ state predicted by Mulliken (3) in 1932. Since very little experimental data on quartet states are available, it seemed profitable to pursue the study of NO in solid matrices in order to establish the nature of the emitting state. Herzberg (4) reports only two transitions involving quartet states, a $^4\Sigma_g^- \rightarrow {}^4\Pi_u$ transition of O_2^+ and a possible $^4\Pi - {}^4\Sigma$ transition in FeCl. Ogawa (5) has reported in low resolution at 8600, 7800, and 7250 Å bands which may arise from the NO $^4\Sigma^- \rightarrow {}^4\Pi$ transition, analogous to the O_2^+ $^4\Sigma_g^- - {}^4\Pi_u$ transition.

Experimental

Deposition of the NO-rare gas mixture was carried out using a continuous flow system. Matheson 99% NO was further purified by passage through a silica gel trap that was maintained at the temperature of a dry ice-acetone bath. The nitric oxide then flowed into a glass manifold through a variable leak. Simultaneously the rare gas "solvent" flowed into the manifold through a Pyrex capillary leak at a rate 3 ± 2 ml STP/min and mixed with the NO. Linde M.S.C. grade rare gases were used in all the experiments. The NO concentration was

controlled by adjustment of the variable leak. Concentrations of 0.1%
to 0.15% NO by volume were used for the lifetime measurements. For
spectra, concentrations of $\leq 0.6\%$ NO by volume were used. After
mixing, the gases impinged upon a liquid helium-cooled cold finger
and solidified.

The emission was excited with 50-kV x rays. The x-ray tube
current load was 45 ma. In both argon and krypton the emissions
were a bright blue color. Spectra were taken in the second order of
an f/10 grating spectrograph which has an 8 Å/mm dispersion in the
first order. A neon filled, iron hollow-cathode discharge tube was
used to provide standard lines. Lifetime measurements were made
using standard techniques. A brass shutter of 0.25 inch thickness
mounted on the x-ray tube cut off the x radiation in about 10 milli-
seconds; the shutter triggered the sweep on the oscilloscope on
closing. The output of a 1P21 photomultiplier tube was fed into the
oscilloscope, and the decaying signal was photographed to obtain the
lifetime curves. A 0.5 meter McPherson Model 235 monochromator
with a band pass of 28 Å was used to isolate individual bands for
lifetime measurements.

Lifetimes

The M-bands have 156, 93, and 35 msec lifetimes in Ne, Ar,
and Kr, respectively. All these values are subject to a 10% error due
to substantial noise in the photomultiplier signal. Within experimental
error the lifetimes are exponential except when the solvent is Kr. In

Kr the emission is nearly exponential but has a weak, longer-lived tail
which may be due to atom recombination in the solid. Several
individual vibrational components of the M-bands were used in
measuring the lifetimes, and the results agreed, as expected, within
experimental error.

In one experiment with neon as matrix, the solid was cooled to
1.8°K by pumping on the helium; the measured lifetime at 1.8°K was
the same as that at 4.2°K. This insensitivity of the lifetime to temper-
ature indicates that only the lowest member of the multiplet is emitting.

In one Ar experiment a nonexponential afterglow was noted
which persisted for more than 30 minutes. In place of the mono-
chromator, a filter which transmitted from 3000 Å to 4200 Å and also
above 6900 Å was used in this experiment. Since the long-lived $^2D \rightarrow$
^4S transition of atomic nitrogen and the long-lived $^1D \rightarrow {}^3P$ transition
of atomic oxygen lie at 5200 Å and 6333 Å (6) respectively, in the gas
phase, these transitions cannot be responsible for the observed
afterglow. It seems probable that the afterglow is due to atom re-
combination in the solid forming NO, N_2, and O_2 in excited states.

Spectra

A densitometer tracing of the spectrum of NO in solid Ar and
in solid Kr is shown in Fig. 1. Plate measurements are given in
Table I. Measurements were made at the darkest part of each line.
There is a considerable solvent effect on the spectra. In both Ar and
Kr the M-bands are broad and degraded to the red. The red tail on
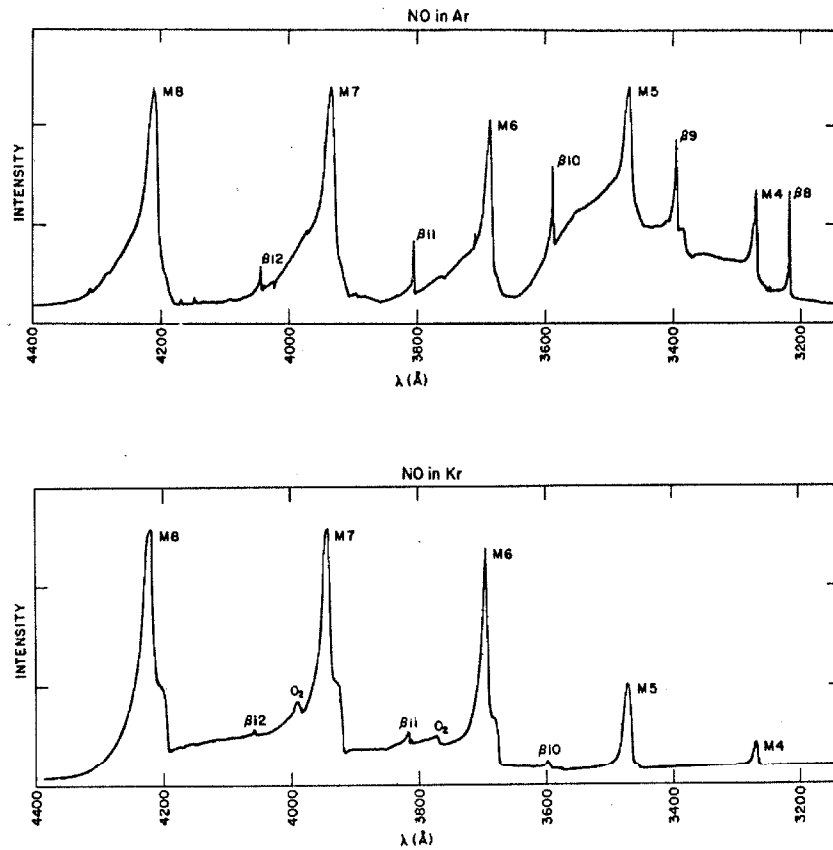
NO in Ar

NO in Kr

Fig. 1.   Densitometer tracing of the emission spectrum of NO
in solid Ar and Kr.   The tracings were made from several plates each
of which had the same exposure time.   As good a match as possible
was made where the plates overlapped.   The tracings from two differ-
ent plates were joined at about 3510 Å to reproduce the Ar spectrum.
Tracings from three different plates were joined at about 3430 Å and
3910 Å to reproduce the Kr spectrum.   The intensity scale is in arbi-
trary units.

TABLE I.   NO emission.

v'	v''	β-Bands ($^2\Pi_{1/2} - {}^2\Pi_{1/2}$)			M-Bands	
		Gas[a]	Ar	Kr	Ar	Kr
0	3		39796		32411	b
0	4	38146.21	38006		30626	30557
0	5	36382.00	36245		28865	28801
0	6	34645.74	b		27135	27070
0	7	32937.54	32810	32711	25428	25372
0	8	31257.27	31132	31041	23753	23701
0	9	29604.99	29481	29396	22101	22055
0	10	27980.71	27862	27779		20436
0	11	26384.44	26271	26188		18844
0	12	24816.31	24707	b		
0	13		23172			

[a]Reference 11.

[b]Observed but not accurately measured.

the M-bands in Ar is especially pronounced. The spectrum of NO in Ar has an intense background between 3200 Å and 3600 Å which may or may not be associated with the M-bands. In Kr there is a strong background throughout the observed region whose relationship to the M-bands is also uncertain. Relative to the M-bands, the β-bands are roughly five times as intense in Ar as in Kr.

The shoulder on the blue edge of the M-bands in Kr is probably due to multiple trapping sites. Another possible explanation is NO dimers.(7). A similar, but much weaker shoulder is associated with the M-bands in Ar. The presence of dimers in these experiments would not be surprising, since Keyser and Kwok (8) using a deposition technique similar to ours have strong infrared evidence for their presence in solid rare gases.

The high purity of the gases combined with the x-ray technique gives rise to NO spectra which are amazingly free of spectral contamination. However, a few other very weak lines do appear on the plates. Most of these lines belong to the Herzberg bands of O_2. They have been previously identified in rare gas solids by Schoen and Broida (9). A few of the weak lines observed here have not been identified. The observed O_2 bands and unidentified lines are given in Table II.

The most accurately measured β-bands and M-bands have been used to make a least squares fit to the equation

$$\nu = a - \omega_e'' (v'' + \tfrac{1}{2}) + \omega_e x_e'' (v'' + \tfrac{1}{2})^2 \tag{1}$$

where ω_e'' and $\omega_e x_e''$ are the vibrational constants for the final state, v''

TABLE II.   Impurity bands.

in Ar	in Kr
	29790 ?
29570 ?	29500 ?
	28190 ?
	27940 O_2
26600 O_2	26500 O_2
25150 O_2	25060 O_2
	22290 ?
22350 O_2	22260 O_2
	20890 O_2

is the vibrational quantum number of the final state, ν is the wave number of the transition in cm^{-1}, and $\underline{a}$ is an additive constant equal to ν_e plus the zero-point energy of the excited state in cm^{-1}. The value of ν_{00} can be obtained from Eq. (1) by substituting v'' = 0. The results are given in Table III. The fit is quite good for the included data, but it is dangerous to extrapolate to other bands. Even the use of this procedure for gas phase data leads to incorrect results when the simple expression in Eq. (1) is used. Adding more empirical terms to Eq. (1) will not necessarily improve the extrapolation properties of the equation. For instance, the infrared $\Delta G_{1/2}$ value of the $^2\Pi_{1/2}$ ground state reported by Gillette and Eyster (10) is 1876.10 cm^{-1}, while the $\Delta G_{1/2}$ value for the same state, as calculated from vibrational constants obtained from vapor phase β-bands, is 1877.70 cm^{-1} (11). Since the effect of the condensed phase on the vibrational constants of the solute molecule is difficult to evaluate, the use of Eq. (1) for the solid phase data can lead only to approximate constants. The work of Keyser and Kwok (8) indicates that $\Delta G_{1/2}$ values calculated from our data are probably too small. Some gas phase and solid phase $\Delta G_{1/2}$ values are given in Table IV for comparison. In preparing the table it has been assumed that the final state of the M-bands is $X^2\Pi_{3/2}$ for reasons stated in the next section. The low value (1858 cm^{-1}) of $\Delta G_{1/2}$ obtained for the β-bands in Kr is probably due to two causes. First, only a few β-bands (five) could be accurately measured; and second, an inordinate extrapolation was used to obtain $\Delta G_{1/2}$, since only bands with v'' $\geq$ 7 were observed.

TABLE III.   Vibrational constants of NO ground state in solid rare gases.

	β-Bands			M-Bands	
	Gas[a]	Ar	Kr	Ar	Kr
$\nu_{00}(\mathrm{cm}^{-1})$	45486.1 $(\mathrm{B}^2\Pi_{1/2} - \mathrm{X}^2\Pi_{1/2})$	45332	45155	37933	37856
$\omega_e(\mathrm{cm}^{-1})$	1904.0 $(\mathrm{X}^2\Pi_{1/2})$	1901.9	1884.6	1894.9	1894.1
$\omega_e x_e(\mathrm{cm}^{-1})$	13.97	14.09	13.36	13.58	13.84

[a]Reference 4, p. 558.

TABLE IV. $\Delta G_{1/2}$ values of NO ground state.

	Gillette and Eyster[a]	Keyser and Kwok[b]		Frosch and Robinson	
	Gas	Ar	Kr	Ar	Kr
$\Delta G_{1/2}(^2\Pi_{1/2})$ (cm^{-1})	1876.10	1874 ± 2	1870 ± 2	1874	1858
$\Delta G_{1/2}(^2\Pi_{3/2})$ (cm^{-1})	1875.63	—	—	1868	1866

[a]Reference 10.

[b]Reference 8.

The Nature of the M-Bands

Although isotopic substitution experiments (1) with $N^{15}O$ and vibrational structure conclusively show that the final state of the M-bands is the NO ground state, the emitting state is still uncertain. Broida and Peyron's suggestion that the emitting state is the $^4\Pi$ state is supported by the following new experimental evidence: 1) The emitting state has a long lifetime indicating that the transition is forbidden. 2) The lifetime becomes progressively shorter in the series Ne, Ar, and Kr. 3) The relative intensity of the M-bands compared with the β-bands is much greater in Kr than in Ar. Because it is difficult to make a Ne deposit stick to the cold finger good spectra were not photographed in this solvent, and therefore no comparison of the relative intensities of the β-bands and the M-bands can be made for a neon matrix. Presumably the β-bands in Ne are at least as strong relative to the M-bands as in Ar and possibly stronger. Points 2 and 3 above are dependent on the fact that spin-forbidden radiative as well as spin-forbidden radiationless processes are enhanced by the presence of heavy atoms, i.e., Ar and Kr.

In brief, this intensity enhancement occurs because in the solid matrix the rare gas states are mixed with the solute states by exchange interactions. Since "heavy atoms" have strong spin-orbit coupling, solute states of different multiplicity are effectively more strongly coupled in a rare gas (or other heavy atom) "solvent" than in the gas phase. This means that heavy atom solvents often substantially shorten the radiative lifetimes of multiplicity forbidden transitions. Since

intersystem crossing is also dependent on the mixing of states of different multiplicity, spin-forbidden radiationless transitions are also enhanced by heavy-atom solvents. Robinson (12) has discussed the heavy-atom enhancement of radiative transitions and Robinson and Frosch (13) have discussed the heavy-atom enhancement of radiationless transitions.

Let us assume that the emitting state of the M-bands is the $^4\Pi$ state predicted by Mulliken. This state is an inverted multiplet. Since the emitting quartet state has a long lifetime, it is reasonable to assume that there is ample time for a Boltzmann distribution over the multiplet members to be established. Inasmuch as kT is 3 cm^{-1} at 4°K, and the multiplet splitting is expected to be greater than 3 cm^{-1}, it can be safely assumed that in the solid the $^4\Pi_{5/2}$ state is the only important emitter in the multiplet. Of course at much higher temperatures other members of the multiplet may also emit.

An energy level diagram for NO is given in Fig. 2. Only mixing with a $^2\Delta_{5/2}$ state can lead to emission from the $^4\Pi_{5/2}$ state. Nitric oxide has a known $^2\Delta_i$ state which probably arises by the promotion of an electron from the ground state $\sigma^2\pi^4\pi$ configuration to a $\sigma\,\pi^4\pi^2$ configuration (15). The 0-0 band of the B' $^2\Delta \leftarrow$ X$^2\Pi_{3/2}$ is at 59 900 cm^{-1}. This means that the energy level separation of the $^2\Delta$ and $^4\Pi$ state is about 21 900 cm^{-1}. The spin-orbit mixing can be calculated from the following formula

$$\left| \langle \psi'' | H_{S.O.} | \psi' \rangle \right| = \left[(f''/f')(v'/v'') \right]^{1/2} [v' - v''], \qquad (2)$$
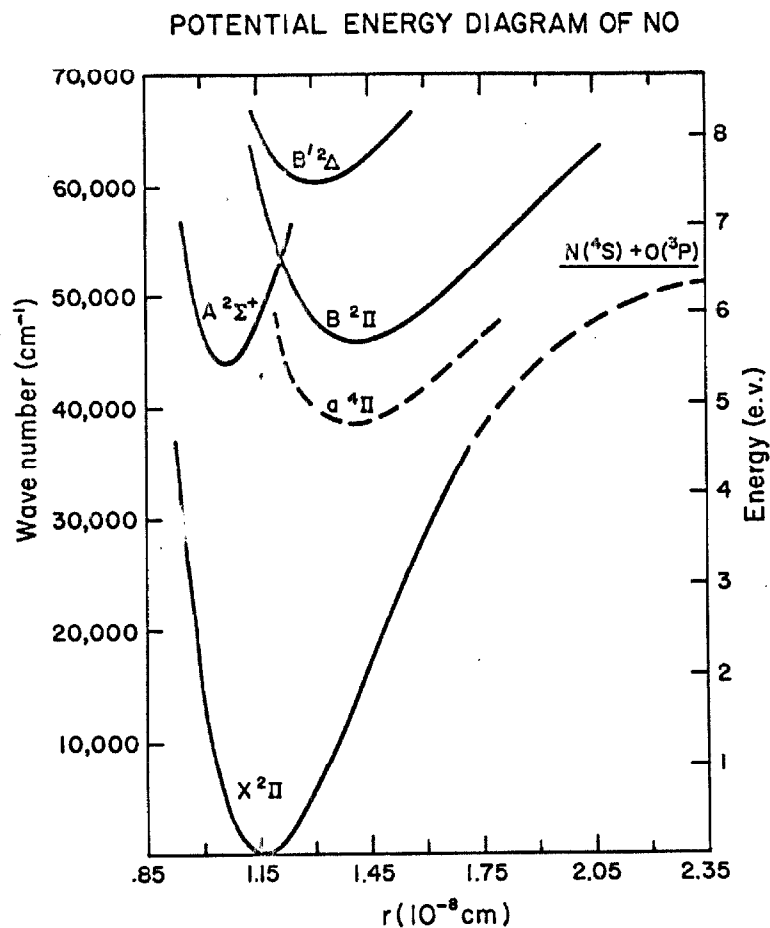
POTENTIAL ENERGY DIAGRAM OF NO

Fig. 2.   Potential energy diagram of NO. The solid portions of the curves were calculated by Vanderslice, Mason, and Maisch (14) using the Rydberg–Klein–Rees method.   The dashed portions of the curves were obtained by fitting the molecular constants to a Hulbert–Hirschfelder potential.

where the primes (') refer to the $^2\Delta_{5/2}$ state and the double primes (") to the $^4\Pi_{5/2}$ state. The oscillator strengths f' and f" and the wave numbers ν' and ν'' are with respect to the ground state. Typical oscillator strengths (16) for formally allowed transitions in NO lie between 0.002 and 0.02. Since $^2\Delta_{5/2} \rightarrow {}^2\Pi_{3/2}$ is a formally allowed transition it will be assumed that $0.002 \leq f' \leq 0.02$. The value of f" is 1.5×10^{-8} (see the calculation below). The energy separations ν', ν'' and $\nu' - \nu''$ are 59 900 cm^{-1}, 38 000 cm^{-1}, and 21 900 cm^{-1}, respectively (17). Using these values one obtains 24 cm$^{-1} \leq \langle \psi'' | H_{S.O.} | \psi' \rangle \leq 75$ cm^{-1}. Such a value seems quite reasonable for a molecule like NO which contains no high-Z atoms.

The other members of the $^4\Pi$ multiplet will mix with other doublet states and, in general, will have different transition probabilities than the $^4\Pi_{5/2}$ state. For instance the $^4\Pi_{3/2}$ state can mix with a $^2\Delta_{3/2}$ or a $^2\Pi_{3/2}$ state.

The Possibility of Observing the M-Bands in High Resolution

Since there are no experimental examples of a gas phase quartet-doublet transition, the observation of the M-bands in high resolution would be an important contribution to the spectroscopic literature. One can estimate the absorption intensity of the individual lines in the M-band fine structure from a knowledge of the geometry and vibrational constants of the upper and lower states, the energy of the transition, and the electronic oscillator strength of the transition.

One can calculate the oscillator strength for the $^4\Pi_{5/2} - {}^2\Pi_{3/2}$ transition from the formula (18)

$$f^{nm} = \frac{mc\, G_n}{8\pi^2 e^2 \nu_{nm}^2\, G_m} \frac{1}{\tau_n} \tag{3}$$

where G_n and G_m are the degeneracy factors for the two states, ν_{nm} is in cm^{-1}, and τ_n is the lifetime in seconds. The Franck-Condon maximum for the M-band emission is about 25 000 cm^{-1}. Using $G_n/G_m = 1$ and $\tau_n = .16$ sec (neon value) one calculates $f = 1.5 \times 10^{-8}$ for emission. Because of the Franck-Condon principle the effective wave number in absorption is greater than the effective wave number in emission. Since the oscillator strength is directly proportional to the transition wave number, the oscillator strength will also be greater in absorption than in emission by the ratio of the effective wave number in absorption to the effective wave number in emission. If we assume that the average wave number of the M-bands in absorption is about 44 000 cm^{-1}, then the oscillator strength for absorption is 2.6×10^{-8}. This value of the oscillator strength can be used to obtain a rough estimate of the path length of NO required to make a high-resolution study of the M-bands. It is possible, of course, that transitions to other members of the multiplet will be more intense since they can mix by spin-orbit interactions with nearby states such as the $B^2\Pi_{1/2, 3/2}$ states.

The absorption intensity of the M-bands will be distributed among the various bands in proportion to their Franck-Condon factors. We have calculated Franck-Condon factors for a transition from the

zeroth vibrational level of the initial $X^2\Pi_{3/2}$ state to the first nine

vibrational levels of the $a^4\Pi_{5/2}$ state. Ogawa's (5) vibrational

constants were used for the excited state, namely ω_e = 1019.0 cm^{-1}

and $\omega_e x_e$ = 12.8 cm^{-1}. The bond length in the excited state was

assumed to be 1.4 Å. This is a reasonable value since it is inter-

mediate between the 1.,385 Å and 1.448 Å bond lengths in the $B^2\Pi_{3/2,\,1/2}$

states (4) which come from the same configuration as the $a^4\Pi_{5/2}$ state.

The $X^2\Pi_{3/2}$ state constants are ω_e = 1903.68 cm^{-1}, $\omega_e x_e$ = 13.97 cm^{-1}

and r_e = 1.1508 Å (4). A method suggested by Brown (19) was used to

correct for anharmonicity. In this method vibrational overlap inte-

grals for a harmonic oscillator are used, but the vibrational constant

is assumed to depend on the vibrational level in the following manner:

$$\omega = \omega_e - \omega_e x_e (v + \tfrac{1}{2}). \tag{4}$$

Brown also corrected for the effect of anharmonicity on r but no cor-

rection was made in our overlap calculations, since the correction

would probably be of the same order of magnitude as the error in our

estimation of r. The calculated Franck-Condon factors (squared

vibrational overlap integrals) for the 0-0 through the 8-0 transitions

are .00011, .0014, .008, .03, .08, .20, .20, and .15, respectively.

The bands in the $a^4\Pi_{5/2} \leftarrow X^2\Pi_{3/2}$ transition will have these factors as

relative intensities. The intensity in each band will be divided among

P, Q, and R branches. The absorption coefficient (20, 21, 22) $k_{\nu p}$ for

the absorption maximum of a line in the P branch of the spectrum is

$$k_{\nu p} = \frac{\pi e^2 NfF(J - \frac{5}{2})(J - \frac{3}{2})}{mc^2\gamma \overline{\Delta\nu}_{1/2} \, 2J(2J + 1)} \approx \frac{\pi e^2 NfF}{4\,mc^2\gamma \overline{\Delta\nu}_{1/2}} \qquad (5a)$$

where e is the electronic charge, N is the number of molecules in one cm^3 of a gas at S. T. P., m is the electronic mass, and F is the Franck-Condon factor for the band in question. The factor γ is 1.06 for a Gaussian-shaped line, $\overline{\Delta\nu}_{1/2}$ is the width of a line in cm^{-1} at half height, and J is the angular momentum quantum number of the initial state. For large J, $k_{\nu p}$ is essentially independent of J as indicated in Eq. (5a). Let $C = \pi e^2 NfF/mc^2\gamma \overline{\Delta\nu}_{1/2}$; then $k_{\nu p} \approx C/4$. Furthermore, for the Q and R branches one has,

$$k_{\nu q} = C \, \frac{(J - \frac{3}{2})(J + \frac{1}{2})(J + \frac{5}{2})}{J(J + 1)(2J + 1)} \approx \frac{C}{2} \qquad (5b)$$

and

$$k_{\nu r} = C \, \frac{(J + \frac{5}{2})(J + \frac{7}{2})}{2(J + 1)(2J + 1)} \approx \frac{C}{4} \, . \qquad (5c)$$

The path length ℓ of NO at one atm pressure and 273°K, required to obtain a given optical density D is then

$$\ell = D/(\alpha_J k_\nu \log_{10} e) \qquad (6)$$

where α_J is the fraction of molecules in the initial state J. For $hcB_v/kT \ll 1$,

$$\alpha_J = \frac{hcB_v(2J+1) \exp \{-hc[B_vJ(J+1) + v_{00}'']/kT\}}{[1 + \exp(-hc\, v_{00}''/kT)]kT} \tag{7}$$

where B_v is the rotational constant and v_{00}'' is the separation in cm^{-1} of the zeroth vibrational levels in the $X^2\Pi_{1/2}$ and $X^2\Pi_{3/2}$ states. The molecular constants (4) for the $X^2\Pi_{3/2}$ state of NO are $B_0 = 1.6957$ and $v_{00}'' = 120.9\ cm^{-1}$. For an NO line at 44 000 cm^{-1} broadened by the Doppler effect, $\Delta v_{1/2} = 5.7 \times 10^{-3}\ T^{1/2}\ cm^{-1}$. This value is a minimum; other effects may further broaden the line, e.g. Λ-type doubling or low spectral resolution (23). Combining Eqs. (5b), (6), and (7) we get

$$\ell_Q = 1.84 \times 10^{-2}\ DT^{3/2}\ \{\exp[2.4\ J(J+1)/T]\}$$

$$\{1 + \exp(170/T)\}/(2J+1)F, \tag{8}$$

where ℓ_Q is in cm and the subscript Q indicates that we refer to the Q branch. The path length needed to obtain a given intensity in the R and P branches will be twice the path length needed to obtain the same intensity in the Q branch. The most intense line in the spectrum will be that for which $J = (T/4.8)^{1/2} - 1/2$.

Let us assume that the desired D is 0.3 and that the NO is at 300°K. The maximum intensity will occur at $J = 15/2$. Substituting T = 300°K, D = 0.3, and J = 15/2 into Eq. (8) we find that $\ell_Q = 8.2/F$ cm. For the 0-0 through the 6-0 bands, ℓ_Q is 750, 59, 10.2, 2.7, 1.0, .59, and .4 meters, respectively. One should bear in mind that ℓ_Q refers to the path length of NO at S.T.P. Since T is 300°K it is necessary that the actual path length be greater by a factor

of 300/273. For J = 5/2 the calculated optical density is reduced from .30 to 0.17, and for J = 25/2 it is reduced from .30 to 0.21. Since the path length of absorbing gas is directly proportional to the optical density, path lengths required for other optical densities can be calculated easily from the above results.

We can also state the approximate wavelength at which the $a^4\Pi_{5/2} \leftarrow X^2\Pi_{3/2}$ transition will lie. From the trends in Table III, one would expect that the 0-0 band would lie at 2631 ± 10 Å. If the correct vibrational constants for the upper state are $\omega_e^! = 1019.0$ cm^{-1} and $\omega_e x_e^! = 12.8$ cm^{-1}, then the 1-0 through 6-0 bands lie at 2564 ± 10 Å, 2502 ± 10 Å, 2444 ± 10 Å, 2390 ± 10 Å, 2341 ± 10 Å, and 2294 ± 10 Å, respectively. The Franck-Condon maximum lies between the 6-0 and 7-0 bands so there is no need to look below 2294 Å.

Bernstein and Herzberg (24) (BH) have searched without success for the $a^4\Pi - X^2\Pi$ transition of NO. Unfortunately they used a Hilger medium quartz spectrograph which limited their chances of observing the bands because of its low resolution. They used paths of 28, 12, 6, and 3 meter-atm at pressures of 700, 300, 150, and 75 mm, respectively. A continuum prevented them from observing below 2600 Å with the longest path. With 12 and 6 meter-atm paths, continuous absorption prevented observation below 2500 Å and 2400 Å, respectively. In the shortest path they observed only the 0-1 transition of the γ-system.

The fact that BH did not observe the M-bands is probably due to both the low resolution of their spectrograph and to the interference of the continuum. Our calculations which may be off by as much as a

factor of two or three indicate that with a higher resolution instrument they should have seen some of the bands. The β and γ systems will not interfere since the 0-0 γ-band and all other γ and β-bands originating in the $v'' = 0$ state lie below 2270 Å. The continuum which BH observed could be due to $(NO)_2$ absorption or to HNO_2 absorption. The dimer concentration can be minimized by using low pressures. The best band to search for is the 4-0 band at 2390 Å, since all bands in the γ or β system originating in the $v'' = 1$ level lie below 2375 Å.

Wilkinson (25) has observed the 6-0 and 7-0 bands of the Vegard-Kaplan system $(^3\Sigma_u^+ - {}^1\Sigma_g^+)$ of N_2 in absorption. He used 13 meter-atm paths and still found the bands "extremely weak." The Franck-Condon factors for the 7-0, 6-0, 1-0, and 0-0 bands of the VK system are 7.9×10^{-2}, 6.8×10^{-2}, 3.3×10^{-3}, and 5.9×10^{-4}, respectively (26). This means that the observation of the 1-0 band of this system would require 260 meter-atm while the observation of the 0-0 band would require 1500 meter-atm of N_2. The similarity of these paths to those calculated for the M-bands is gratifying since the 0.9 sec lifetime (27) of the VK bands is similar to the .16 sec lifetime of the M-bands. Also the Franck-Condon factors for the two systems are similar.

It is also possible that high-resolution spectra of the M-bands might be seen in emission. The problem in obtaining an emission spectrum is to minimize nonradiative deexcitation through collision with the container walls and with other NO molecules. The Vegard-Kaplan bands of N_2 can be observed in emission even though they undergo many collisions during their 0.9 sec radiative lifetime (27).

There would therefore seem to be a good chance of observing the shorter-lived M-bands in emission. Because NO in the $^4\Pi$ state reacts with ground state NO (see next section), it would be best to use a continuous-flow in search for the emission. Although it would be difficult in gaseous NO to obtain either an emission or absorption spectrum of the M-bands, if our calculations are correct, the absorption spectrum would seem to offer the best chance of success.

Discussion

The observed vibrational structure of the NO ground state in Ar and Kr is surprisingly similar to the vibrational structure of the NO ground state in the gas phase. One would expect to see some evidence of a repulsive effect on the higher vibrational levels, but no effect was observed. In Ar the β-bands were seen up to v = 13. In fact there is a general red shift in the vibrational spacings which is evident in both solvents. This red shift, as expected, is somewhat greater in Kr than in Ar. The β-bands because of their broad Franck-Condon envelope would make a good series for further study of the effect of a solid environment on the optential energy curves of diatomic molecules.

The fact that the β-bands rather than the γ-bands are excited in solid rare gases is somewhat surprising since in the gas phase the 0-0 γ-band is 1287 cm^{-1} lower than the 0-0 β-band. The appearance of the β-bands rather than the γ-bands could be due to one of two causes. Either the B$^2\Pi$ state, in which the β-bands originate, is lower

in the solid than the $A^2\Sigma^+$ state, in which the γ-bands originate, or the $B^2\Pi$ state is much more readily excited by x rays than the $A^2\Sigma^+$ state. In the latter case one would still have to postulate a rather slow radiationless transition from $B^2\Pi$ to $A^2\Sigma^+$. A radiationless transition slow compared with the $\sim 10^{-7}$ sec emission lifetime is not unreasonable in view of the large difference in internuclear distance in the two states.

Strausz and Gunning (28) (SG) have performed some interesting vapor phase photochemical experiments with NO and Hg. They use a mercury light source to excite mercury atoms in their reaction vessel. They have shown that the Hg atoms are deexcited by the NO in the following manner:

$$Hg^* + NO \longrightarrow Hg + NO^* . \qquad (9)$$

The NO^* can then be used to initiate chemistry either by reaction with ground state NO or, in the presence of hydrocarbon, by the abstraction of a hydrogen atom from RH to form the free radical R•. Other experiments by SG suggest, but do not prove, that while the $^3P_1$ state of Hg reacts with NO in the manner indicated by Eq. (9), the $^3P_0$ state of Hg does not. Prior to these experiments, Fallon, Vanderslice, and Mason (29) had suggested that mercury-photosensitized reactions involving NO could go through the $^4\Pi$ state of NO. SG have accepted this hypothesis and indicate that NO^* is probably an NO molecule in the $^4\Pi$ state.

Our results are also consistent with the suggestion that the NO^* in Eq. (9) is the $^4\Pi$ state of NO. The $^3P_0$, $^3P_1$, and $^3P_2$ states of the Hg lie at 37 645 cm^{-1}, 39 412 cm^{-1}, and 44 042 cm^{-1} respectively (6).

On energy grounds it is unlikely that the $^3P_0$ state of Hg is the sensitizer, since the 0-0 band of the $a^4\Pi_{5/2} - X^2\Pi_{3/2}$ transition lies probably quite near 38 000 cm^{-1}, or 355 cm^{-1} above the $^3P_0$ state of mercury. Primary radiative excitation of the $^3P_2$ state from the $^1S_0$ state of mercury is forbidden, and therefore, the $^3P_2$ state is probably not the sensitizer either. This leaves the $^3P_1$ level as the most probable state of Hg* in Eq. (9). The 1-0 band of the $a^4\Pi - X^2\Pi$ transition lies at approximately 39 114-nA where n is 0, 1, 2, or 3 for the $^4\Pi_{5/2}$, $^4\Pi_{3/2}$, $^4\Pi_{1/2}$, or $^4\Pi_{-1/2}$ state respectively and $\underline{A}$ is the coupling constant for the $a^4\Pi$ state. Since the $a^4\Pi$ state is inverted, -nA is a positive quantity. The coupling constants (4, 11) for the $X^2\Pi$ and $B^2\Pi$ states of NO are 124 cm^{-1} and 33 cm^{-1}, respectively. Therefore, a coupling constant that would place the $a^4\Pi$ state of NO less than 25 cm^{-1} below the $^3P_1$ state of Hg is not unreasonable. Rotation of the NO molecule could bring the two states even closer together in energy.

It is somewhat surprising that the M-bands have not been reported in auroral or airglow spectra. However, a brief search of the literature indicates that the M-bands, if present at all, are weak in atmospheric spectra.

Finally we feel that the evidence presented in this paper strongly points to the $^4\Pi_{5/2}$ state of NO as the emitter of the M-bands. Although it is not certain that the M-bands can be observed in high resolution, the chances of success are sufficiently great to justify a reexamination of this problem.

Acknowledgments

References

1. H. P. Broida and M. Peyron, J. Chem. Phys. 32, 1068 (1960);

   M. Peyron and H. P. Broida, J. Chem. Phys. 30, 139 (1959).

2. L. Vegard, Ann. Physik 79, 377 (1926).

3. R. S. Mulliken, Revs. Modern Phys. 4, 1 (1932).

4. G. Herzberg, Molecular Spectra and Molecular Structure I. Spectra of Diatomic Molecules, pp. 266, 558, 560, D. Van Nostrand, New York (1950).

5. M. Ogawa, Sci. of Light (Tokyo) 3, 39 (1954); also references by other authors listed here.

6. C. E. Moore, "Atomic Energy Levels," Vol. I (1949), pp. 32, 45; Vol. III (1958), p. 192, Circular No. 467 of the National Bureau of Standards.

7. A. L. Smith, W. E. Keller, and H. L. Johnston, J. Chem. Phys. 19, 189 (1951).

8. L. F. Keyser and J. Kwok, unpublished work. Keyser and Kwok have infrared evidence for the presence of dimers of NO in solid Kr ≥ 0.2 mole % in NO. They deposit on a window cooled to 8°K and observe the infrared spectrum which consists of four absorption lines at 1870 cm^{-1}, 1862 cm^{-1}, 1773 cm^{-1}, and 1767 cm^{-1}. Warming the deposit to 15–25°K and recooling causes three of these lines to increase in intensity relative to the other line at 1870 cm^{-1}. The frequencies of these three lines can be correlated with the infrared spectrum of liquid NO (7) which contains a broad feature centered at 1770 cm^{-1} (unresolved doublet) and a

narrower feature at 1863 cm^{-1}. [The spectrum of NO in liquid krypton (7) contains lines at about 1770, 1783, and 1864 cm^{-1}.] Since liquid NO is believed to be almost 100% dimer (see Reference 7 for details) the assignment of the Keyser and Kwok lines to dimers is reasonable.

9. L. J. Schoen and H. P. Broida, J. Chem. Phys. 32, 1184 (1960).

10. R. H. Gillette and E. H. Eyster, Phys. Rev. 56, 1113 (1939).

11. F. A. Jenkins, H. A. Barton, and R. S. Mulliken, Phys. Rev. 30, 150 (1927).

12. G. W. Robinson, J. Mol. Spectroscopy 6, 58 (1961).

13. G. W. Robinson and R. P. Frosch, J. Chem. Phys. 38, 1187 (1963).

14. J. T. Vanderslice, E. A. Mason, and W. G. Maisch, J. Chem. Phys. 31, 738 (1959).

15. E. Miescher, Can. J. Phys. 33, 355 (1955). The A constant of the $^2\Delta$ state is -2.

16. H. A. Ory, J. Chem. Phys. 40, 562 (1964).

17. Here the 0-0 bands have been used rather than the Franck-Condon maxima. This should not affect the result appreciably.

18. G. W. Robinson in Methods of Experimental Physics: Molecular Physics, V. 3, p. 243-44, Dudley Williams, ed., Academic Press, New York (1962).

19. W. G. Brown, Z. Physik 82, 768 (1933).

20. Reference 18. The formulas given in the reference have been suitably modified to correspond to the conditions described here.

21. The relative intensities of the P, Q, and R branches are taken
     from I. Kovács and A. Budó, Z. Physik $\underline{117}$, 612 (1941).

22. The absorption coefficients given in Eqs. (5a), (5b), and (5c) are
     valid only if both initial and final states belong to the case (a)
     coupling limit. Kovács and Budó (21) have given intensity
     formulas for the situation where either or both states belong to
     case (b). The use of the formulas when case (b) coupling applies
     is more complicated than when case (a) coupling applies. In
     case (a) coupling the intensities of the P, Q, and R branches are
     directly proportional to square of the spin-orbit coupling which
     mixes doublet and quartet states. However, in the case (b)
     limit the intensities of the P, Q, and R branches depend on the
     spin-orbit coupling in different ways. For instance, if a state
     were coupled to two other states with matrix elements H_1 and
     H_2, the intensity might be proportional to $(H_1 + H_2)^2$ in one branch
     and to $(H_1 - H_2)^2$ in another. For this reason we cannot calculate
     the rotational intensities in the case (b) limit from our experi-
     mental lifetimes. Since in high rotational states there is usually
     a transition from the case (a) to the case (b) coupling limit due to
     spin uncoupling, our intensity formula will not be valid for high J.

23. In calculating the path length required to see the M-bands in
     absorption, we have assumed that only the Doppler effect is im-
     portant in broadening the lines. Actually the resolving power of
     the spectrograph may be of comparable importance. If we call
     $\overline{\Delta\nu_{1/2}(D)}$ the broadening due to the Doppler effect and $\overline{\Delta\nu_{1/2}(R)}$
     the broadening due to the instrument, then the overall line

broadening $\overline{\Delta\nu_{1/2}} = [\overline{\Delta\nu_{1/2}(D)}^2 + \overline{\Delta\nu_{1/2}(R)}^2]^{1/2}$. For the M-bands $\overline{\Delta\nu_{1/2}} = (3.2 \times 10^{-5} \, T + 1.9 \times 10^9/R^2)^{1/2}$ where R is the resolving power of the spectrograph. If the instrumental broadening is comparable to the Doppler broadening, our path lengths should be multiplied by the factor $(9.6 \times 10^{-3} + 1.9 \times 10^9/R^2)^{1/2}/9.8 \times 10^{-2}$.

24. H. J. Bernstein and G. Herzberg, J. Chem. Phys. 15, 77 (1947).

25. P. G. Wilkinson, J. Chem. Phys. 30, 773 (1959).

26. R. W. Nicholls, J. Research Natl. Bur. Standards 65A, 451 (1961).

27. E. C. Zipf, J. Chem. Phys. 38, 2034 (1963).

28. O. P. Strausz and H. E. Gunning, Can. J. Chem. 39, 2549 (1961); O. P. Strausz and H. E. Gunning, ibid. 41, 1207 (1963).

29. R. J. Fallon, J. T. Vanderslice, and E. A. Mason, J. Phys. Chem. 63, 2082 (1959).

D. Emission and Absorption Spectra of Various Species — Especially

C_2 — Produced by the X Irradiation of Acetylene

Introduction

Several studies of matrix isolated C_2 have appeared in the literature. The most complete published study is that of McCarty and Robinson (1, 2) who trapped C_2 (produced in rare gas-methane and rare gas-acetylene discharges) in solid Ar and Xe matrices. They observed the Swan bands in both emission and absorption. More recently Weltner, Walsh, and Angell (3) have observed the Swan bands in absorption in Ne and Ar matrices. They vaporized graphite to produce the radicals. Schoen (4) has also reported the observation of the Swan band emission and a transition which he attributes to the $A^3\Pi \rightarrow x^1\Sigma_g^+$ transition of C_2. This assignment seems rather unlikely in view of the doubly forbidden character of the transition, and since the $A^3\Pi_g \rightarrow X'^3\Pi_u$ transition (Swan bands) is allowed. The work of Schoen will be further discussed below in light of the results reported here.

Additional work was needed to test some of the earlier observations. Of particular interest was the observation by McCarty and Robinson (1, 2) that the upper $(A^3\Pi_g)$ and lower $(X'^3\Pi_u)$ states of the Swan system have much larger vibrational separations in rare gas matrices than in the gas phase. McCarty and Robinson also reported a possible reverse anharmonicity in the vibrational structure of the $X'^3\Pi_u$ state when the solvent was Xe, but the experiments reported here do not support this finding.

The ground state of C_2 is of considerable interest. Until recently the ground state was believed to be the lower state of the Swan bands because of the observation of the Swan bands in cometary absorption spectra (6). The Phillips bands, whose lower state $(^1\Sigma_g^+)$ is the alternative possibility for the C_2 ground state are not observed in cometary spectra. McCarty and Robinson assigned the $^3\Pi_u$ state as the ground state in solid rare gases, but more recently Ballik and Ramsay (7) have shown conclusively that, in the gas phase, the $^1\Sigma_g^+$ state lies 610 ± 5 cm^{-1} below the $^3\Pi_u$ state.

The work to be described below has repeated much of the above matrix isolation work in a slightly different manner as well as produced some new bands not previously observed in the solid.

Experimental

The C_2 was produced by the x irradiation of C_2H_2 and C_2D_2 trapped in Ar, Kr, and Xe lattices cooled to liquid helium temperatures. In brief the gases were mixed in a glass manifold and then allowed to impinge on a liquid helium-cooled cold finger. Acetylene concentrations of 1% or less were used. The C_2H_2 which was obtained from the Matheson Co. and reported by them to have a 99.6% purity was used without further purification. The C_2D_2 (isotopic purity 99%) was obtained from Merck Sharp and Dohme of Canada and also used without further purification. The rare gases which were used as supplied by the manufacturer were Linde M.S.C. grade. Spectra were taken in the second order of an f/10 grating spectrograph with a second order

dispersion of 4 Å/mm. Kodak 103a-O, 103a-D, 103a-F, 1-N, and hypersensitized 1-M and 1-Z plates were used in the proper spectral regions.

The formation of C_2 from the acetylene was essentially complete in a half hour when 50-kV x rays produced by a 45 mamp stream of electrons were used to irradiate the sample. The x rays were also used to excite the C_2 emission spectra. A tungsten ribbon filament lamp was used to take absorption spectra. Broad band pass filters were used to separate the orders of the spectrograph.

Results

The observed spectra are compiled in Table I. The most prominent spectra obtained are the Swan bands of C_2 ($A^3\Pi_g - X'^3\Pi_u$) in both emission and absorption and two band series with common lower states (labeled a and b in Table I) which are also probably due to C_2. An energy level diagram for C_2 is shown in Fig. 1, and a microdensitometer tracing of the emission obtained from C_2D_2 in solid Kr is given in Fig. 2. Features which cannot be ascribed to C_2 have also been observed and will be discussed below.

The Swan bands have been observed in all three rare gas solvents. An experiment with C^{13} enriched acetylene confirmed that the assignment of the Swan bands is correct. Some of the strong features of the Swan bands appear as multiplets. For instance the 0-0 band is a triplet with a line separation of 30-40 cm^{-1} in all three solvents. One of the most striking features of the spectrum is

TABLE I.[†]   Electronic spectra obtained from x-irradiated C_2H_2 and

C_2D_2 in solid rare gases.

(cm^{-1})	I	$\Delta\nu_{1/2}$(cm^{-1})	Assignment and Remarks
C_2H_2 in Ar			
absorption			
19185	m	6	Swan Band 0-0
21132	w	7	Swan Band 1-0
emission			
23070	m	3	?
22973	m	6	a
22728	w	5	?
21493	m	5	?
21353	vs	15	a
21238	m	5	b 1-0?
21143	w	14	Swan Band 1-0
21026	w	11	Swan Band 1-0
19752	s	5	a
19619	m	5	b 1-1?
19363	w	13	Swan Band 1-1
19189	m	20	Swan Band 0-0 ⎫
19142	m	20	Swan Band 0-0 ⎬ overlap
19082	m	60	Swan Band 0-0 (degraded to red) ⎭
18926	w	3	?

Table I (continued)

C$_2$H$_2$ in Ar (continued)			
18653	m	3	?
18412	w	3	?
18177	vs	11	a
18024	m	4	b 1-2?
17612	w	12	Swan Band 1-2
17418	m	12	Swan Band 0-1
17312	w	12	Swan Band 0-1
17011	w	≤2	P
16906	w	≤2	P
16624	s	4	a
16431	w	≤2	P
16379	w	≤2	P
16273	w	≤2	P
16151	vw	≤2	P
16017	vw	≤2	P
15991	vw	≤2	P
15094	vw	3	a

C$_2$H$_2$ in Kr			
absorption			
*19144	m	12	Swan Band 0-0
*21085	m	9	Swan Band 1-0

Table I (continued)

C$_2$H$_2$ in Kr (continued)			
*23001	vw	13	Swan Band 2-0
emission			
*27074H?	w	9	c
*25371H?	w	8	c
*25154H?	w	10	C$_4$H$_2$?
*24210H?	w	7	C$_4$H$_2$?
*23922H?	w	14	C$_4$H$_2$?
*23698H?	m	9	c
*22694H?	w	6	C$_4$H$_2$?
22385	w	5	?
*22055H?	m	8	c
*21762H?	m	15	C$_4$H$_2$?
19138	s	15	Swan Band 0-0 (part of broad feature ~ 100 cm^{-1} wide)
*16352H?	w	≤ 2	P
*16286H?	w	≤ 2	P
*16247H?	w	≤ 2	P
*16196H?	w	≤ 2	P
*16062H?	w	≤ 2	P
*16036H?	w	≤ 2	P
*15976H?	w	≤ 2	P
*15948H?	w	≤ 2	P
*15936H?	w	≤ 2	P

Table I (continued)

C₂H₂ in Kr (continued)			

*15886H?	w	≤ 2	P
*15787H?	w	≤ 2	P
*15670H?	w	≤ 2	P
*15545H?	w	≤ 2	P
*15010	w	4	a

C₂D₂ in Kr			

emission

25319	w	5	?
24123	vw	7	?
24099	w	9	?
24076	w	7	?
23839	m	9	?
23674	m	11	?	bleaches
23164	vw	13	?
22971	m	7	?
22940	w	6	?
22930	w	6	?
22907	m	7	?
22872	vs	13	a
22779	m	4	?
22619	w	9	?

Table I (continued)

C_2D_2 in Kr (continued)			
22602	w	4	?
22286	m	12	? bleaches
21400	s	9	?
21366	m	5	?
21348	m	5	?
21338	m	5	?
21304	m	5	?
21255	vs	18	a
21166	s	7	b 1-0?
21149	m	5	?
21085	m	11	Swan Band 1-0
21045	m	13	Swan Band 1-0
21017	w	9	Swan Band 1-0
20951	s	7	?
19655	vs	9	a
*19550	m	6	b 1-1?
*19309	m	10	Swan Band 1-1
*19267	vw	10	Swan Band 1-1
*19246	vw	7	Swan Band 1-1
18325	m	4	?
18158	vw	4	?
18086	s	12	a

Table I (continued)

C₂D₂ in Kr (continued)				
17957	m	5	b	1-2?
17558	m	9	Swan Band 1-2	
*17517	vw	9	Swan Band 1-2	
*17496	vw	9	Swan Band 1-2	
17367	s	10	Swan Band 0-1	
17303	m	6	Swan Band 0-1	
*17035	vw	2	?	
16822	w	3	?	
16796	w	3	?	
*16630D?	w	≤2	P	
*16603D?	w	≤2	P	
16536	s	7	a	
*16496D?	vw	≤2	P	
*16445D?	vw	≤2	P	
16387	vw	3	b	1-3?
*16279D?	vw	≤2	P	
*15903D?	vw	≤2	P?	
15830	w	5	Swan Band 1-3	

C₂H₂ in Xe				

absorption

| *18975 | s | 9 | Swan Band 0-0 | |

Table I (continued)

C$_2$H$_2$ in Xe (continued)			
20911	s	7	Swan Band 1-0
emission			
*26297	w	11	C$_4$H$_2$?
*25060	m	10	C$_4$H$_2$?
*24116	w	9	C$_4$H$_2$?
*23832	m	14	C$_4$H$_2$?
*22892	m	13	C$_4$H$_2$?
*22601	w	8	C$_4$H$_2$?
*22546	w	8	C$_4$H$_2$?
*21952	m	10	C$_4$H$_2$?
*21672	s	8	C$_4$H$_2$?
*21625	w	6	C$_4$H$_2$?
*21386	vw	5	C$_4$H$_2$?
*21343	vw	7	C$_4$H$_2$?
*21312	vw	4	C$_4$H$_2$?
21049	w	7	?
20908	m	10	Swan Band 1-0
20872	m	10	Swan Band 1-0
*20737	m	8	C$_4$H$_2$?
*20459	vw	7	C$_4$H$_2$?
*20401	vw	8	C$_4$H$_2$?
19145	s	7	Swan Band 1-1

Table I (continued)

C$_2$H$_2$ in Xe (continued)			
18974	s	7	Swan Band 0-0
18959	s	10	Swan Band 0-0
18939	s	9	Swan Band 0-0
*17060H?	w	≤5	P
17030H?	w	≤5	P
*16964H?	vw	6	P
*16829H?	vw	≤2	P
*16760H?	vw	≤2	P
*16748H?	vw	≤4	P
*16720H?	vw	≤2	P
*16665H?	vw	≤2	P
*16619H?	vw	≤4	P
*16496H?	vw	≤2	P
*16432H?	vw	≤2	P
*16231H?	vw	≤2	P

C$_2$D$_2$ in Xe			
absorption			
22680	s	300	? possibly present with C$_2$H$_2$ in Xe
*23610	s	130	?⎫ no plates available in this
*24030	m	60	?⎭ region with C$_2$H$_2$ in Xe

Table I (continued)

C$_2$D$_2$ in Xe (continued)			
*24380	s	70	?
*24720	m	60	?
*25060	w	80	?
*25700	w	90	?

no plates available in this region with C$_2$H$_2$ in Xe

emission

*17407	m	13	Swan Band 1-2
*17208D?	s	≤ 2	P
*17176D?	s	≤ 2	P
*17110D?	m	≤ 2	P
17031D?	m	≤ 2	P
*16987D?	s	≤ 2	P
*16896D?	w	≤ 2	P
*16854D?	s	≤ 2	P
*16312D?	w	≤ 2	P
*16261D?	m	≤ 2	P
*16155D?	vw	≤ 2	P
*16070D?	vw	≤ 2	P
*16037D?	w	≤ 2	P
*15904D?	w	≤ 2	P
*15879D?	vw	≤ 2	P
*15819D?	vw	≤ 2	P

Table I (continued)

C_2D_2 in Xe (continued)			
*15783D?	vw	≤ 2	P
*15582D?	vw	≤ 2	P

†An asterisk in the first column indicates that the line was not observed with both ordinary and perdeuteroacetylene. Often the reason may be that the line was very weak. Those measurements followed by H? (or D?) are considered particularly likely to be lines from hydrogen (deuterium) containing molecules. In the intensity column s, m, and w mean strong, medium, and weak, respectively. The letter v stands for very. The series labeled c is reduced in intensity by about 50% after a 2 minute exposure to x rays. A complete set of emission spectra was not obtained with C_2D_2 in Xe. No C_2D_2 experiments were done in Ar.

ENERGY LEVELS OF C$_2$
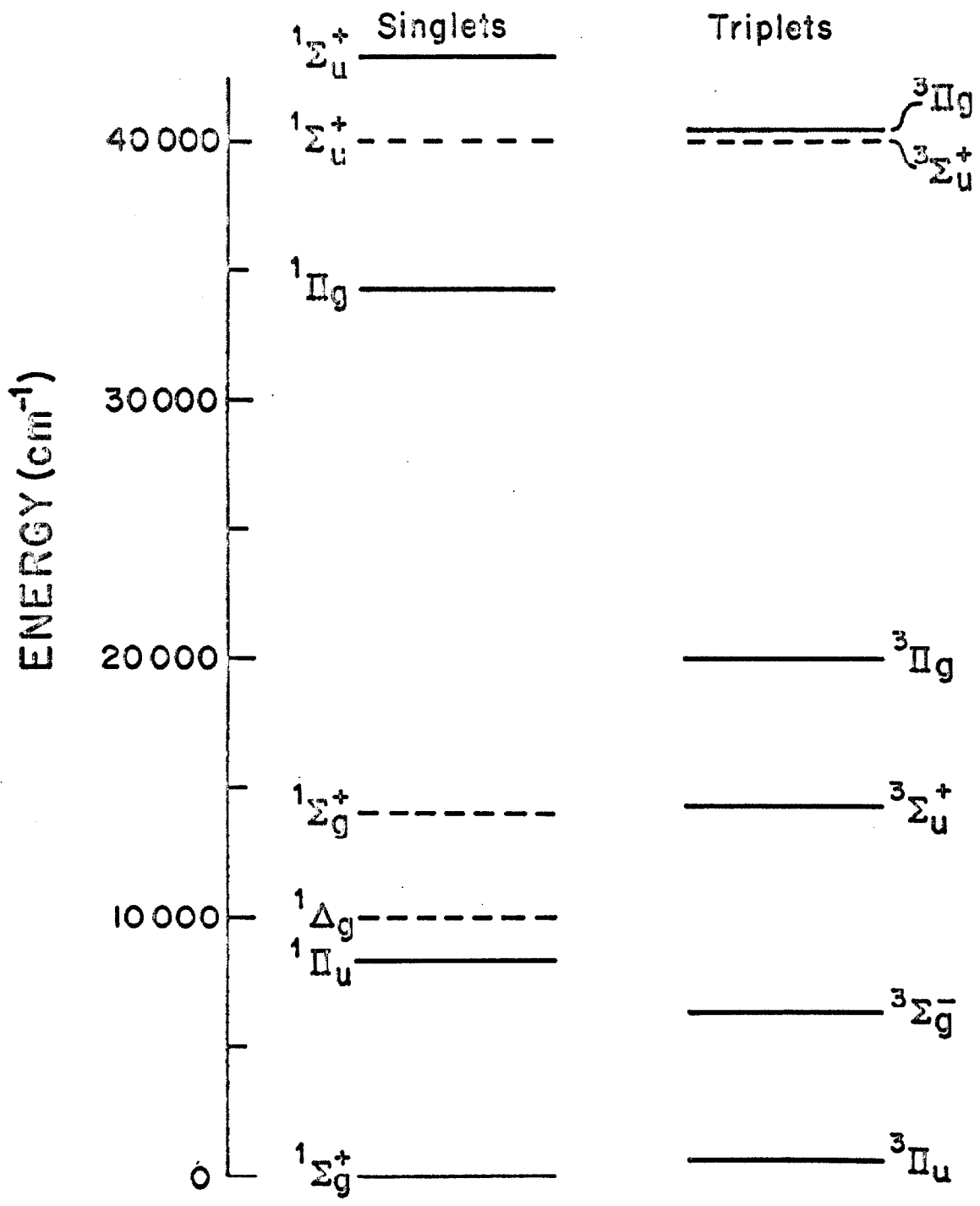
Fig. 1.
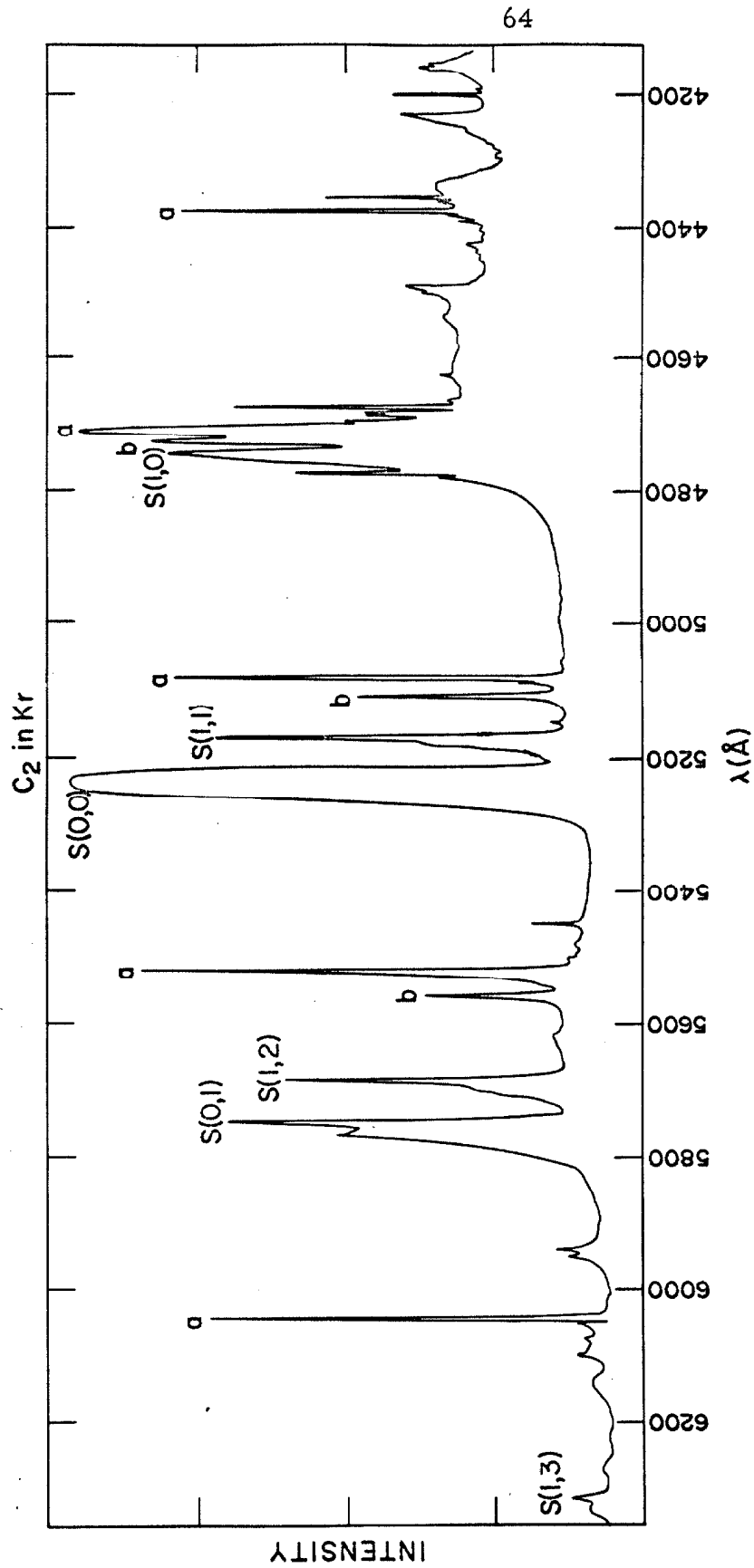
Fig. 2.   Microdensitometer tracing of the emission spectrum of C_2 in solid Kr.

emission from the first vibrational level of the upper electronic state. Normally vibrational relaxation in solid media occurs prior to emission. Two other homonuclear diatomics have also been reported to emit from excited vibrational levels when dissolved in a rare gas solid. Emission has been observed from the $v' = 0$, $v' = 1$, and $v' = 2$ of the Vegard-Kaplan bands of N_2 in solid Ar and Kr (10, 11) and from the $v' = 0$ and $v' = 1$ levels of the Herzberg bands of O_2 in solid Xe (11).

A vibrational analysis of the Swan bands is given in Table II. The large increase in the solid phase ΔG values of both upper and lower states compared with the gas phase should be noted. Such a large change in vibrational spacings in the solid phase is exceptional. The 0-0 and 1-0 emission bands reported here for C_2 in Xe are not appreciably matrix shifted with respect to the corresponding absorption bands, while McCarty and Robinson (1,2) (MR) reported 50 cm^{-1} red shifts of the 0-0 and 1-0 band emissions with respect to the absorption. The vibrational spacings of the $X'^3\Pi_u$ state of C_2 in Xe as reported by MR (using the apparent 50 cm^{-1} matrix shift of the emission) indicated an inverse anharmonicity effect, i.e. $\Delta G_{3/2} > \Delta G_{1/2}$, but the newer results indicate that the anharmonicity is normal in Xe and also in Ar and Kr. The values for the Swan band absorption in Ar, namely 21270 cm^{-1} and 19220 cm^{-1}, reported by Weltner, Walsh, and Angell (3) (WWA) differ markedly from those reported in this work and from those reported by MR for some unexplained reason. The absorption in Xe reported by WWA, however, agrees with the present work and that of MR.

TABLE II. Swan bands. Where an individual emission band was a multiplet, the most intense feature was used in this table. In cases of equal intensity the feature overlapping the absorption was used.

v'	v''	Gas[a]		Argon		Krypton		Xenon	
Absorption									
2	0	22856				23001			
			1722				1916		
1	0	21134		21132		21085		20911	
			1756		1947		1941		1936
0	0	19378		19185		19144		18975	
Emission									
0	0	19378		19189		19138		18974	
			1618		1771		1771		
0	1	17760		17418		17367			
1	0	21134		21143		21085		20908	
			1618		1780		1776		1763
1	1	19516		19363		19309		19145	
			1595		1751		1751		1738
1	2	17921		17612		17558		17407	
			1571				1728		
1	3	16350				15830			

[a]Calculated from data given on p. 513 of Reference 6.

Two other series of emission bands of C_2 with a common lower state have been observed in solid Ar and Kr but are entirely absent in solid Xe. These bands which are labeled a and b, respectively, in Table I are tabulated with their vibrational assignments in Table III. Shifts obtained from preliminary experiments using C^{13} enriched acetylene indicate that the b bands may originate in the $v' = 1$ vibrational level rather than the $v' = 0$ level. It was believed at first that the a bands and b bands were part of the same system, but the fact that the origin of the b bands in Ar is 1735 cm^{-1} to the red of the a-band origin in Ar, while in Kr the origins are separated by only 1706 cm^{-1} indicates that the two band systems have different upper states. The bands also differ somewhat in appearance.

Up to now attempts to assign these two band systems to known or predicted states of C_2 have failed. Assignments are difficult in the case of C_2 both because of the large number of low-lying electronic states and because of possible changes in vibrational separations such as the increase in the ΔG values of both the upper and lower states of the Swan band system. One would like to say that the a bands belong to the Deslandres-d'Azambuja system, ($^1\Pi_g - ^1\Pi_u$ transition, Fig. 1, p. 63), since $\Delta G_1/_2$ for the lower state of this system is 1584 cm^{-1} in the gas phase compared with a $\Delta G_1/_2$ value of the lower electronic state of the a bands in solid Ar of 1620 cm^{-1}. Such an assignment would require an unusually large red shift relative to the gas phase of 2996 cm^{-1} and 3097 cm^{-1} in Ar and Kr, respectively. It is probable that the b bands are the same as the bands reported by Schoen (4) (extending from 4700Å to 6075Å)

TABLE III.   The a bands and the b bands.

v''	Argon		Krypton	
	a Bands	b Bands	a Bands	b Bands
0	22973	21238	22872	21166
	1620	1619	1617	1616
1	21353	19619	21255	19550
	1601	1595	1600	1593
2	19752	18024	19655	17957
	1575		1569	1570
3	18177		18086	16387
	1553		1550	
4	16624		16536	
	1530		1526	
5	15094		15010	

which he attributes to the $A^3\Pi_g \rightarrow x^1\Sigma_g^+$ transition. Such an assignment seems highly unlikely, even in the solid, in view of the doubly forbidden character of the transition and the fact that radiation from the $A^3\Pi_g$ to the $X'^3\Pi_u$ state (Swan bands) is highly allowed.

Besides the bands which can definitely be associated with C_2 a number of other bands have been observed which can be correlated with one another to form systems. Benzene phosphorescence was particularly prominent during some, but not all, experiments with C_2H_2 in Ar and Kr and C_2D_2 in Kr. The identification is certain, since comparison could be made with earlier experiments with C_6H_6 and C_6D_6 in rare gas matrices (part IF, this thesis). It is possible that benzene was present as an impurity in the acetylene, since no effort was made remove impurities from the acetylene. The other alternative, of course, is that the benzene was produced in the lattice by, a reaction of three neighboring acetylenes. Further work is required to distinguish between the two possibilities.

Besides benzene phosphorescence three groups of emission lines have been observed. One of these series (labeled c bands in Table I) was observed during two different C_2H_2 in Kr experiments. The bands are easily bleached being diminished by about 50% after only 2 minutes exposure to x rays. The c band system has the appearance of a diatomic band system, but it is hard to see what diatomic molecule with a fundamental frequency near 1700 cm^{-1} could be so easily photolyzed. Unfortunately the experimental data do not allow one to assign the 27074 cm^{-1} band unequivocally as the 0-0 band. The fundamental frequency does not match any C_2H_2 ground state

frequencies (12). One intriguing possibility is that the c bands are emission from the HC_2 radical which has not been previously observed. From the considerations of Walsh (13) one would expect HC_2 to be linear in both its ground and lower excited states. The c bands could easily be analogous to the violet bands of CN (0-0 band at 25800 cm^{-1}) with which HC_2 is isoelectronic. The reduction in $\Delta G_{1/2}$ from 2043 cm^{-1} to an apparent 1700 cm^{-1} could easily be explained by the fact that not all the electrons are concentrated in the C—C bond of HC_2. A crude estimation of the C—C stretching frequency of HC_2 can be made by assuming that the ratio of the C—C stretching frequency in HC_2 to the CN stretching frequency should be nearly equal to the ratio of the C—N stretching frequency in HCN to the N_2 stretching frequency. $\Delta G_{1/2}$ is equal to 2135, 2043, and 2332 cm^{-1} in HCN (5), CN (6), and N_2 (6), respectively. These values give a $\Delta G_{1/2}$ for the C—C stretching frequency of 1862 cm^{-1} which, although higher than the observed $\Delta G_{1/2}$ of 1700 cm^{-1}, does not exclude the possibility of HC_2. Further experiments, especially absorption spectra, are necessary to check this possible identification.

Another series of emission bands which definitely come from a polyatomic molecule were observed with C_2H_2 in Kr and more strongly in Xe. After their appearance the bands remain undiminished in intensity during further x irradiation. On the basis of the observed frequencies these bands seem most likely to be due to the diacetylene phosphorescent state. Evans (14) reports the onset of singlet-triplet absorption in diacetylene as being at 27020 cm^{-1}, while the corresponding band in Xe observed by the author is at 26297 cm^{-1}. This is

good agreement in view of matrix shifts and the possibility that either or both origins may not be the 0-0 band but rather the 0-0 band plus one unit of some vibrational mode. Furthermore, the ~2180 cm^{-1} separation observed in the spectrum matches well with the 2184 cm^{-1} symmetric stretching mode of C_4H_2 (15). The 1215-1254 cm^{-1} separations observed in the spectrum also correlate well with the very weak 1241 cm^{-1} Raman line of diacetylene (15) believed to be due to two quanta of one of the bending modes. If diacetylene is bent in the excited state (it is linear in the ground state), changes of two quanta in the bending mode should be prominent in the emission spectrum.

One other group of emissions, the P bands, is listed in Table I. The bands are quite narrow (≤ 2 cm^{-1}) and not stable in time. Possibly there is one set of stable bands and one similar set which is unstable. Similar bands which appear in all three solvents are also obtained when deuterated acetylene is the solvent but are shifted with respect to those obtained when ordinary acetylene is used. No identification of the bands has been made other than that their complexity indicates they are emitted by a polyatomic molecule. Actually the P band intensity accounts for only a small amount of the light emitted by the sample, probably < 0.1%, and it is only the narrowness of the bands which makes them experimentally observable.

A few other unidentified emission lines are listed in Table I.

A number of broad absorption bands were noted after x irradiation when C_2D_2 was deposited in Xe. The bands are also apparently present with C_2H_2 in Xe, but only the first one was observed because no plates were taken which extended further to the blue. No attempt

was made to observe these absorptions in Ar or Kr. The identity of these bands is at present unknown. They do not appear to correlate with the C_3 absorption spectrum in Xe reported by Weltner and Walsh (16).

Discussion

Because of the large number of low-lying electronic states, C_2 is a unique molecule. The ground state configuration of C_2 is $1s\sigma_g^2 1s\sigma_u^2 2s\sigma_g^2 2s\sigma_u^2 2p\pi_u^4$ which gives a $^1\Sigma_g^+$ ground state. However, electron-electron repulsion terms in the Hamiltonian makes states arising from the $1s\sigma_g^2 1s\sigma_u^2 2s\sigma_g^2 2s\sigma_u^2 2p\pi_u^3 2p\sigma_g$ configuration very close to the ground state in energy. In fact the $^3\Pi_u$ state arising from the first "excited" configuration was long thought to be the ground state of C_2 (6, 7). Many other configurations have low-lying electronic states. This large number of low-lying states makes it difficult to interpret C_2 spectra and also difficult to do theoretical calculations of the C_2 energies. For this reason and because of perturbations of the vibrational separations the a bands and b bands have not been assigned to any particular electronic state. On the other hand there is no doubt about the Swan band assignment.

The failure to observe the Phillips bands in absorption below 9080 Å in Xe, below 9940 Å in Kr, and below 10300 Å in Ar leaves little doubt that $^3\Pi_u$ is the ground state of C_2 in solid rare gases. Since the work of Ballik and Ramsay (7) indicates that in the gas phase the lowest vibrational level of the $^1\Sigma_g^+$ state lies 610 cm^{-1} below

the lowest vibrational level of the $^3\Pi_u$ state, the position of the two levels is apparently reversed in the solid.

It is possible to explain this reversal of the ground states in a qualitative manner. Configuration interaction will be less important in the solid, since the medium will attract the solute electrons and effectively create electron-electron correlation. Therefore, both the $^1\Sigma_g^+$ state and the $^3\Pi_u$ state are probably red shifted in the solid. Clementi and Pitzer (8, 9) predict another $^1\Sigma_g^+$ state 14000 cm^{-1} above the x $^1\Sigma_g^+$ state. There is no other $^3\Pi_u$ lying close to the lowest $^3\Pi_u$ state. If only the two lowest $^1\Sigma_g^+$ states and the $^3\Pi_u$ state are considered, the secular equation for the problem is

$$\begin{vmatrix} H_{11} - E & H_{12} & 0 \\ H_{21} & H_{22} - E & 0 \\ 0 & 0 & H_{33} - E \end{vmatrix} = 0 \, ,$$

or

$$E = \frac{H_{11} + H_{22}}{2} \pm \frac{H_{11} - H_{22}}{2} \left[1 + \frac{4 H_{12} H_{21}}{(H_{11} - H_{22})^2} \right]^{\frac{1}{2}} ,$$

and

$$E = H_{33} \, .$$

In the above equations H_{11}, H_{22}, and H_{33} are the energies of the two lowest $^1\Sigma_g^+$ states and the $^3\Pi_u$ state, respectively, before configuration interaction has been considered. The diagonal elements will all be more negative in the solid because electron-electron repulsion terms

are less important. $H_{12} = H_{21}^*$ is the off diagonal expectation value of the electron-electron repulsion part of the Hamiltonian. Since H_{12} is smaller in the solid than in the gas, the two lowest $^1\Sigma_g^+$ states will be closer together in the solid than in the gas phase. This could give rise to the situation depicted in Fig. 3 which shows the $^3\Pi_u$ state lower in energy than the $^1\Sigma_g^+$ state in the solid.

It is more difficult to explain the vibrational perturbation observed in the Swan bands. The most surprising aspect of the perturbation is that it is about the same in all three rare gases. For instance the increase in the $\Delta G_{1/2}$ value of the $^3\Pi_g$ upper state in Ar, Kr, and Xe is 191, 185, and 180 cm^{-1}, respectively. The situation is similar in the lower state (Table II). The explanation may be that the C_2 accepts "part of an electron" in partially filled bonding orbitals thus increasing the magnitude of the molecular force constant. Further studies are needed with molecules having low-lying unfilled bonding orbitals such as CN and BN to see whether the large vibrational perturbation is a common effect in solid media. Robinson (17) has briefly discussed the problem of calculating vibrational perturbations. Unfortunately the a priori determination of changes in vibrational energies in solid media requires a long and tedious quantum mechanical calculation.

GROUND STATE OF C$_2$

Gas   Solid   Solid   Gas

$^1\Sigma_g^+$

$a^1\Sigma_g^+$

$X'^3\Pi_u$
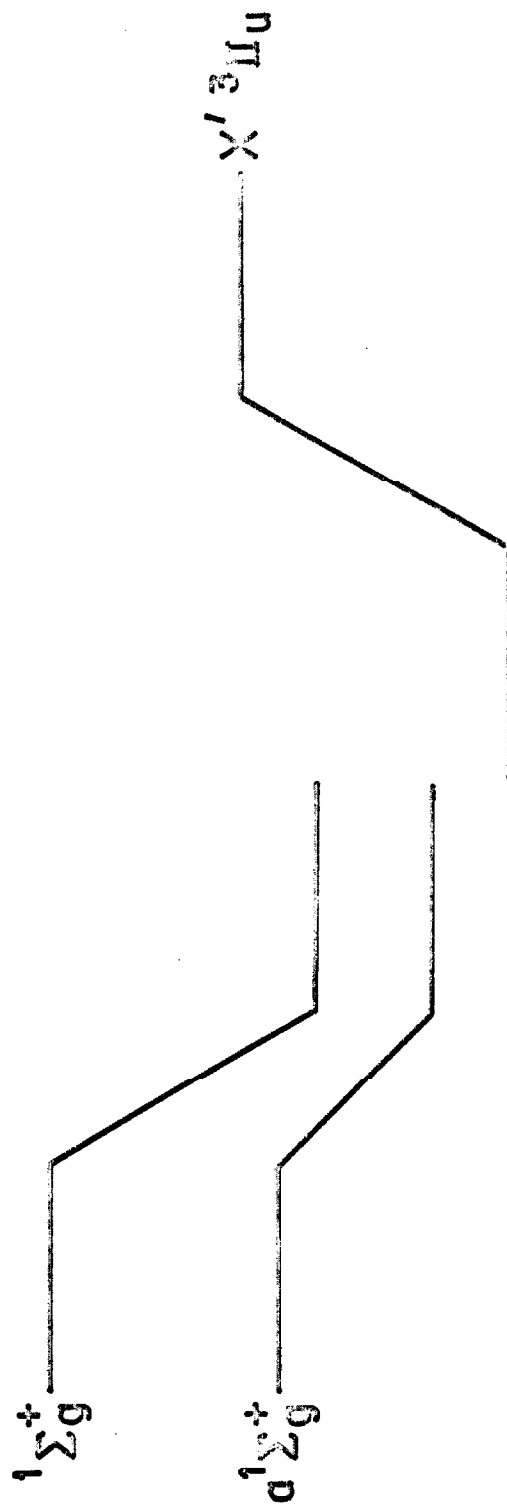
Fig. 3.

References

1. M. McCarty and G. W. Robinson, J. chim. phys. 56, 723 (1959).

2. M. McCarty, Thesis, Johns Hopkins University (1960).

3. W. Weltner, P. N. Walsh, and C. L. Angell, J. Chem. Phys. 40, 1299 (1964).

4. L. J. Schoen, 5th Intern. Symp. Free Radical Stabilization, Uppsala, Sweden (1961).

5. A. E. Douglas and D. Sharma, J. Chem. Phys. 21, 448 (1953).

6. G. Herzberg, Molecular Spectra and Molecular Structure I (D. Van Nostrand Co., Inc., Princeton, N. J., 1950), p. 488.

7. E. A. Ballik and D. A. Ramsay, Astrophys. Jour. 137, 61 (1963); ibid. 137, 84 (1963).

8. E. Clementi and K. S. Pitzer, J. Chem. Phys. 32, 656 (1960).

9. E. Clementi, Astrophys. Jour. 133, 303 (1961).

10. H. P. Broida and M. Peyron, J. Chem. Phys. 32, 1068 (1960).

11. L. J. Schoen and H. P. Broida, J. Chem. Phys. 32, 1184 (1960).

12. G. Herzberg, Molecular Spectra and Molecular Structure II. Infrared and Raman Spectra of Polyatomic Molecules (D. Van Nostrand Co., Inc., Princeton, N. J., 1945), p. 290.

13. A. D. Walsh, J. Chem. Soc. 2288 (1953).

14. D. F. Evans, J. Chem. Soc. 1735 (1960).

15. A. V. Jones, Proc. Roy. Soc. A211, 285 (1952).

16. W. Weltner and P. N. Walsh, J. Chem. Phys. 37, 1153 (1962).

17. G. W. Robinson, Advances in Chemistry Series No. 36, 10 (1962).

E. The X Irradiation of Carbon Dioxide in Solid Rare Gas

One problem which can be readily worked on using x-ray excitation is the observation of phosphorescence spectra and the measurement of triplet state lifetimes of molecules stable to x irradiation. The triplet state of CO_2 has never been identified spectroscopically. However, it has been suggested that very complicated emission bands from the carbon monoxide flame may originate in a triplet state of CO_2 (1). Gaydon has suggested that the flame bands are a triplet to ground state transition, while Walsh (2) attributes them to a transition between two triplet states. The flame bands which are superposed on a stronger continuum are strongest between 3500 and 4500 Å. Broida and Gaydon (3) have shown that the reaction of CO with atomic oxygen gives the bands but not the continuum. At the present time the nature of the bands and continuum is still unknown, although the evidence for CO_2 as the emitter is quite strong.

It was thought that the phosphorescence of CO_2 might be excited in a rare gas matrix with x rays. Krypton and xenon matrices with CO_2 concentrations of about 1% and 0.5%, respectively, were deposited on the liquid helium cooled cold finger, and x-ray excited emission spectra were photographed. Unfortunately there was no sign of the flame bands in the emission. A continuum which was most intense between 3650 and 3930 Å was very strong in Xe. It was also present in Kr but only very weakly. The continuum may or may not have the same cause as the continuum observed with the flame bands. Besides the continuum a series of bands was observed in Kr which has been

tentatively identified as the Herzberg bands (4) of CO. The bands whose measurements are given in Table I are very broad. They are cut off sharply on the blue edge but are only slowly degraded to the red. Their width at half height is approximately 100 cm^{-1}. Besides the bands a broad line was observed in Kr at 5625 Å which has been identified by Schoen and Broida (5) as being due to the forbidden $^1S-^1D$ transition of atomic oxygen. The presence of atomic oxygen in the lattice supports the assignment of the bands to a CO transition. Two of the bands (Table I) have also been observed in solid Xe. The bands are much weaker in Xe and only about 15 cm^{-1} in breadth. The above features are the only emission observed between 3180 and 5760 Å in Kr and between 3180 and 5470 Å in Xe.

If the identification of the Herzberg bands of CO is correct, the results are particularly interesting for two reasons. First the bands are one of the few cases where the spectrum in Xe is blue shifted with respect to the spectrum in Kr. The Herzberg bands of O_2 are also progressively further to the blue in the series Ar, Kr, and Xe (5). The second fact about the bands which is interesting is that they represent a transition between two highly excited states of CO. The upper state is the $C^1\Sigma^+$ state for which T_e = 91926 cm^{-1}, while the lower state is $A^1\Pi$ for which T_e = 65075 cm^{-1}. Because of radiationless decay, emission from highly excited states is rare in condensed media. However, because there is only one molecular vibrational mode, radiationless decay in diatomic molecules may be slower than in polyatomic molecules. Even more surprising is the fact that the emission is apparently coming from a state of CO higher

TABLE I. Herzberg bands of CO (cm^{-1}).

v'	v''	Gas*		Kr†		Xe	
		ν	ΔG	ν	ΔG	ν	ΔG
0	0	27174		27970			
			1481		1447		
0	1	25693		26523			
			1447		1430		
0	2	24246		25093		25140	
			1412		1411		1430
0	3	22834		23682		23710	
			1377		1389		
0	4	21457		22293			

*Reference 4.

†Measured at blue edge of band.

in energy than the lowest exciton state of the rare gas crystal, i.e. an embedded state. The lowest excited states of crystalline Kr and Xe are at 80390 and 66310 cm^{-1}, respectively (6). Excitation probably occurs in two steps. First the $A^1\Pi$ state is probably excited. This requires an energy of 64746 cm^{-1} in the gas phase. The $A^1\Pi - X^1\Sigma^+$ transition of CO is analogous to the $a^1\Pi_g - X^1\Sigma_g^+$ transition of N_2. Because the g-u selection rule should apply weakly in CO the lifetime of the $A^1\Pi$ state should be long enough to allow the second step to occur. The second step is, of course, excitation of the $C^1\Sigma^+$ state or some other state that can relax back to the $C^1\Sigma^+$ state.

The fact that the CO bands are only weakly excited in Xe may be because the CO_2 is not readily decomposed by the amount of energy available from the Xe lattice. Alternatively the lowest exciton level of the Xe lattice may not have a high enough energy to efficiently excite the $A^1\Pi$ level of CO. Again it must be emphasized that further work is needed to confirm the above results. Deposition experiments using isotopically substituted CO would be particularly helpful in corroborating the results.

References

1. A. G. Gaydon, The Spectroscopy of Flames (John Wiley and Sons, Inc., New York, 1957),pp. 91–111 and other references cited here.

2. A. D. Walsh, J. Chem. Soc. 2266 (1953).

3. H. P. Broida and A. G. Gaydon, Trans. Faraday Soc. 49, 1190 (1953).

4. G. Herzberg, Molecular Spectra and Molecular Structure I. Spectra of Diatomic Molecules (D. Van Nostrand Co., Inc., Princeton, N. J., 1950),p. 522.

5. L. J. Schoen and H. P. Broida, J. Chem. Phys. 32, 1184 (1960).

6. O. Schnepp and K. Dressler, J. Chem. Phys. 33, 49 (1960).

F.   The Spectra and Triplet State Lifetimes of Benzene

and Naphthalene in Rare Gas Matrices

Although the literature contains numerous articles on the
spectra and lifetimes of benzene and naphthalene the useful study of
the electronic structure of these molecules has by no means been
exhausted. We[*] have carried out a study of the spectra of these two
molecules trapped in a rare gas, H_2, or CH_4. The phosphorescence
lifetimes of these molecules have also been measured in the same
solvents. The experimental apparatus used did not differ in any im-
portant essentials from that described in the section on apparatus in
this thesis.[†] Phosphorescence spectra were made with a set of
rotating disks.   To measure the lifetimes, the phosphorescence was
passed through an interference filter (except in a few cases when the
emission was very weak) and focused on the cathode of a 1P21 RCA
photomultiplier tube. The output of the tube was fed into an oscillo-
scope and the decaying signal photographed from the face of the scope.
Lifetimes were measured directly from the photographs.

Our results along with the results of some other workers are
shown in Table I. The deuterium effect on the measured triplet state

---

[*]Most of the experimental work discussed in this section was
done jointly with Dr. M. R. Wright.

[†]Glass stopcocks were used in the glass system in place of
metal valves. Careful cleaning of the stopcocks was necessary when-
ever the solute was changed, since both benzene and napthalene dis-
solve readily in stopcock grease. These solutes dissolve less readily
in silicone greases than in hydrocarbon base greases.

TABLE I. Phosphorescence lifetimes.

Solvent Compound	Matrices at 4.2°K					Durene* at 77°K	EPA† at 77°K	van der Waals‡
	H₂	CH₄	Ar	Kr	Xe			
benzene		16	16	1	.07		7.0	
benzene–d₆		22	26	1	.07			
naphthalene	2.3	2.2	1.7	.4	.07	2.1	2.6	
naphthalene–d₈			13			16		
anthracene							<.1	
anthracene–d₈								.7

*C. A. Hutchison and B. W. Mangum, J. Chem. Phys. 32, 1261 (1960).

†D. S. McClure, J. Chem. Phys. 17, 905 (1949).

‡J. H. van der Waals, private communication.

lifetimes is apparently general among the polyacenes. An explanation of the deuterium effect is given in the section of this thesis devoted to electronic relaxation. An intermolecular heavy atom effect is also apparent from the lifetime variation in the series Ar, Kr, and Xe.

The measured lifetime can be separated into a radiative and a nonradiative portion,

$$1/\tau \;=\; 1/\tau_r \;+\; 1/\tau_{nr} \;. \tag{1}$$

Here τ is the measured lifetime, τ_r is the radiative lifetime, and τ_{nr} is the nonradiative lifetime. An explanation of the heavy atom effect on the radiative lifetime has been given by Robinson (1). The heavy atom effect on the nonradiative lifetime is discussed later in this thesis.

The qualitative features of the benzene spectra are interesting. The heavy atom effect mentioned above is evident not only in the lifetimes but also in the vibronic features of the phosphorescence spectrum itself. This indicates that at least part of the heavy atom effect on the phosphorescence lifetime is due to a change in the radiative part of the measured lifetime. In Kr and Xe two series of symmetric (a_{1g}) vibrations are about equal in intensity. One series has its origin in the 0-0 band. The other series, in addition to the symmetric vibration, has one quantum of the 1600 cm^{-1} carbon stretching vibration (e_{2g}). On the other hand in a "lower molecular weight solvent" like argon the series containing the 0-0 band has less than 10% of the overall intensity of the series which begins with the

1600 cm^{-1} vibration indicating that in this low molecular weight solvent the intermolecular perturbation is relatively unimportant as a mechanism for the radiative decay of the triplet state. The 0-0 band also appears weakly in the phosphorescence spectrum of benzene in EPA* at 77°K (2). This solvent perturbation may account for the fact that benzene has a shorter lifetime in EPA than in CH_4 or Ar. In Xe and Kr the phosphorescence is relatively strong and is easily observed superposed on the background continuum of an absorption spectrum. No fluorescence has been observed with Kr or Xe solvents indicating rapid intersystem crossing. On the other hand in Ar weak fluorescence whose intensity is 10% of the phosphorescence intensity can be seen. In methane the fluorescence is very strong. In one experiment using an H_2 matrix no phosphorescence could be detected. Additional experiments are needed to get relative fluorescence-phosphorescence quantum yields. In napthalene as in benzene, Q_F/Q_P is highly solvent dependent. Here, Q_F is the fluorescence and Q_P the phosphorescence quantum yield. Napthalene in hydrogen does, however, emit detectable phosphorescence.

Absorption to the lowest benzene singlet ($^1B_{2u} \leftarrow {}^1A_{1g}$) is similar to the gas phase absorption in that more than 90% of the intensity is concentrated in a series of totally symmetric vibrations plus one quantum of the 521 cm^{-1} C-bending vibration. Up to four or five quanta of the symmetric breathing vibration can be observed in

---

*EPA is a glass consisting of 5 parts ether, 5 parts isopentane, and 2 parts alcohol. Reference 3.

this series. The absorption is interesting because the individual bands show structure. In Ar and Kr this structure is a triplet. The splitting in Ar is of the order of 100 cm^{-1}, and the intensity (from an eye estimate) of the three members is from red to blue 25:1:10. The spectrum in Kr is very similar. The spectrum of benzene in Xe is broadened too much to observe any structure which may be present in the lines. In H_2 the structure in each absorption band is quite complex. A microdensitometer trace of the first strong absorption is shown in Fig. 1. The spacing of about 10 cm^{-1} excludes the possibility of the fine structure being due to free rotation of either H_2 or C_6H_6, since the B constant for H_2 is 29 cm^{-1} (4) and that for C_6H_6 is 0.12 cm^{-1} (5). The most probable explanation is that the fine structure is due to an interaction of the benzene with the lattice, although it is difficult to pinpoint the exact nature of this interaction. The Debye frequency (6) of an H_2 lattice is 73 cm^{-1} which is much higher than the observed 10 cm^{-1} spacing of the fine structure. Of course frequencies other than the Debye maximum may show up, but frequencies close to ν_{max} are most likely to appear in the spectrum because these frequencies are the ones associated with localized vibrations.

Emission spectra from the hydrogen matrix have not been correlated with the benzene spectrum. Further work with benzene and benzene-d_6 in hydrogen and deuterium is necessary to pin down the mechanism of the degradation of benzene excitation in hydrogen lattices.

The theoretical assignment of the lowest triplet state of benzene as a $^3B_{1u}$ has been questioned by some workers. Since a
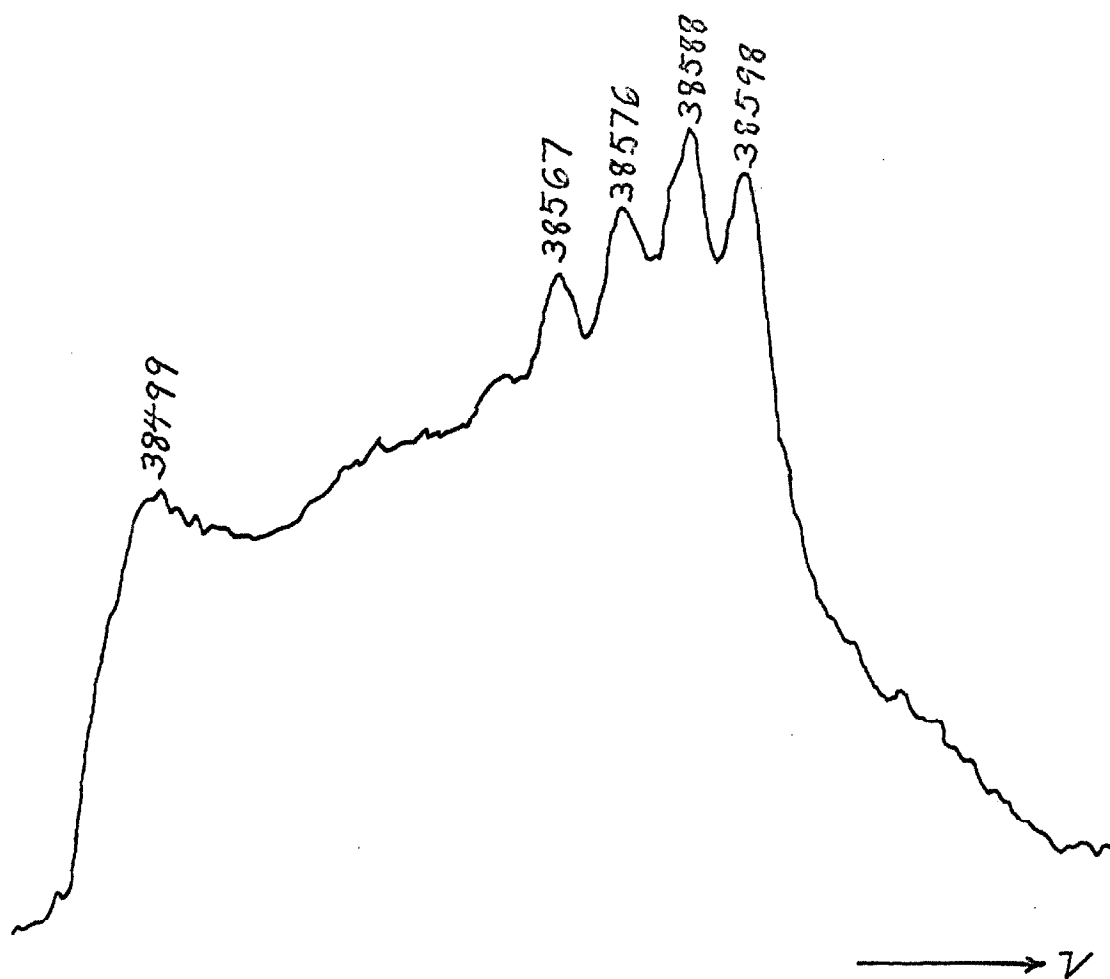
Fig. 1. A microdensitometer tracing of the first absorption band of
the benzene $^1B_{2u} \leftarrow {}^1A_{1g}$ transition. The solvent is ordinary
hydrogen. The line measurements are in reciprocal centi-
meters.

$^3B_{1u}$ would mix through spin-orbit interaction with a $^1B_{2u}$, it was expected that the vibrational structure of the emission from a $^3B_{1u}$ state would be similar to the vibrational structure of emission from a $^1B_{2u}$ state. However, in benzene the 606 cm^{-1} (e_{2g}) vibration is excited in the fluorescence, while the 1596 cm^{-1} (e_{2g}) vibration is excited in the phosphorescence. However, as Albrecht (7) has pointed out, another possible mechanism for the phosphorescence is for the $^3B_{1u}$ state to mix vibronically with a $^3E_{1u}$ state which can in turn mix through spin-orbit coupling with a $^1E_{1u}$ state. If this is the case, then there is no reason why the fluorescence and phosphorescence should have the same vibrational structure.

References

1. G. W. Robinson, J. Mol. Spec. 6, 58 (1961).

2. H. Shull, J. Chem. Phys. 17, 295 (1949).

3. D. S. McClure, J. Chem. Phys. 17, 905 (1949).

4. G. Herzberg, <u>Molecular Spectra and Molecular Structure I</u> (D. Van Nostrand and Co., Inc., Princeton, N. J., 1950) p. 532.

5. Calculated using a 1.39 Å carbon-carbon bond length and a 1.01 Å carbon-hydrogen bond length.

6. H. P. Gush, W. F. J. Hare, E. J. Allen, and H. L. Welsh, Can J. Phys. 38, 176 (1960).

7. A. C. Albrecht, J. Chem. Phys. 33, 937 (1960).

II. Theory of Electronic Relaxation in the Solid Phase

A. A Brief Summary and Some New Thoughts

Robinson and Frosch have published two papers on the subject
of electronic relaxation in solid media (Parts IIB and IIC of this
thesis). This part contains a summary of the ideas in those papers
and also some new thoughts on the subject.

For many years it has been known that molecules which are
dissolved in a condensed medium do not normally exhibit resonance
fluorescence but rather relax by some radiationless process to lower
vibrational and electronic states before reemitting. Electronic relax-
ation can occur between states of the same multiplicity in which case
it is called internal conversion or between states of different multi-
plicity in which case it is called intersystem crossing. Normally
relaxation from all but the lowest excited state of a given multiplicity
is more efficient than radiation and consequently phosphorescence and
fluorescence normally originate in these lowest vibronic states.
Quantum yield measurements show, however, that even the lowest
states relax in part by a nonradiative mechanism. For instance
Lim (1) reports the quantum yield of C_6H_6 in EPA as 0.20 ± 0.02 for
both fluorescence and phosphorescence. This requires that 0.6 of the
excited molecules decay by a nonradiative mechanism. The possible
ways in which an electronically excited molecule can relax are de-
picted in Fig. 1.

More recently it has been observed that perdeuterated compounds
have longer phosphorescence lifetimes than perprotonated ones. See
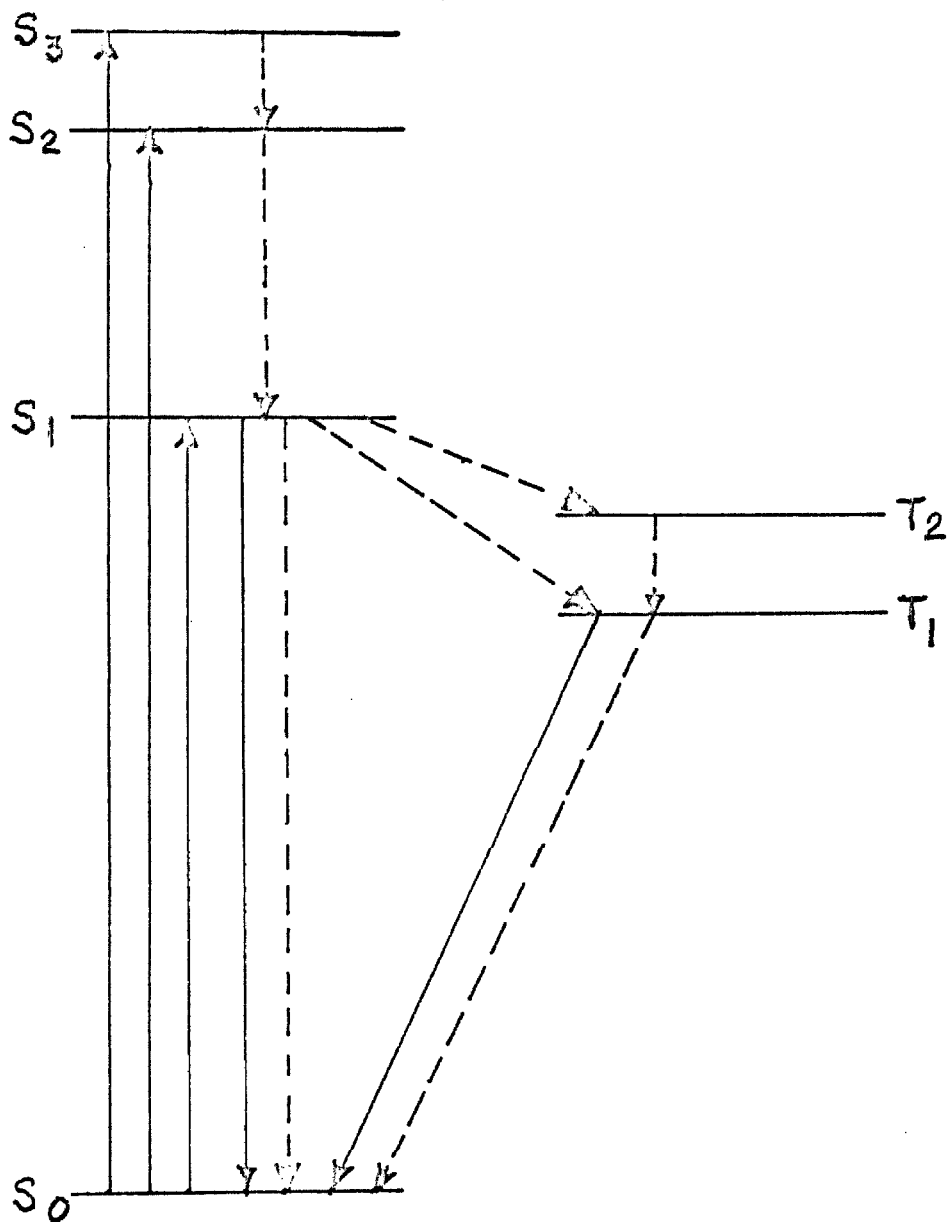
Fig. 1.   Common electronic excitation and relaxation paths in a typi-
cal molecule.   The solid lines represent radiative and the
dashed lines nonradiative processes.

Table I, section IF. de Groot and van der Waals (2) have shown that the radiative lifetimes of perdeutero and ordinary napthalene are the same. Therefore, the phosphorescence lifetime increase from two to seventeen seconds on deuteration is entirely due to an increase in the nonradiative lifetime. The theory of Robinson and Frosch explains the experimental observations (especially the deuterium effect) in a semiquantitative manner.

In principle any isolated system can be described by the time-dependent Schroedinger equation

$$H\Psi = -\frac{\hbar}{i}\frac{\partial\Psi}{\partial t} , \qquad (1)$$

where Ψ is a function of both time and space (including spin) coordinates while H is independent of time. The formal solution to the problem is

$$\Psi(t) = \exp(-iHt/\hbar)\Psi(o) , \qquad (2)$$

where $\exp(-iHt/\hbar)$ is the usual exponential operator. Equation (2) shows that, if $\Psi(o)$ is an eigenstate of H, all measurable properties of the system are time independent, i.e.

$$\Psi(t) = \exp(-iEt/\hbar)\Psi(o) . \qquad (3)$$

On the other hand, if $\Psi(o)$ is not an eigenstate of H, but rather a member of a degenerate group of states then the properties of the system will indeed be time dependent. Of course this hypothetical isolated system is not very meaningful; it does not allow for any measurement on the system because such a measurement would

require an external perturbation. Unfortunately Eq. (2) is not very useful for solving practical problems. A solution to any desired degree of accuracy within the confines of the uncertainty principle can, however, be obtained by the use of time-dependent perturbation theory (3).

Suppose we have a system whose Hamiltonian can be written as the sum of a large part H_0 and a small perturbation λV where $0 \leq \lambda \leq 1$, and V may or may not depend explicitly on the time. In addition let us assume that we know the eigenfunctions of H_0 and that they constitute a complete set. The wave function can be expanded in terms of this complete set.[*] Then

$$\Psi(t) \;=\; \sum_i C_i(t) \exp(-iE_i t/\hbar)\psi_i \;, \tag{4}$$

where the ψ_i's are independent of t. Substitution of Eq. (4) in Eq. (1), multiplication through by ψ_k^* and integration then yields

$$\dot{C}_k(t) \;=\; \frac{1}{i\hbar} \sum_i C_i(t) \exp[i(E_k - E_i)t/\hbar] < \psi_k |\lambda V| \psi_i > \tag{5}$$

This is as far as we can go without assuming an explicit functional dependence of V on the time. Suppose we expand the C_i's in a power series in λ

---

[*]In Eq. (4) it has been assumed that only discrete values of the energy are possible. If a continuum is also present, as is often the case, this omission can easily be corrected by adding an integral to the sum in Eq. (4).

$$C_i = C_i^{(0)} + \lambda C_i^{(1)} + \lambda^2 C_i^{(2)} + \dots , \tag{6}$$

and substitute Eq. (6) into Eq. (5), while assuming that $C_i(o) = \delta_{im}$ and that V does not depend explicitly on the time. We then obtain the $C_k(t)$'s by equating powers of λ and integrating. The first and second order constants are

$$C_k^{(1)}(t) = \{ 1 - \exp[i(E_k - E_m)t/\hbar] \} < \psi_k | \lambda V | \psi_m > \Big/ (E_k - E_m), \tag{7a}$$

and

$$C_k^{(2)}(t) = \sum_i < \psi_k | \lambda V | \psi_i > < \psi_i | \lambda V | \psi_m > \Big/ (E_i - E_m)$$

$$X \left\{ \frac{\exp[i(E_k - E_m)t/\hbar] - 1}{E_k - E_m} - \frac{\exp[i(E_k - E_i)t/\hbar] - 1}{E_k - E_i} \right\}. \tag{7b}$$

Higher order terms can, of course, be obtained, but this won't be necessary for our purposes. Now suppose that $C_k^{(1)}(t)$ is small for all k. Then we can neglect the first order contribution to $C_k(t)$ and concentrate on the second order contribution. The second term in Eq. (7b) arises from the mathematically convenient, but physically artificial assumption that V is turned on suddenly. Therefore the second term can be ignored. Setting $\lambda = 1$ we then obtain

$$|C_k(t)|^2 = 4 \left| \frac{\sum_i < \psi_k | V | \psi_i > < \psi_i | V | \psi_m >}{E_i - E_m} \right|^2$$

$$X \frac{\sin^2[(E_k - E_m)t/2\hbar]}{(E_k - E_m)^2} \tag{8}$$

Now let us examine the application of Eq. (8) to electronic relaxation. The system consists of an impurity molecule, the solute, embedded in a solid lattice, the solvent. It is assumed that the solution is sufficiently dilute that interactions between solute molecules are unimportant. The system wave function can be taken as the product of an electronic part (including any solvent effects on the electronic wave function), a solute vibrational part, and a phonon part. That such a product wave function is approximately valid is evident from the fact that the spectrum of a solute such as benzene or napthalene is only weakly perturbed (except of course for the lack of rotation) in a van der Waals solid such as a rare gas or EPA glass (4, 5, 6). Only few if any phonon frequencies stand out strongly in the observed spectra. The separation of electronic and vibrational parts is, of course, just the first term in a Taylor's expansion of the Born–Oppenheimer wave function about the equilibrium position. We can now write our wave function as $\psi_a(x)\phi_{a\ell}(R)\chi_{a\alpha}(Q)$ where $\psi_a(x)$ is the electronic wave function of the $\underline{a}$th electronic state, $\phi_{a\ell}(R)$ is a product function over all the normal modes in the ath state, and $\chi_{a\alpha}(Q)$ is a product function over all the phonon modes. Where it is necessary to designate the normal modes explicitly, $\phi_{a\ell}(R)$ will be written $\phi_{a\ell}(R) = \Pi\phi_{an_\ell}(R_\ell)$ where the product is taken over all normal modes ℓ and n_ℓ is the occupation number of the $\underline{\ell}$th normal mode. A similar product function will be used for the phonon modes.

The basis set has been chosen so that

$$H_o\psi_a\phi_\ell\chi_\alpha = (E_a + E_\ell + E_\alpha)\psi_a\phi_\ell\chi_\alpha \ . \tag{9}$$

The assumed perturbation is the sum of an electronic part $H_1(x)$, and a part which provides for the interaction between phonon and molecular vibrational motion, $H_2(Q, R)$. H_1, for instance, might be spin-orbit mixing in the case of intersystem crossing or electron-electron repulsion terms in the case of internal conversion. H_1 can also be a vibronic interaction, an electronic interaction introduced by the lattice, or some combination of these terms. Such lattice terms are responsible for the heavy atom effect on electronic relaxation discussed in section IIC of this thesis. H_2 is the difference in the vibrational Hamiltonian of the isolated lattice and molecular systems and the combined system. Since H_1, in general, only mixes different electronic states of the solute, while H_2 only mixes different phonon and vibrational states within the same electronic state, the problem must be solved in the second order perturbation approximation where $V = H_1 + H_2$. From Eq. (8)

$$|C_{a\ell\alpha}(t)|^2 = 4 \left| \sum_{b, m, \beta} < \psi_a \phi_{a\ell} X_{a\alpha} |H_1 + H_2| \psi_b \phi_{bm} X_{b\beta} > \right.$$

$$\left. X \; \frac{< \psi_b \phi_{bm} X_{b\beta} |H_1 + H_2| \psi_c \phi_{cn} X_{c\gamma} >}{E_b + E_m + E_\beta - E_c - E_n - E_\gamma} \right|^2$$

$$X \; \frac{\sin^2[(E_a + E_\ell + E_\alpha - E_c - E_n - E_\gamma)t/2\hbar]}{(E_a + E_\ell + E_\alpha - E_c - E_n - E_\gamma)^2} \; , \tag{10}$$

where $|C_{cn\gamma}(0)|^2 = 1$. Since it has been assumed that H_1 only mixes electronic states and H_2 allows for interconversion of molecular

vibrational and phonon energy, Eq. (10) can be rewritten[*]

$$|C_{a\ell\alpha}(t)|^2 = 4\beta_{e\ell}^2 \left| \sum_{m,\beta} < \phi_{a\ell}\chi_{a\alpha} |H_2| \phi_{am}\chi_{a\beta} > \right.$$

$$\times \left. \frac{<\phi_{an}|\phi_{cn}><\chi_{a\beta}|\chi_{c\gamma}>}{E_a+E_m+E_\beta-E_c-E_n-E_\gamma} \right|^2 \frac{\sin^2[(E_a+E_\ell+E_\alpha-E_c-E_n-E_\gamma)t/2\hbar]}{(E_a+E_\ell+E_\alpha-E_c-E_n-E_\gamma)^2} , \quad (11)$$

where $\beta_{e\ell}^2 = |<\psi_a|H_1|\psi_c>|^2$. It has been assumed in Eq. (11) that there is only one important final electronic state in the relaxation process. The quantities $<\phi_{am}|\phi_{cn}>$ and $<\chi_{a\beta}|\chi_{c\gamma}>$ are vibrational overlap integrals for solute and phonons, respectively.

---

[*]Actually another term should be added to Eq. (11). In Eq. (11) electronic interaction first takes place between initial and final electronic states, and then phonon coupling takes place in the final electronic state. The reverse process is also possible. Phonon coupling can occur first in the initial electronic state and then electronic state interaction can occur. Since the phonon coupling in the initial electronic state will be different than the phonon coupling in the final electronic state, a slightly different perturbation Hamiltonian must be used, call it $H_1 + H_2'$. The missing term in Eq. (11) is then

$$|C_{a\ell\alpha}(t)|^2 = 4\beta_{e\ell}^2 \left| \sum_{m,\beta} < \phi_{a\ell} | \phi_{cm} > < \chi_{a\alpha} | \chi_{c\beta} > \right.$$

$$\times \left. \frac{< \phi_{cm}\chi_{c\beta} |H_2'| \phi_{cn}\chi_{c\gamma} >}{E_m + E_\beta - E_n - E_\gamma} \right|^2$$

$$\times \frac{\sin^2[(E_a + E_\ell + E_\alpha - E_c - E_n - E_\gamma)t/2\hbar]}{(E_a + E_\ell + E_\alpha - E_c - E_n - E_\gamma)^2} .$$

Since the above equation has the same form as Eq. (11), it will not be carried along in the body of the paper.

We must now consider the specific form of H_2. It is shown in appendix A that if the solvent and solute can each be described by a quadratic potential, and if their interaction potential is quadratic, then H_2 will have the form

$$H_2 = \sum_{j, k, \ell}{}' \xi_{jk\ell} R_j Q_k e^{-i\vec{k} \cdot \vec{\ell}} , \qquad (12)$$

where R_j is the jth molecular normal coordinate and Q_k is the kth phonon normal coordinate. The coefficient ξ is the magnitude of the interaction between the molecular and phonon vibrations. In the exponential of Eq. (12), $\vec{k}$ is the wave vector of the phonon labeled k, and ℓ is the vector position of the ℓth unit cell. The prime on the summation indicates that those lattice sites which are occupied by the solute are not included in the summation. The product $\vec{k} \cdot \vec{\ell}$ can take on values from $-\pi$ to $+\pi$ and, in general, for every positive value of k there corresponds a negative value. Also $Q_{-k} = Q_k^*$. If we take Q_k to be real, Eq. (12) then reduces to

$$H_2 = \sum_{j, k, \ell}{}' \eta_{jk\ell} R_j Q_k \cos \vec{k} \cdot \vec{\ell} , \qquad (13)$$

where the summation is over positive $|\vec{k}|$ and $\eta_{jk\ell} = 2 \xi_{jk\ell}$. Use of a quadratic interaction like that in Eq. (12) excludes the possibility (to the second order of approximation) of coupling involving more than one vibrational mode and/or one phonon mode.

Since little is known about the detailed coupling of molecular vibrational states with phonon states, i. e. about the magnitude of the coupling coefficient η in Eq. (13), and since, in general, there will be a large number of different coupling coefficients, H_2 as expressed in Eq. (13) is not very useful for comparison with experiment. Fortunately, however, a number of simplifying assumptions can be made on the basis of physical arguments. Some of these will be made clear in the next few paragraphs.

It is known, at least in the case of napthalene, that radiationless decay is relatively insensitive to the details of the lattice coupling. For instance napthalene at 77°K has a measured lifetime of 2.1 sec in durene (7) and 2.6 sec in EPA (5). Wright, Frosch, and Robinson (6) have obtained 1.9 sec and 2.3 sec, respectively, for the lifetime of napthalene in Ar and H_2 at liquid helium temperatures. The somewhat low result for napthalene in Ar may be due to a heavy atom effect.

Remembering that the detailed structure of the lattice does not appreciably change the nonradiative lifetime, we can now considerably simplify Eq. (13). The first point is that only interactions between nearby lattice sites will be important. This is equivalent to saying that $\xi_{jk\ell} \approx 0$ unless $\vec{\ell}$ is a nearby lattice point. We can take the solute molecule as origin of the vector $\vec{\ell}$. Then in general $|\vec{\ell}|$ will be small. H_2 will be a maximum for $|\vec{k}| = 0$ and for $\vec{k} \cdot \vec{\ell} \approx \pi$. The limit $|\vec{k}| = 0$ simply refers to a translation of the system as a whole and is not of interest in the problem of electronic relaxation. The other limit $\vec{k} \cdot \vec{\ell} \approx \pi$ is that for which $\lambda \approx \dfrac{1}{2|\vec{\ell}|}$. That is H_2 is a maximum when the motion of the solute and its nearest neighbors is 180° out of phase.

Physically this is exactly what would have been predicted. We can make use of the fact that only phonons with a value of $|\vec{k}|$ near $|\vec{k}|_{max}$ are important by assuming an average phonon frequency and incorporating it into H_2 in place of the sum over all phonon frequencies. The result is

$$H_2 = \sum_j \eta_j R_j Q , \qquad (14)$$

where Q is now an average phonon normal coordinate with associated energy $h\nu$. The coefficient η_j is a measure of the average mixing of the molecular and phonon systems. By substitution of Eq. (14) into Eq. (11) we then obtain

$$|C_{a\ell\alpha}(t)|^2 = 4\beta_{e\ell}^2 | \sum_{m,\beta,\nu} \eta_\nu <\phi_{a\ell}|R_\nu|\phi_{am}><\chi_{a\alpha}|Q|\chi_{a\beta}>$$

$$X <\phi_{am}|\phi_{cn}><\chi_{a\beta}|\chi_{c\gamma}>/(E_a + E_m + E_\beta - E_c - E_n - E_\gamma)|^2$$

$$X \frac{\sin^2[(E_a + E_\ell + E_\alpha - E_c - E_n - E_\gamma)t/2\hbar]}{(E_a + E_\ell + E_\alpha - E_c - E_n - E_\gamma)^2} . \qquad (15)$$

Since our basis set for the phonons is orthonormal, we can set $\beta = \gamma$ in the summation in Eq. (15) and obtain

$$|C_{a\ell\alpha}(t)|^2 = 4\beta_{e\ell}^2 |<\chi_\alpha|Q|\chi_\gamma>|^2$$

$$X \left| \frac{\sum\limits_{m,v} \eta_v < \phi_{a\ell} | R_v | \phi_{am} > < \phi_{am} | \phi_{cn} >}{E_a + E_m - E_c - E_n} \right|^2$$

$$X \frac{\sin^2[(E_a + E_\ell + E_\alpha - E_c - E_n - E_\gamma)t/2\hbar]}{(E_a + E_\ell + E_\alpha - E_c - E_n - E_\gamma)^2} \quad . \qquad (16)$$

The matrix element $< \chi_\alpha | Q | \chi_\gamma >$ is zero unless $\alpha = \gamma \pm 1$. For $\alpha = \gamma \pm 1$ we obtain for the matrix elements

$$< \chi_{\gamma+1} | Q | \chi_\gamma > = \frac{1}{2\pi} \left[\frac{h(\gamma+1)}{2\nu} \right]^{\frac{1}{2}} , \qquad (17a)$$

and

$$< \chi_{\gamma-1} | Q | \chi_\gamma > = \frac{1}{2\pi} \left[\frac{h\gamma}{2\nu} \right]^{\frac{1}{2}} , \qquad (17b)$$

where ν is the average phonon frequency and γ is the quantum number of the phonon state. Equation (17a) corresponds to the absorption of a phonon by the lattice and Eq. (17b) to the emission of a phonon.

One can now consider the temperature effect on the transition. It will be assumed that the lattice constitutes an infinite heat sink which is always in thermal equilibrium. Then since phonons obey Bose-Einstein statistics (8)

$$\gamma = \{\exp(h\nu/kT) - 1\}^{-1} \qquad (18)$$

Combining Eqs. (16), (17), and (18) we get

$$| C_{a\ell \gamma+1}(t) |^2 = \frac{h\beta_{e\ell}^2}{2\pi^2\nu} \{1 - \exp(-h\nu/kT)\}^{-1}$$

$$X \quad \left| \frac{\sum_{m,v} \eta_v < \phi_{a\ell} | R_v | \phi_{am} > < \phi_{am} | \phi_{cn} >}{E_a + E_m - E_c - E_n} \right|^2$$

$$X \quad \frac{\sin^2[(E_a + E_\ell - E_c - E_n + h\nu)t/2\hbar]}{(E_a + E_\ell - E_c - E_n + h\nu)^2} \quad , \qquad (19a)$$

and

$$\left| C_{a\ell\,\gamma-1}(t) \right|^2 = \frac{h\beta_{e\ell}^2}{2\pi^2\nu} \{\exp(h\nu/kT) - 1\}^{-1}$$

$$X \quad \left| \frac{\sum_{m,v} \eta_v < \phi_{a\ell} | R_v | \phi_{am} > < \phi_{am} | \phi_{cn} >}{E_a + E_m - E_c - E_n} \right|^2$$

$$X \quad \frac{\sin^2[(E_a + E_\ell - E_c - E_n - h\nu)t/2\hbar]}{(E_a + E_\ell - E_c - E_n - h\nu)^2} \qquad (19b)$$

Of course the result we want is not the build-up of any particular final state but the decay of the initial state. This can be obtained by simply subtracting the final state build-up from the initial state population which is taken as unity. The probability W that the initial state is no longer excited at time t is

$$W = 1 - \frac{h\beta_{e\ell}^2}{2\pi^2\nu} \{\exp(h\nu/kT) - 1\}^{-1} \sum_\ell$$

$$\left| \frac{\sum_{m,v} \eta_v < \phi_{al} \left| R_v \right| \phi_{am} > < \phi_{am} \left| \phi_{cn} >}{E_a + E_m - E_c - E_n} \right|^2$$

$$X \left\{ \frac{\sin^2[(E_a + E_l - E_c - E_n + h\nu)t/2\hbar]}{(E_a + E_l - E_c - E_n + h\nu)^2} \exp(h\nu/kT) \right.$$

$$\left. + \frac{\sin^2[(E_a + E_l - E_c - E_n - h\nu)t/2\hbar]}{(E_a + E_l - E_c - E_n - h\nu)^2} \right\} . \tag{20}$$

This is the master equation. It has been assumed that only one final electronic state is important. If more than one state is important, the result can be summed over all final electronic states. We can further simplify Eq. (20) by observing that

$$< \phi_{al} \left| R_v \right| \phi_{am} > = < \phi_{an_l} \left| R_v \right| \psi_{an_m} > \tag{21a}$$

where n_l and n_m are the quantum numbers of the $\underline{v\text{th}}$ normal mode. For $n_m = n_l + 1$

$$< \phi_{al} \left| R_v \right| \phi_{am} > = \frac{1}{2\pi} \left[\frac{h(n_v + 1)}{2\nu_v} \right]^{\frac{1}{2}} , \tag{21b}$$

and

$$< \phi_{al} \left| R_v \right| \phi_{am} > = \frac{1}{2\pi} \left(\frac{hn_v}{2\nu_v} \right)^{\frac{1}{2}} , \tag{21c}$$

for $n_m = n_l - 1$. Substituting in Eq. (20), we then obtain

$$W = 1 - \frac{h\beta_{e\ell}^2}{2\pi^2\nu} \{\exp(h\nu/kT) - 1\}^{-1} \sum_{\ell}$$

$$\left| \sum_{v} \left\{ \frac{\eta_v \frac{1}{2\pi} \left[\frac{h(n_v + 1)}{2\nu_v}\right]^{\frac{1}{2}} < \phi_{a\ell+1} | \phi_{cn} >}{E_c + E_n - E_a - E_\ell - h\nu_v} \right. \right.$$

$$\left. \left. + \frac{\eta_v \frac{1}{2\pi} \left(\frac{hn_v}{2\nu_v}\right) < \phi_{a\ell-1} | \phi_{cn} >}{E_c + E_n - E_a - E_\ell + h\nu_v} \right\} \right|^2$$

$$X \left\{ \exp(h\nu/kT) \frac{\sin^2[(E_a + E_\ell - E_c - E_n + h\nu)t/2\hbar]}{(E_a + E_\ell - E_c - E_n + h\nu)^2} \right.$$

$$\left. + \frac{\sin^2[(E_a + E_\ell - E_c - E_n - h\nu)t/2\hbar]}{(E_a + E_\ell - E_c - E_n - h\nu)^2} \right\} \tag{22}$$

For long t

$$\frac{\sin^2 \alpha t}{\pi t \, \alpha^2} = \delta(\alpha) , \tag{23}$$

where $\delta(\alpha)$ is the Dirac delta function. By use of Eq. (23) and re-membering that $\delta(cx) = \frac{1}{|c|} \delta(x)$ we obtain from Eq. (22)

$$W = 1 - \frac{\beta_{e\ell}^2 t}{2\nu} \{\exp(h\nu/kT) - 1\}^{-1} \sum_{\ell}$$

$$\left| \sum_{v} \left\{ \frac{\eta_v \frac{1}{2\pi} \left[\frac{h(n_v + 1)}{2\nu_v} \right]^{\frac{1}{2}} < \phi_{a\ell + 1} | \phi_{cn} >}{E_c + E_n - E_a - E_\ell - h\nu_v} \right. \right.$$

$$\left. \left. + \frac{\eta_v \frac{1}{2\pi} \left(\frac{hn_v}{2\nu_v} \right)^{\frac{1}{2}} < \phi_{a\ell - 1} | \phi_{cn} >}{E_c + E_n - E_a - E_\ell + h\nu_v} \right\} \right|^2$$

$$X \; \{ \exp(h\nu/kT)\delta(E_a + E_\ell - E_c - E_n + h\nu)$$

$$+ \; \delta(E_a + E_\ell - E_c - E_n - h\nu) \} \quad . \tag{24}$$

We note from Eq. (24) that the probability that relaxation has occurred at the end of time t is directly proportional to t, as expected. We can take the time derivative of W to obtain the rate of decay. Differentiating and making use of the properties of the delta function we get

$$\frac{dw}{dt} = \frac{-\beta_{e\ell}^2}{2\nu} \{ \exp h\nu/kT - 1 \}^{-1} \int_{-\infty}^{\infty} \left\{ \left| \sum_{v} \frac{\eta_v}{2\pi} \left(\frac{h}{2\nu_v} \right)^{\frac{1}{2}} \right. \right.$$

$$X \left. \left[\frac{(n_v + 1)^{\frac{1}{2}} < \phi_{a\ell + 1} | \phi_{cn} >}{h\nu - h\nu_v} + \frac{n_v^{\frac{1}{2}} < \phi_{a\ell - 1} | \phi_{cn} >}{h\nu + h\nu_v} \right] \right|^2$$

$$X \; \exp(h\nu/kT)\delta(E_a + E_\ell - E_c - E_n + h\nu)$$

$$+ \left| \sum_{v} \frac{\eta_v}{2\pi} \left(\frac{h}{2\nu_v} \right)^{\frac{1}{2}} \left[\frac{(n_v + 1)^{\frac{1}{2}} < \phi_{a\ell + 1} | \phi_{cn} >}{h\nu + h\nu_v} \right. \right.$$

$$+ \left.\left.\frac{n_v^{\frac{1}{2}} < \phi_{a\ell-1} | \phi_{cn} >}{h\nu - h\nu_v}\right]\right|^2 \delta(E_a + E_\ell - E_c - E_n - h\nu)\right\} dE_\ell. \quad (25)$$

Equation (25) cannot be further simplified without considering a specific molecule and solvent.[*] Even then we would have to guess at

---

values of the effective phonon frequency $h\nu$ and the solute-solvent coupling η_v. However, a number of important inferences can be drawn from Eq. (25). In the first place the rate of electronic relaxation is proportional to the square of the mixing of initial and final electronic states. Second because of the $h\nu - h\nu_v$ and $h\nu + h\nu_v$ in the denominators, low frequency molecular vibrations will be more efficient in transferring energy to the lattice than high frequency ones. Third vibrational overlap is an important factor in determining the rate of relaxation. Large vibrational overlap integrals for big energy gaps require a major difference of geometry and force constants in initial and final states. As a rule the greater the difference in the vibrational quantum numbers in initial and final states, the smaller the overlap integrals will be. Therefore large electronic energy gaps lead to slow relaxation.

Equation (25) indicates that there will be a small temperature effect on the rate of relaxation. In discussing the effect of temperature one must consider not only the initial phonon state but also the initial vibronic state. Since electronic relaxation is usually slow compared with vibrational relaxation, one is justified in assuming a Boltzmann population of vibrational levels in the initial electronic state. This has not been done in Eq. (25), although it could easily be done formally by summing over all initial states weighted by an appropriate Boltzmann factor. Rather it has been assumed for the sake of simplicity that the initial state is the lowest vibrational state of the initial electronic state. Since typical vibrational overlap integrals do not appear to be very sensitive to the initial vibrational state, and

since molecular vibrational energies are usually large compared to kT at room temperature, the omission is probably not important at room temperature and below. As an example kT at room temperature is 210 cm^{-1}, so for a typical minimum vibrational frequency of 300 cm^{-1}, the population of the v = 1 state is only 0.2 that of the v = 0 state. This, of course, is an extreme case. For a typical aromatic C—C stretching mode of 1000 cm^{-1} the population of the v = 1 state is only 0.009 that of the v = 0 level. One other factor related to temperature has been neglected in Eq. (25); namely, the value of the molecule—phonon interaction η_v will be temperature dependent due to lattice expansion. In spite of the above weaknesses some idea of the importance of temperature can be obtained from the theory. In Fig. 1 $e^x/(e^x - 1)$ and $1/(e^x - 1)$ have been plotted. Of course x = hν/kT. From Fig. 1 it can be seen that the rate of decay should be constant at low temperatures and then start to increase approximately linearly with temperature. If the two squared terms inside the integral of Eq. (25) are of comparable magnitude, which is a reasonable assumption, then the decay rate should go as [exp(hν/kT) + 1]/[exp(hν/kT) − 1] (upper curve in Fig. 1). A reasonable value for hν would be about 100 cm^{-1}. If we take this value, then the radiationless decay rate should be constant with temperature below about 45°K and then increase slowly until at 300°K the radiationless decay rate is 4.3 times as fast as at 0°K.

There is not too much data in the literature on the dependence of phosphorescence lifetimes on temperature. Hadley, Rast, and Keller (9) studied the lifetime of napthalene and napthalene–d$_8$ in

Plot of $e^x/(e^x - 1)$, $1/(e^x - 1)$, and $(e^x + 1)/(e^x - 1)$
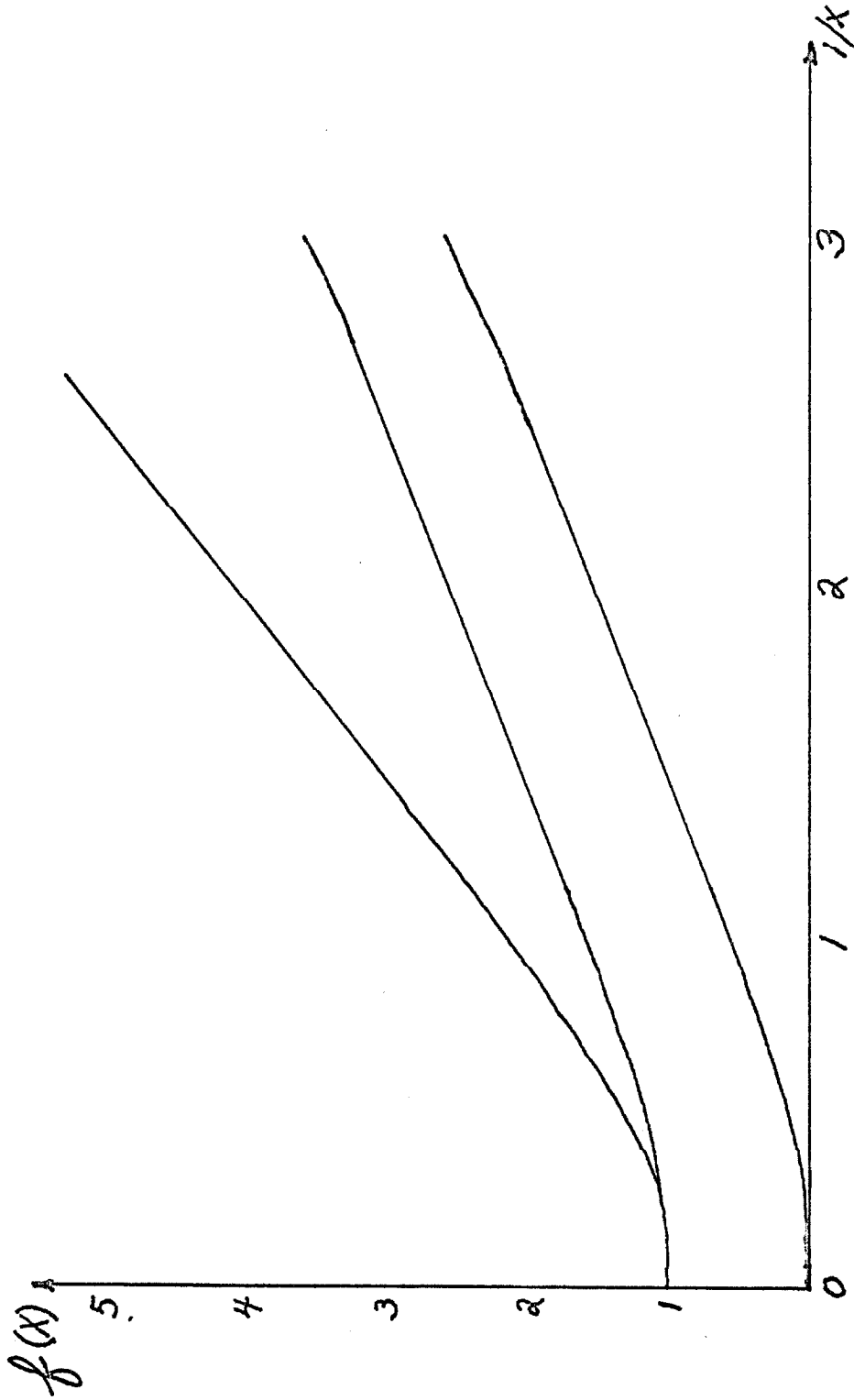
Fig. 1.

durene between 77°K and 325°K. They observed a sharp decrease in the lifetime of both the ordinary and perdeuterated molecules above 210°K in 0.02 mole fraction solutions. Unfortunately it is not possible to separate the unimolecular decay process in their experiments from a possible bimolecular triplet-triplet annihilation process which can take place through virtual states of the durene.

Eisenthal and Murashirge (10) have measured the lifetime of napthalene in lucite at 77°K and room temperature. They obtain 2.2 sec and 1.2 sec, respectively, at the two temperatures. Since the lifetimes are exponential and independent of concentration at low concentrations they should be a measure of the unimolecular process only. If it is assumed that 2.2 sec is an upper limit to the lifetime and that room temperature is 300°K, we can estimate $h\nu$ from Fig. 1. The result is $h\nu = 260$ cm^{-1} which seems quite high. However, it does give a correct order of magnitude.

A short comparison of electronic relaxation theory as presented in this section with the theory of Robinson and Frosch as presented in the next two sections is in order here. The primary difference is in the treatment of H_2. Here a specific form for H_2 has been assumed and has been used to treat the problem with second order perturbation theory. The treatment results in a moderate dependence of the lifetime on temperature. In the earlier Robinson-Frosch treatment a large number of degenerate final states was assumed. Only one of these final states was coupled directly to the initial state. The coupling among the final states was given by a matrix element α which was assumed to be independent of temperature

and the same for each pair of final states, while the coupling of the initial and directly coupled final state was given by a matrix element β which corresponds to H_1. It was assumed that $\beta \ll \alpha$ and the matrix which described the coupling among final states was diagonalized to give a final state band each member of which is coupled to the initial state with magnitude approximately equal to $\beta/\sqrt{N}$ where N is the total number of final states. Summation over each state in the band then gives $w_n(t) = (2\beta_n^2/\alpha h) \sec^{-1}$ where $w_n(t)/t$ is the rate of decay to the nth directly coupled final state. The matrix element β_n^2 is the product of an electronic part $\beta_{e\ell}^2$ and a vibrational overlap factor $\left| < \phi_n'' | \phi_o' > \right|^2$. The $w_n(t)/t$ must then be summed over all directly coupled final states in order to obtain the total rate of electronic relaxation. The theory is useful because of its simplicity and because it emphasizes two of the most important factors in determining radiationless transition rates, namely the electronic coupling between initial and final states $\beta_{e\ell}^2$ and the Franck-Condon factors $\left| < \phi_n'' | \phi_o' > \right|^2$. The parameter α is useful because it can be related to vibrational relaxation times and therefore linewidths through the uncertainty principle relationship $\alpha \tau_{vib} \geq \hbar$. This leads to $w_n(t)/t = 2\beta_{e\ell}^2 \tau_{vib} \left| < \phi_u'' | \phi_o' > \right|^2/\hbar^2$. The fact that slow vibrational relaxation seems to lead to fast electronic relaxation is at first glance quite surprising. The reason is that for large α (small τ_{vib}) the final state band becomes very broad and consequently the number of states in near resonance becomes small. Actually the dependence of the overall rate on τ_{vib} will be largely lost in the summation over directly coupled states, since the number of important directly coupled

states will increase in direct proportion to α.

Gouterman's theory (11) uses a first order perturbation technique. He assumes a perturbation Hamiltonian of the form $H'' = \sum_{\alpha} \eta_{\alpha} x_{\alpha} F_x \cos{(\omega t + \vec{k} \cdot \vec{r}_{\alpha})}$ where the α's in the summation refer to the αth particle in the solute molecule, r_{α} is the position coordinate of the αth particle, η_{α} is the coupling to the phonon field, F_x is the force exerted on the solute by the phonon field, ω is the phonon frequency, and $\vec{k}$ is the phonon wave vector. From H'' he obtains for the radiationless transition rate

$$W_{n \rightarrow m}(t) = \frac{4\omega^3 \left| \vec{\mu}_{mn} \right|^2}{3 \hbar c_s^3} \left[1 - \exp(\hbar\omega/kT) \right]^{-1}$$

where $\left| \vec{\mu}_{mm} \right|^2$ is the mixing between initial and final states and c_s is the velocity of sound in the solvent. In order to take account of the fact that a solid is not a continuous medium, Gouterman sets a maximum limit on ω such that $\hbar\omega_{max} = k\theta_D$, where θ_D is the Debye θ for the solvent. Unfortunately Gouterman does not try to sum over all possible final states. Also his Hamiltonian does not mix states of different multiplicity so that his theory cannot be used as it stands to explain intersystem crossing.

Perhaps comparison with another type of relaxation theory would be useful. Such a theory is the theory of nuclear spin relaxation in liquids and gases (12). Usually in discussing spin relaxation, use is made of the density matrix whose elements are defined as

$$\rho_{mn} = (m|\rho|n) \equiv \overline{a_m a_n^*} \tag{26}$$

where the bar over $a_m a_n^*$ designates the ensemble average and the a's are the constants in the expansion in Eq. (27). The operator ρ is both linear and Hermitian. Expanding $\Psi(t)$ in terms of a complete set

$$\Psi(t) = \sum_n a_n(t)\psi_n \tag{27}$$

and substituting in the time-dependent Schroedinger equation we obtain

$$\dot{a}_k(t) = \frac{1}{\hbar i} \sum_n a_n(t) <k|H|n> . \tag{28}$$

Equation (28) is identical to Eq. (5) except that here the $\exp(iEt/h)$ terms have been included in the constants. It is easy to show with the use of Eq. (28) that

$$\frac{d\rho}{dt} = \frac{i}{\hbar} [\rho, H] . \tag{29}$$

Now suppose that H can be expressed as the sum of a large time-independent part H whose eigenfunctions are the ψ_n's in Eq. (27) and a much smaller perturbation H_1. If H_1 were zero, then the solution to Eq. (29) would be

$$\rho(t) = \exp(-iH_0 t/\hbar)\rho(o)\exp(iH_0 t/\hbar) . \tag{30}$$

We can now define a quantity $\rho^*(t)$ such that

$$\rho(t) = \exp(-iH_0 t/\hbar)\rho^*(t)\exp(iH_0 t/\hbar) , \tag{31}$$

and substitute Eq. (31) in Eq. (29) obtaining

$$- \frac{i}{\hbar} [H_0, \rho] + \exp(-iH_0 t/\hbar) \frac{d\rho^*}{dt} \exp(iH_0 t/\hbar)$$

$$= \frac{i}{\hbar} [\rho, H_0 + H_1] \quad . \tag{32}$$

Rearranging and defining

$$H_1^* \equiv \exp(iH_0 t/\hbar) H_1 \exp(-iH_0 t/\hbar) \quad , \tag{33}$$

we then obtain

$$\frac{d\rho^*}{dt} = \frac{i}{\hbar} [\rho^*, H_1^*(t)] \quad . \tag{34}$$

One can easily show that the relationship between ρ and ρ^* is closely connected to the two alternative methods of expanding Ψ used in Eqs. (4) and (27), namely

$$a_n(t) = c_n(t) \exp(-iE_n t/\hbar) \quad . \tag{35}$$

Similarly

$$(m | \rho^* | n) = (m | \exp(iH_0 t/\hbar) \rho(t) \exp(-iH_0 t/\hbar) | n)$$

$$= \exp[i(E_m - E_n) t/\hbar] (m | \rho | n) \quad . \tag{36}$$

Thus we find that

$$\rho_{mn}^* = \overline{c_m c_n^*} \quad . \tag{37}$$

Equation (34) has the solution

$$\rho^*(t) = \rho^*(0) + \frac{i}{\hbar} \int_0^t [\rho^*(t'), H^*(t')] \, dt' \ . \tag{38}$$

Since we do not know $\rho^*(t')$ Eq. (38) cannot be integrated directly, but it can be solved by an iterative procedure equivalent to the expansion of the c's of Eq. (6) in a power series in λ. Using two iterations we get

$$\rho^*(t) = \rho^*(0) + \frac{i}{\hbar} \int_0^t \left[(\rho^*(0) + \frac{i}{\hbar} \int_0^{t'} [\rho^*(0), H_I^*(t'')] \, dt''), \right.$$

$$\left. H_I^*(t') \right] dt' \ . \tag{39}$$

After collecting terms we obtain

$$\rho^*(t) = \rho^*(0) + \frac{i}{\hbar} \int_0^t [\rho^*(0), H_I^*(t')] \, dt'$$

$$+ \left(\frac{i}{\hbar} \right)^2 \int_0^t \left[\int_0^{t'} [\rho^*(0), H_I^*(t'')] \, dt'', H_I^*(t') \right] dt' \ . \tag{40}$$

Suppose that at $t = 0$ the system is in the state labeled m. Then

$$(k|\rho^*(0)|n) = (k|\rho(0)|n) = \delta_{km}\delta_{nm} \tag{41}$$

Suppose we are interested in the population of some state k (not the initial state) at time t. Then

$$\rho_{kk}^{*}(t) \; = \; (k|\rho^{*}(0)|k) \; + \; \frac{i}{\hbar} \int_{0}^{t} \left[\sum_{n} (k|\rho^{*}(0)|n)(n|H_{1}^{*}(t')|k) \right.$$

$$\left. - \; (k|H_{1}^{*}(t')|n)(n|\rho^{*}(0)|k) \right] dt'$$

$$+ \left(\frac{i}{\hbar}\right)^{2} \int_{0}^{t} \sum_{n,\,p} \left\{ \int_{0}^{t'} \left[[(k|\rho^{*}(0)|n)(n|H_{1}^{*}(t'')|p) \right.\right.$$

$$\left. - \; (k|H_{1}^{*}(t'')|n)(n|\rho^{*}(0)|p) \right] dt'' \, (p|H_{1}^{*}(t')|k)$$

$$- \; (k|H_{1}^{*}(t')|n) \int^{t'} [(n|\rho^{*}(0)|p)(p|H_{1}^{*}(t'')|)$$

$$\left. - \; (n|H_{1}^{*}(t'')|p)(p|\rho^{*}(0)|k)] dt'' \right\} dt' \quad . \tag{42a}$$

Because of Eq. (41), Eq. (42a) reduces to

$$\rho_{kk}^{*}(t) \; = \; \left(\frac{1}{\hbar}\right)^{2} \int_{0}^{t} \left\{ \int_{0}^{t'} (k|H_{1}^{*}(t'')|m) dt'' \, (m|H_{1}^{*}(t')|k) \right.$$

$$\left. + \; (k|H_{1}^{*}(t')|m) \int_{0}^{t'} (m|H_{1}^{*}(t'')|k) dt'' \right\} dt' \quad . \tag{42b}$$

If H_{1} does not depend explicitly on the time then Eq. (42) reduces to

$$\rho^*_{kk}(t) = \rho_{kk}(t) = \frac{|(k|H_1|m)|^2}{\hbar^2} \int_0^t \left\{ \int_0^{t'} e^{i(E_k - E_m)t''/\hbar} dt'' \right.$$

$$\left. X\ e^{i(E_m - E_k)t'/\hbar} + e^{i(E_k - E_m)t'/\hbar} \int_0^{t'} e^{i(E_m - E_k)t''/\hbar} dt'' \right\} dt' \quad (43)$$

After performing the integration we get

$$\rho_{kk}(t) = 4|(k|H_1|m)|^2 \frac{\sin^2[(E_k - E_m)t/2\hbar]}{(E_k - E_m)^2} \quad (44)$$

This is identical to the familiar result obtained with first order time-dependent perturbation theory thus demonstrating that the perturbation method and the density matrix method are the same. Since we are interested in a decay rate, it is customary to work with the time derivative of Eq. (42b).

$$\frac{d\rho^*_{kk}(t)}{dt} = \frac{1}{\hbar^2} \int_0^t [(k|H_1^*(t')|m)(m|H_1^*(t)|k)$$

$$+ (k|H_1^*(t)|m)(m|H_1^*(t')|k)] dt' \quad . \quad (45a)$$

Again Eq. (45a) is identical to the perturbation result. We can now replace ρ^*_{kk} by ρ_{kk} and $H_1^*(t)$ by its value in terms of $H_1(t)$. We also use the relations $E_m = \hbar\omega_m$, $E_k = \hbar\omega_k$, and $E_k - E_m = \hbar\omega_{km}$. The result is

$$\frac{d\rho_{kk}}{dt} = \frac{1}{\hbar^2} \int_0^t [(k|H_1(t')|m)(m|H_1(t)|k)e^{i\omega_{km}(t'-t)}$$

$$+ (k|H_1(t)|m)(m|H_1(t')|k)e^{i\omega_{km}(t-t')}] dt' . \qquad (45b)$$

At this point the treatment of spin relaxation in fluids deviates significantly from the treatment of electronic relaxation in solids. The perturbation $H_1(t)$ causes a mixing of the nuclear spin states which depends on the motions of the surrounding medium. In the solid the perturbation can be treated as independent of the time since the local environment of a lattice point is constant in time. In a liquid or gas it is, of course, possible in principle to consider a time-independent Hamiltonian by simply writing down all the interactions between particles. However, since the local environment is constantly changing in a fluid medium, it is possible to add the effects of the medium together to give a field at the nucleus which varies randomly with time. Thus the surrounding medium simply acts as a randomly fluctuating thermal bath which can absorb energy from the system of interest or emit energy to the system.

It is now necessary to discuss the random fluctuations of the fluid in a little more detail. In the first place it will be assumed that, if the value of H_1 is known at time t, the value of H_1 at time t' depends only on the difference

$$t - t' = \tau . \qquad (46)$$

Let us define

$$G_{km}(\tau) = \overline{(k|H_1(t-\tau)|m)(m|H_1(t)|k)} \quad , \tag{47}$$

where the overbar indicates that we are taking the average value of a random fluctuation. Then since $G_{km}(\tau)$ does not depend on t

$$G_{km}(\tau) = \overline{(k|H_1(t)|m)(m|H_1(t+\tau)|k)}$$

$$= \overline{(m|H_1(t+\tau)|k)(k|H_1(t)|m)}$$

$$= G_{mk}(-\tau) \quad . \tag{48}$$

We now obtain from Eqs. (45b), (46), and (48) and the fact that the perturbation is random in time that

$$\frac{d\rho_{kk}}{dt} = \frac{1}{\hbar^2} \int_0^t \left[G_{km}(\tau)e^{-i\omega_{km}\tau} + G_{km}(-\tau)e^{i\omega_{km}\tau} \right] d\tau$$

$$= \frac{1}{\hbar^2} \int_{-t}^t G_{km}(\tau)e^{-i\omega_{km}\tau} d\tau \quad . \tag{49}$$

The properties of our random perturbation are such that

$$\overline{(k|H_1(t)|m)} = 0 \quad , \tag{50a}$$

but

$$\overline{|(k|H_1(t)|m)|^2} \geq 0 \quad . \tag{50b}$$

Therefore if τ is large enough that the system at time $t + \tau$ does not "remember" its position at time t, we can write

$$G_{mk}(\tau) = \overline{(m|H_1(t)|k)(k|H_1(t+\tau)|m)}$$

$$= \overline{(m|H_1(t)|k)}\;\overline{(k|H_1(t+\tau)|m)}$$

$$= 0 \tag{51}$$

We can define a critical time τ_c called the correlation time for which $G(\tau > \tau_c) = 0$. If we are interested in the decay rate for times at which $\tau_c \ll t$, as is usual, we can set the limits on the integral in Eq. (49) at infinity and obtain

$$\frac{d\rho_{kk}}{dt} = \frac{1}{\hbar^2}\int_{-\infty}^{\infty} G_{km}(\tau)e^{-i\omega_{km}\tau}\,d\tau \quad . \tag{52}$$

Let us define the spectral density of $G_{km}(\tau)$ by

$$J_{km}(\omega) = \int_{-\infty}^{\infty} G_{km}(\tau)e^{-i\omega\tau}\,d\tau \quad . \tag{53}$$

The Wiener-Khintchine Theorem (13) permits us to take the Fourier transform of $J_{km}(\tau)$ and obtain

$$G_{km}(\tau) = \frac{1}{2\pi}\int_{-\infty}^{\infty} J_{km}(\omega)e^{i\omega\tau}\,d\omega \quad . \tag{54}$$

By setting $\tau = 0$ in Eq. (54) we see that the total area under the curve $J_{km}(\omega)$ is independent of τ_c. Making use of Eq. (53) we obtain from Eq. (52) that

$$\frac{d\rho_{kk}}{dt} = J_{km}(\omega_{km})/\hbar^2 \ . \tag{55}$$

For $1/\omega_{km} \gg \tau_c$ Eq. (55) goes to zero. If we assume that $J_{km}(\omega)$ is approximately constant for $1/\omega < \tau_c$ then, since the area under $J(\omega)$ is constant, the transition probability in Eq. (52) will have a maximum when $1/\omega_{km} \cong \tau_c$. Since the spectral density and τ_c will in general depend on the temperature $d\rho_{kk}/dt$ may approach a maximum at some particular temperature.

From Eq. (51) we see that $G(\infty) = 0$. It is also obvious from Eq. (44) that $G_{km}(0) = \overline{|(k|H_1(t)|m)|}^2$. A little reflection shows that $G_{km}(0)$ is a maximum value of $G_{km}(\tau)$. Physical arguments can be made that normally $G(\tau)$ is a monotonically decreasing function. The assumption is often made (14) that

$$G_{km}(\tau) = G_{km}(0)\exp(-\tau/\tau_c) \ , \tag{56a}$$

or

$$G_{km}(\tau) = \overline{|(k|H_1(t)|m)|}^2 \exp(-\tau/\tau_c) \ . \tag{56b}$$

By use of Eqs. (52) and (56) we then obtain that

$$\frac{d\rho_{kk}}{dt} = \frac{\overline{(k|H_1(t)|m)(m|H_1(t)|k)}}{\hbar^2} \frac{2\tau_c}{1 + \tau_c^2 \omega_{km}^2} \ . \tag{57}$$

Equation (57) is still very general and might be used to describe many different relaxation processes which depend on a randomly fluctuating force field, e.g. vibrational relaxation in a liquid or gas. For nuclear spin relaxation we may write the interaction as

$$H(t) = -\gamma_n \hbar \, \overrightarrow{H(t)} \cdot \vec{I} , \tag{58}$$

where γ_n is the gyromagnetic ratio of the relaxing nucleus, $\overrightarrow{H(t)}$ is a randomly fluctuating magnetic field due to the medium at the nucleus, and $\vec{I}$ is the nuclear spin. The magnetic field $\overrightarrow{H(t)}$ may be caused by the random motions of other nuclei, by the random motions of electrons, or in a number of other conceivable ways. If we further assume that $H_q(t)$ is independent of $H_{q'}(t)$ unless $q = q'$ where q and q' are x, y, and z, we obtain on substitution of Eq. (58) in Eq. (57) that

$$\frac{d\rho_{kk}}{dt} = \gamma_n^2 \left(\frac{2\tau_c}{1 + \tau_c^2 \omega_{km}^2} \right) \sum_q \overline{H_q^2} \, |(k|I_q|m)|^2 . \tag{59}$$

It should be noted that the average value of the square of the perturbing field does not depend on the time. In order to carry the calculation further one must assume a specific value of I. It is important to note that Eqs. (57) and (59) have a maximum at $\tau_c = 1/\omega_{km}$.

Both Eqs. (57) and (59) give the rate of increase in the population of state k if state m initially had a unit population. If more than one state is initially excited, as is usually the case for nuclear spins, we must sum over all initial states. We then obtain

$$\frac{d\rho_{kk}}{dt} = \sum_{m} (R_{mk}\rho_{mm} - R_{km}\rho_{kk}) \quad , \tag{60}$$

where $R_{km} = R_{mk}$ is the right-hand side of Eq. (57) or (59). Equation (60) leads to an eventual equal population of all states, contrary to observation, because we have treated the medium as if it could exchange infinite amounts of energy with the spin system. This flaw in the theory is most easily corrected by replacing $\rho_{e\ell}$ by $\rho_{e\ell} - \rho_{e\ell}^{\,o}$ where $\rho_{e\ell}^{\,o}$ is the value of $\rho_{e\ell}$ at thermal equilibrium, i.e.

$$\rho_{e\ell}^{\,o} = \exp(-E_\ell/kT)/\sum_{n} \exp(-E_n/kT) \tag{61}$$

Equation (54) then becomes

$$\frac{d\rho_{kk}}{dt} = \sum_{m}{}' R_{mk}(\rho_{mm} - \rho_{mm}^{\,o}) \quad , \tag{62}$$

where the prime on the summation simply indicates that $k \neq m$. The above treatment of transitions induced by randomly fluctuating fields is, of course, by no means complete, since many pages have been devoted to the subject, but it does outline the main plan of attack on a difficult problem.

The use of a correlation function as in the treatment of spin relaxation greatly differs from the use of time-independent perturbations which have been used here in the treatment of electronic relaxation is not always treated by using the assumption of a randomly fluctuating field. An example of a treatment where the perturbation

does not depend on the time (even randomly) is the relaxation of nuclei in metals (12). It would be possible to replace the H_2 used here in the treatment of electronic relaxation by a perturbation Hamiltonian fluctuating randomly in time, but this is not usually profitable in the treatment of relaxation processes in solids. However, a randomly fluctuating perturbation Hamiltonian in place of H_2 might be very useful in treating electronic relaxation processes in the liquid and gas phases which are characterized by randomly fluctuating fields. For instance one might choose a perturbation function of the form

$$V = H_1 + \xi(t) \sum_v R_v , \qquad (63)$$

where H_1 is the H_1 used earlier in the presentation of electronic relaxation, but the earlier H_2 has been replaced by $\xi(t) \sum_v R_v$. In Eq. (63) $\xi(t)$ is a randomly varying function of the time subject to the conditions that $\overline{\xi(t)} = 0$, $\overline{\xi(t)^2} \leq 0$, and $\overline{\xi(t)\xi(t+\tau)} \geq 0$ for times shorter than some critical time τ_c but zero for $t > \tau_c$. Of course τ_c will be a function of the temperature.

Accurate lifetimes of solutes in liquid solutions are much more difficult to measure than in solid solutions because minute amounts of impurity can quench the triplet state. Porter and Stief (15) have used 9, 10-dibromoanthracene, which has a very short lifetime, to overcome this problem. They have studied the lifetime as a function of temperature in propylene glycol, 3-methyl pentane and isopentane. They find that at high temperatures the unimolecular decay rate is the

same in all three solvents (k $\approx 10^4$ sec^{-1}) at a given temperature and
only varies slowly with temperature. A similar situation holds for
low temperatures except that k ≈ 300 sec^{-1}. The change between these
two lifetime extremes is solvent dependent and occurs in a tempera-
ture range of 50-60°. In the case of propylene glycol the change in
lifetime is greatest about 50° above the melting point, while in the
other two solvents the change is greatest near the melting point. All
the lifetimes were measured in the (sometimes supercooled) liquid
state. The work of Porter and Stief is important because it demon-
strates that there are probably two distinct types of electronic relax-
ation. The slower process which occurs in solids and high viscosity
liquids has been discussed in detail in this thesis. The fast process
is apparently the result of the rapidly changing environment in a
liquid. It has not, as yet, been treated theoretically in a detailed
manner, but such a treatment should be possible using a Hamiltonian
similar to Eq. (63). Since H_1 is common to both processes, effects,
such as the deuterium effect, which depend on H_1 should be present
in both the fast and slow processes. Unfortunately, at present, no
experimental information is available on the lifetimes of perdeuterated
compounds in liquid solution.

No discussion of the effect of the environment and vibronic
interactions on H_1 has been made in this section, but these subjects
are discussed rather thoroughly in the second paper by Robinson and
Frosch (section IIC, this thesis).

References

1. E. C. Lim, J. Chem. Phys. 36, 3497 (1962).

2. M. S. de Groot and J. H. van der Waals, Mol. Phys. 4, 189 (1961).

3. For example, see L. I. Schiff, Quantum Mechanics (McGraw-Hill Book Co., Inc., New York, 1949), Chap. VIII.

4. M. R. Wright, R. P. Frosch, and G. W. Robinson, J. Chem. Phys. 33, 934 (1960).

5. D. S. McClure, J. Chem. Phys. 17, 905 (1949).

6. This thesis.

7. C. A. Hutchison and B. W. Mangum, J. Chem. Phys. 32, 1261 (1960).

8. J. M. Ziman, Electrons and Phonons (Oxford University Press, London, 1962), p. 44.

9. S. G. Hadley, H. E. Rast, and R. A. Keller, J. Chem. Phys. 39, 705 (1963).

10. K. B. Eisenthal and R. Murashirge, J. Chem. Phys. 39, 2108 (1963).

11. M. Gouterman, J. Chem. Phys. 36, 2846 (1962).

12. A very complete discussion of nuclear spin relaxation is found in A. Abragam, The Principles of Nuclear Magnetism (Oxford University Press, London, 1961), pp. 264-423. A good but shorter discussion of nuclear spin relaxation is found in C. P. Slichter, Principles of Magnetic Resonance (Harper and Row, New York, 1963), pp. 115-159.

13. N. Davidson, <u>Statistical Mechanics</u> (McGraw–Hill Book Co., Inc., New York, 1962),pp. 290–295.

14. See C. P. Slichter, Reference 12, p. 141 for a discussion of this assumption; also Reference 13.

15. G. Porter and L. J. Stief, Nature $\underset{\sim}{195}$, 991 (1962).

B. Theory of Electronic Energy Relaxation in the Solid Phase*

G. W. ROBINSON† AND R. P. FROSCH

Gates and Crellin Laboratories of Chemistry,‡ California Institute of Technology, Pasadena, California

(Received May 17, 1962)

A theory of electronic energy relaxation in the solid phase is presented. This process is sometimes called *internal conversion* when applied to states of the same multiplicity, or *intersystem crossing* when applied to states of different multiplicity. The physical limit where the electronic transition is slow compared with vibrational relaxation is shown to be a well-defined mathematical limit in the theory. In the other limit, where the electronic transition is rapid compared with the vibrational relaxation time, vibrational relaxation plays the dominant role in the over-all relaxation process. The result derived from a continuum model for the final states is justified only in the first limit and only then providing the assumption of a large number of final states is physically justified. Two different models are used to illustrate the source of the mathematical limitations and the range of applicability of the theory. These models remove the ambiguities which arise from the normalization of continuum states in the continuum model. The most important conclusions of the paper are embodied in Eqs. (22), (23), (40), (48), and (50).

1. INTRODUCTION

IN this paper we examine theoretically the important problem of radiationless transitions among electronic states of molecules in a solid environment. The paper is primarily concerned with the phenomena called internal conversion and intersystem crossing.[1,2] A second paper[3] in this series will discuss some broader aspects of the more general problem of radiationless transitions in solids. The applications of the present theoretical results also will be described there.

The ground rule which we lay down in this paper limits the discussion to *those radiationless transitions which are slow compared with vibrational relaxation times*, i.e., $\tau_{el} \gg \tau_{vib}$. Because of this, transitions always originate from a *Boltzmann distribution* of vibrational levels. The discussion is considerably simplified if only a single initial state is assumed, and for low temperatures the most appropriate initial state is the zeroth vibrational state belonging to the initial electronic state of the entire system of molecule plus lattice. The theory as presented here will generally be written in terms of this zeroth vibrational initial state. The results obtained are therefore only rigorously applicable at 0°K. A more general result would require a Boltzmann average of the transition probability over all the thermally available vibrational states of the molecule plus the lattice. Actually, if the excitation of lattice vibrations does not greatly modify the purely electronic coupling between the initial and final states, the result obtained for the zeroth vibrational state will be very nearly the same as that obtained from the Boltzmann average providing the temperature is sufficiently low that internal (molecular) vibrations are not appreciably excited. One of the premises of this paper is that in a

[1] M. Kasha, Chem. Revs. 41, 401 (1947).

[2] M. Kasha, Discussions Faraday Soc. No. 9, 14 (1950).

[3] G. W. Robinson and R. P. Frosch (to be published); paper II of this series.

majority of the systems where radiationless transitions have been studied experimentally (EPA, hydrocarbon "glasses," rare-gas "solvents," and mixed crystals), the coupling between electronic motions in the molecule and lattice vibrations is sufficiently weak that the above simplification is physically justified.

The choice of the limit $\tau_{el} \gg \tau_{vib}$ is not made only to avoid the rather trivial process of averaging over a nonequilibrium distribution of initial states. Rather, it is a well-defined mathematical limit in which a simplifying perturbation procedure can be used. When the electronic coupling is strong, the language of perturbation theory and the very meaning of initial and final electronic states becomes indistinct. It is interesting to think about radiationless transitions between electronic states which are so very rapid compared with vibrational relaxation that the vibrational relaxation time itself determines the rate of the over-all radiationless process. Radiationless transitions between certain electronic states, more highly excited than the ones considered here, are no doubt in this category, and, through studies using monochromatic excitation, examples of such rapid transitions may be found at some future time.[4]

In the simplest case, the solvent plays no role in the radiationless transition other than to act as a collection of phonon oscillators into which energy in the form of lattice vibrations may ultimately flow. Many cases exist, however, where the solvent itself, through relatively weak electronic interactions with the solute, modifies the radiationless transition probability. Such effects, i.e., the "heavy atom effect" on multiplicity forbidden radiationless transitions, are discussed in II and are not discussed here. The presence of strong solvent–solute electronic interactions would complicate the present theory. They are not discussed.

---

[4] Some very interesting results have been reported recently[5] which can be interpreted[5] in terms of a "singlet–triplet" radiationless process which can compete with vibrational relaxation.

[5] M. O'Dwyer, M. A. El-Bayoumi, and S. J. Strickler, J. Chem. Phys. 36, 1395 (1962).

The systems which are treated consist of the molecule of interest (the solute) plus the surrounding medium (the solvent).[6] We assume a highly dilute system where intermolecular resonance interactions, directly or through virtual states of the solvent, can be neglected. The phenomenon of electronic relaxation is simply a result of radiationless transitions among nearly degenerate nonstationary states[7] of the *over-all system*. It is important to realize at the outset that even the so-called "electronic states" of a free solute molecule are not true stationary states but are mixed through electronic and vibronic interactions. Radiationless transitions between these states would occur in the gas-phase molecule providing the appropriate degeneracies existed. Placing the solute in a surrounding medium substantially increases the degeneracy of the system states because superpositions of solute and solvent vibrational and electronic states can occur. Irreversibility is built into the problem of radiationless transitions in an environment since it becomes statistically improbable for the system to return to the initial state when the total number of final states nearly degenerate with the initial state becomes large.

It is convenient to define the nonstationary states as the zero-order eigenstates of a certain incomplete Hamiltonian. The difference H' between the complete and incomplete Hamiltonian is the perturbation term which causes the zero-order states to be nonstationary. *In this paper the terms "initial state" and "final state" always imply nonstationary states of the system.* A measuring scheme capable of distinguishing between the zero-order states,[9] and rapid compared with transitions

---

[6] The terms *solute* and *solvent* are convenient and are used throughout this paper.

[7] According to the qualitative discussion in the Introduction only a single initial state is considered. The "final states nearly degenerate with the initial state" consist of the final electronic state plus molecular vibrational additions plus lattice vibrational additions. The radiationless transition can therefore occur by way of a time-independent perturbation to final states which are electronically nondegenerate with the initial state but which are degenerate with the initial state, or nearly so, when molecular and lattice vibrational additions to the final electronic state are included. The final states giving the largest contribution to the transition probability in complex molecules are generally those where the molecular vibrational energy greatly dominates the lattice vibrational energy. This point has to do with the Franck-Condon principle applied to the total system of molecule plus lattice. It was explained in a qualitative way in a previous paper, reference 8, pp. 79–82.

[8] G. W. Robinson, J. Mol. Spectroscopy 6, 58 (1961).

[9] We assume a large number of solute molecules so that the measurement itself does not contribute a measurable perturbation. It is well known by experimentalists that quantum yields, intensities of triplet–triplet absorption, and signal strengths in ESR experiments can be used to measure the distribution of molecules among the various excited states as a function of time. That the measuring device does not itself perturb the radiationless lifetime is evident from the fact that the measured values of radiationless transition probabilities do not depend upon the kind of detection used. A discussion of these topics as they apply to radiationless transitions will appear in paper II, and the appropriate references will be cited there.

between them, is able to follow the decay and buildup of nonstationary states as a function of time.[10] The experimental study of relaxation phenomena becomes, therefore, a study of radiationless transitions among states which are almost but not quite stationary. Since the states are nonstationary, they will have intrinsic width in accordance with the uncertainty principle. The criterion of energy conservation referred to the zero-order states is thus modified, but except for this modification, energy is conserved between the initial and final states of the system.

3. PERTURBATION HAMILTONIAN

Those parts of the total Hamiltonian which are to be included in the perturbation H' are by no means arbitrary but depend upon the experiment of interest. Any term in H' which is so large that no designed experiment can follow the time factors associated with it must be included as part of the zero-order Hamiltonian. On the other hand, small terms in H' can be associated with physically detectable time variations of the zero-order eigenfunctions. It is important to realize that H_0 and H' refer to the entire system of molecule plus surroundings. The Hamiltonian H_0+H' therefore

---

[10] The question of just how the system is initially "prepared" in the nonstationary state has often been raised by others. For two weakly coupled classical oscillators one merely flicks one or the other of the oscillators with his finger, and if the coupling is indeed weak it is absolutely no trick at all to watch the oscillation alternately build-up and decay in the two oscillators. The analog for the present electronic relaxation problem requires that one of the oscillators be highly damped, i.e., it is coupled strongly, compared with the coupling between the oscillators, to a complicated spring system with many degrees of freedom, say a *bedspring* (we acknowledge H. M. McConnell for providing us with this "notation"). The experiment which measures the "lifetime of the radiationless transition" in this case consists of measuring the decrease of vibrational amplitude of the initial oscillator with time. In the quantum-mechanical problem, in the absence of the environment, the system is placed initially in states represented by the time independent functions $(1-\lambda^2)^{\frac{1}{2}}\psi_1+\lambda\psi_2$ and $\lambda\psi_1-(1-\lambda^2)^{\frac{1}{2}}\psi_2$, where $0\leq\lambda\leq2^{-\frac{1}{2}}$. If an environment coupled strongly to ψ_2 and having many available degrees of freedom is present, then there are a large number of final states of the transition which consist of linear combinations of ψ_2 and the environmental states. Placing the system initially into the "state" $(1-\lambda^2)^{\frac{1}{2}}\psi_1+\lambda\psi_2$ therefore has no meaning. However, providing the coupling between ψ_1 and ψ_2 plus environment is weak compared with the coupling among the final states, preparing the system in states of the type $(1-\lambda_f^2)^{\frac{1}{2}}\psi_1+\lambda_f\psi_f$, where ψ_f signifies a particular linear combination of zero-order final states, does have meaning. Section 2 describes how these stationary states contain the nonstationary states along with the appropriate time factors. Any process such as direct absorption of radiation or radiationless transitions from higher states essentially prepares the system in the almost, but not quite, stationary state ψ at a well-defined time, $t=0$. The physical justification for coupling ψ_2 directly to the environmental levels, but coupling ψ_1 to the environment only through ψ_2, has to do basically with the fact that ψ_2 is a vibrationally highly excited state of the over-all system of molecule plus lattice while, in the limit of interest $\tau_{el}\gg\tau_{vib}$, ψ_1 is in Boltzmann equilibrium with the lattice states. Vibrational relaxation can therefore occur from ψ_2 but not from ψ_1. For the special case when $T=0^\circ K$, ψ_1 is in its zeroth molecular-lattice vibrational state and is vibrationally nondegenerate. On the other hand, ψ_2 has a high degree of vibrational degeneracy. The points cited in this footnote and footnotes 7 and 9 are, we feel, basic and should be kept in mind when reading the quantitative theory later in the paper.

contains terms originally present in the free molecule possibly modified by the surroundings, terms belonging to the surroundings possibly modified by the presence of the molecule, and terms representing coupling between the molecule and its surroundings. Providing they are sufficiently small, terms in any of the above three categories can be associated with experimentally observable radiationless transitions. For example, terms coupling molecular vibrational levels to each other through the lattice must be considered if the experiment to be described has to do with the radiationless transition called *vibrational relaxation*; coupling terms among the lattice vibrations must be considered if one wishes to describe the radiationless transition called *heat conduction*; and coupling between vibronic states of the entire system must be considered if, as in the present case, radiationless transitions among electronic states are to be discussed. The perturbation may be oscillatory with time or it may be time independent. For an oscillatory perturbation having angular frequency ω, transitions with the highest probability occur about a region where the energy difference between initial and final states is equal to $\hbar\omega$. A stationary perturbation can also cause radiationless transitions, but in this case those of highest probability occur to final states which are in near resonance with the initial state.

For multiplicity allowed transitions, the zero-order states are mixed by electrostatic coupling. Coulombic interactions among the electrons and nuclei of the system are therefore the perturbation terms which are responsible for the nonstationary character of the electronic zero-order states. It is doubtful that oscillatory electric fields caused by lattice vibrations are of measurable importance[11] when compared with time-independent terms already in the free-molecule Hamiltonian. Only states having the same symmetry are mixed by H', since the Hamiltonian must be totally symmetric. In those instances where the first-order matrix elements of H' are small or vanishing because of symmetry, vibronic terms become important. One may thus have symmetry-forbidden but vibronically allowed radiationless transitions, analogous to those which are well known for the radiative process.[12,13] A Taylor's series expansion in the normal coordinates of the initial and final electronic eigenfunctions, and of H' itself, about the equilibrium positions of the nuclei provides a standard method by which weak vibronic interactions caused by the breakdown of the Born–Oppenheimer approximation may be treated theoretically.

For multiplicity-forbidden processes, an oscillatory electric field like that provided by pure electrostatic interactions or lattice vibrations is not sufficient to

[11] But see, M. Gouterman, J. Chem. Phys. **36**, 2846 (1962), where a different point of view is taken.
[12] G. Herzberg and E. Teller, Z. physik Chem. **B21**, 410 (1933).
[13] A. C. Albrecht, J. Chem. Phys. **33**, 156 (1960).

cause a transition. A magnetic perturbation, such as a spin–orbit interaction, is required. Electrostatic interactions or lattice vibrations can at most modulate the magnetic perturbation, providing there is some coupling between the two kinds of motion. In all but possibly a few pathological cases, the higher-order coupling between the lattice vibrations and the magnetic contributions to the molecular Hamiltonian must certainly be small compared with the magnetic terms already present in H'. The time *independent* spin-orbit terms will thus play by far the greatest role in the radiationless transition process involving states of different multiplicities.

The probability that any of these interactions are grossly modified by the environment seems remote except in special instances where there exist strong solute–solvent electrostatic interactions or where heavy atom effects are superimposed on weak intramolecular spin–orbit coupling.[3] *It is the premise of this paper that, except in such cases, the matrix elements for the electronic relaxation problem in the limit $\tau_{el} \gg \tau_{vib}$ are determined by the presence of perturbations, already present in the free molecule, between electronic states which are almost, but not quite, stationary.* For those cases where the initial and final states ψ' and ψ'' are strongly mixed so that "transitions back and forth between the two" take place rapidly compared with the vibrational time scale, the vibrational levels for the system can no longer be thought of as belonging to ψ' or to ψ'' separately, but rather to the electronic stationary states given by the appropriate linear combinations of ψ' and ψ''. The transfer of molecular excitation energy to the lattice would then depend upon the rate at which vibrational energy associated with the electronic states $a\psi'+b\psi''$ can be transferred to lattice vibrations. Thus, the vibrational relaxation time, not the magnitude of the matrix element mixing ψ' and ψ'', becomes the only quantity of significance in the radiationless transition probability.

4. RADIATIONLESS TRANSITIONS IN THE ABSENCE OF AN ENVIRONMENT

Resonant States

The discussion of radiationless transitions between two nonstationary states of an isolated molecule is a conceptually simple problem, related, however, to the more complicated problem of energy transfer in a solid. For this reason it seems appropriate to use the simple problem as a starting point in the treatment of the more complicated one. Here, and for the remainder of the paper we discuss only transitions induced by stationary perturbations. The initial state and the final state may or may not be in exact resonance. We discuss the case of resonance[14] first, and then the case where an energy gap Γ between the initial and final

---

[14] The states are degenerate before the perturbation "is applied." The perturbation, of course, removes the degeneracy.

states exists. In principle the total transition probability in the free molecule can be obtained by summing the individual transition probabilities, each with its own energy gap and its own matrix element, over all the final states. The total transition probability in a free molecule thus becomes a very complex function of the time, since there is in general no coherence between the time variations in the individual probabilities. In the next section we show how the introduction of an environment modifies the results obtained in this section. In the limiting case where $\tau_{el} \gg \tau_{vib}$, it is seen that the presence of the environment actually simplifies the treatment of the radiationless transition problem.

The quantum mechanical problem of excitation transfer back and forth between a single initial state and a single final state in resonance is analogous to the classical mechanical problem of two coupled oscillators or pendulums. The classical problem and the quantum-mechanical problem are long-standing textbook exercises.[15-17] They may be solved by finding the solutions to two simultaneous differential equations involving the time. For the present purpose a more illustrative solution to the quantum mechanical problem, for the case where the perturbation does not involve the time, may be obtained by direct calculation of the *stationary-state* eigenvalues and eigenfunctions of the coupled system. The stationary-state eigenfunctions so obtained contain the nonstationary initial and final-state eigenfunctions of interest with their appropriate time factors. An examination of these time factors allows the time variation of the nonstationary states to be deduced.[18]

Let the two states in resonance be designated *initial* and *final* and allow these to be mixed by a time-independent perturbation H'. The time independent eigenfunctions and energies of the coupled system are

$$\psi_{\pm}(\mathbf{x}) = 2^{-\frac{1}{2}}[\psi'(\mathbf{x}) \pm \psi''(\mathbf{x})], \tag{1}$$

$$E_{\pm} = E_0 \pm \beta, \tag{2}$$

where E_0 is the unperturbed energy and β is the matrix element of H' between $\psi''(\mathbf{x})$ and $\psi'(\mathbf{x})$. Solving now for $\psi'(\mathbf{x})$ and $\psi''(\mathbf{x})$ in terms of $\psi_+(\mathbf{x})$ and $\psi_-(\mathbf{x})$, which are stationary states, and introducing the proper time factors $\exp(-iE_{\pm}t/\hbar)$ for these stationary states yields for the time-dependent eigenfunctions $\psi'(\mathbf{x}, t)$ and $\psi''(\mathbf{x}, t)$

$$\psi',''(\mathbf{x}, t) = 2^{-1}\{\psi_+(\mathbf{x}) \exp(-i\beta t/\hbar)$$
$$\pm \psi_-(\mathbf{x}) \exp(+i\beta t/\hbar)\} \exp(-iE_0 t/\hbar). \tag{3}$$

[15] L. A. Pipes, *Applied Mathematics for Engineers and Physicists* (McGraw-Hill Book Company, Inc., New York, 1945), Chap. VIII.

[16] N. W. McLachlan, *Theory of Vibrations* (Dover Publications, Inc., New York, 1951), Chap. IV.

[17] L. Pauling and E. B. Wilson, Jr., *Introduction to Quantum Mechanics* (McGraw-Hill Book Company, Inc., New York, 1935), pp. 314–325.

[18] L. D. Landau and E. M. Lifshitz, *Quantum Mechanics Non-Relativistic Theory* (Pergamon Press, Ltd., London, 1958), Chap. VI.

In Eq. (3) the upper sign refers to prime and the lower one refers to double prime. The functions $\psi',''(\mathbf{x}, t)$ are seen to be nonstationary since their squared moduli oscillate between $\psi'^2(\mathbf{x})$ and $\psi''^2(\mathbf{x})$ with a period of $h\beta^{-1}$. For example, at $t=0$, $\psi'^*(\mathbf{x}, t)\psi'(\mathbf{x}, t)=\psi'^2(\mathbf{x})$, while at $t=\frac{1}{4}h\beta^{-1}$, $\psi'^*(\mathbf{x}, t)\psi'(\mathbf{x}, t)=\psi''^2(\mathbf{x})$; and, in general, for this initial condition, the squared modulus of $\psi'(\mathbf{x}, t)$ is given by,

$$\psi'^*(\mathbf{x}, t)\psi'(\mathbf{x}, t) = \cos^2\!\beta t/\hbar\psi'^2(\mathbf{x}) + \sin^2\!\beta t/\hbar\psi''^2(\mathbf{x}). \quad (4)$$

The time-dependent coefficient $c''^*c''= \sin^2\!\beta t/\hbar$ gives the "transition probability" $w(t)$ for a transition $\psi'(\mathbf{x})\rightarrow\psi''(\mathbf{x})$ under the constant perturbation.

It is clear that a measuring process which is rapid compared with a time scale $t \approx \hbar\beta^{-1}$ and capable of distinguishing between $\psi'(\mathbf{x})$ and $\psi''(\mathbf{x})$ would be able to follow the time variation of the eigenfunctions. If at $t=0$ the system is placed in the nonstationary state $\psi'(\mathbf{x})$, the alternate decay of $\psi'(\mathbf{x})$ and buildup of $\psi''(\mathbf{x})$ at all subsequent times could be followed. Emission from the initial state to lower states, absorption from the initial state to higher states, or paramagnetic resonance of the initial state could act as such a measuring device.

Nonresonant States

The methods used in the last subsection for two degenerate states may also be used when the states are not initially degenerate. Here, however, the two stationary-state eigenfunctions are no longer symmetric and antisymmetric combinations of $\psi'(\mathbf{x})$ and $\psi''(\mathbf{x})$. Instead, the well-known exact result for an energy gap[19] $\Gamma = E' - E''$ becomes[18]

$$\psi_1(\mathbf{x}) = a\psi'(\mathbf{x}) + b\psi''(\mathbf{x}), \quad (5)$$

$$\psi_2(\mathbf{x}) = b\psi'(\mathbf{x}) - a\psi''(\mathbf{x}), \quad (6)$$

$$E_1 = E + \tfrac{1}{2}\epsilon, \quad (7)$$

$$E_2 = E - \tfrac{1}{2}\epsilon, \quad (8)$$

where

$$a = [(\epsilon+\Gamma)/2\epsilon]^{\frac{1}{2}} \quad (9)$$

and

$$b = [(\epsilon-\Gamma)/2\epsilon]^{\frac{1}{2}}. \quad (10)$$

For convenience, we have introduced the quantities

$$E = E' - \tfrac{1}{2}\Gamma \quad (11)$$

and

$$\epsilon = (4\beta^2 + \Gamma^2)^{\frac{1}{2}}. \quad (12)$$

The quantity β is the matrix element of the perturbation Hamiltonian H' mixing $\psi'(\mathbf{x})$ and $\psi''(\mathbf{x})$. The time

---

[19] It will be of utmost importance to distinguish between what we call energy gap Γ and electronic energy difference ΔE. The first is the energy difference between initial and final states inclusive of vibrational energy while the second refers to the *electronic* energy difference between the two states. Generally, $0 \leq \Gamma \leq 1$ cm^{-1}, while $\Delta E > 1000$ cm^{-1}.

dependent functions $\psi'(\mathbf{x}, t)$ and $\psi''(\mathbf{x}, t)$ in this case become

$$\psi'(\mathbf{x}, t) = \{a\psi_1(\mathbf{x}) \exp(-i\epsilon t/2\hbar)$$

$$+ b\psi_2(\mathbf{x}) \exp(+i\epsilon t/2\hbar)\} \exp(-iEt/\hbar), \quad (13)$$

$$\psi''(\mathbf{x}, t) = \{b\psi_1(\mathbf{x}) \exp(-i\epsilon t/2\hbar)$$

$$- a\psi_2(\mathbf{x}) \exp(+i\epsilon t/2\hbar)\} \exp(-iEt/\hbar). \quad (14)$$

With initial condition $\psi'^2(\mathbf{x}, t) = \psi'^2(\mathbf{x})$ at $t = 0$, the squared modulus of the coefficient of $\psi''(\mathbf{x})$ becomes

$$c''^* c'' = [4\beta^2/(4\beta^2 + \Gamma^2)] \sin^2[\tfrac{1}{2}(4\beta^2 + \Gamma^2)^{\frac{1}{2}}]t/\hbar, \quad (15)$$

which reduces to the result for two degenerate states when $\Gamma = 0$. It is seen that $\psi'^2(\mathbf{x}, t)$ oscillates back and forth between $\psi'(\mathbf{x})$ and $\psi''(\mathbf{x})$ with a frequency $\hbar^{-1}[\beta^2 + \tfrac{1}{4}\Gamma^2]^{\frac{1}{2}}$. For states where $\Gamma \gg \beta$ this frequency is much higher than that for the case of resonance. The maximum amplitude of $\psi''(\mathbf{x})$ in $\psi'(\mathbf{x}, t)$, however, is much lower than unity because of the large energy denominator. Thus at very short times compared with the time scale $t \approx \hbar\beta^{-1}$, the transition probability for transitions from $\psi'(\mathbf{x})$ to states very near resonance is given by

$$w(t) \approx \beta^2 t^2/\hbar^2 \qquad (t \ll \hbar\beta^{-1}, \quad \Gamma \approx \beta), \qquad (16)$$

while for states far removed from resonance one has

$$w(t) \approx (4\beta^2/\Gamma^2) \sin^2 \tfrac{1}{2}\Gamma t/\hbar \qquad (\Gamma \gg \beta). \quad (17)$$

The result given in Eq. (17) is the same as would be obtained if first-order energies[20] and eigenfunctions obtained by a perturbation approach were used at the beginning of the calculation. A major point of interest for our purposes is that, if there is a very large number of final states over which one must sum to obtain the total transition probability for *leaving* $\psi'(\mathbf{x})$, contributions for which $\Gamma \gg \beta$ will dominate those for which $\Gamma \approx \beta$ when $t \ll \hbar\beta^{-1}$.[21] This condition holds over the time range of physical importance providing β between the initial state and each one of the final states is sufficiently small. For radiationless transitions of a molecule in an environment, the full electronic matrix element β divides itself among a large number of vibrational levels of the final electronic state associated with the superposition of internal and lattice modes. The division of β over the final states greatly simplifies an otherwise complex time dependency of the transition probability, since the contributions from levels very

[20] The first-order correction to the energy is, of course, zero.

[21] These considerations are just statements of the uncertainty relationship $\Delta\Gamma\Delta t \approx \hbar$. The reason for stressing throughout the paper the conditions under which contributions from states where $\Gamma \gg \beta$ dominate those where $\Gamma \approx \beta$ has to do with the applicability of first-order perturbation theory in obtaining results like those embodied in Eqs. (17), (22), (44), and (48). When these conditions are not met, first-order perturbation theory cannot be used and a linear time dependence of the transition probability is not obtained. It is this linear time dependence which results in the usual exponential law for the decay of an excited state.

near resonance are minimized. The importance of this statement will become apparent in the subsequent sections where the effect of the environment is discussed.

5. EFFECT OF THE ENVIRONMENT ON THE RADIATIONLESS TRANSITION PROBABILITY

In the next section a rigorous perturbation calculation based upon a simplified, but physically reasonable, model for electronic relaxation is presented. In this section we use intuitive reasoning to construct a plausible set of final states which has very simple mathematical properties. This allows a simple evaluation of the radiationless transition probability between electronic states of a molecule in an environment.

States in Near Resonance

Assume that there is a set of molecular vibrational levels of the final electronic state which *in the free molecule are in near resonance with the initial state.* They are coupled directly to the initial state rather than indirectly to the initial state through mechanical coupling in the lattice. We say that such free-molecule final states are *directly coupled* to the initial state. The matrix element between the initial state and any one of this set of directly coupled final states may be designated β_n. The quantities β_n may be derived from β_{el}, the full electronic matrix element, providing the appropriate vibrational factors are known. When the molecule is placed in a solid environment, the free-molecule energy levels are of course modified. Except for the case of rotation, the modification of the free molecule energy levels is slight for the kind of weak solute–solvent coupling considered. Of greater importance here is the fact that, in the solid, lattice modes may be superimposed upon the molecular modes, so that each directly coupled final state derived from the modified free-molecule energy-level diagram may be further modified by the superposition of lattice modes. The importance of stressing directly coupled final states which in the free molecule are in near resonance with the initial state follows from the Franck–Condon principle applied to the total system of molecule plus environment. Large units of molecular energy cannot easily be converted *in a one-step process* to high-lying lattice levels because of the need for keeping the over-all Franck–Condon factors of reasonable magnitude. Therefore any path for a radiationless transition involving a large change in lattice vibrational quantum number cannot appreciably contribute to the total transition probability unless that particular lattice vibration were associated with some large change in the solute-solvent intermolecular structure.[8] Generally, therefore, for the kind of weak solute–solvent coupling discussed in this paper, the most important directly coupled final states for a complex molecule in an environment contain primarily molecular vibrational energy added to small amounts of lattice vibrational energy. According to the premise stated at the end of

Sec. 3, we assume that *the presence of the environment has no effect on β_{el}, and has an effect on β_n only through the presence of lattice contributions to the Franck–Condon factors*. Environmental perturbations which contribute to β_{el} certainly exist in some systems, and such effects are briefly discussed in Paper II as a simple extension of the present theory.

If the total eigenfunction $\psi(\mathbf{x}, \eta)$ in terms of electronic and nuclear coordinates, respectively, can be, as a first approximation, resolved into an electronic and a vibrational part[22,23]

$$\psi(\mathbf{x}, \eta) = \Theta(\mathbf{x}, \eta)\phi(\eta), \qquad (18)$$

then β_n is related to β_{el} through vibrational overlap integrals. More is said about these vibrational factors in the next subsection. Here it suffices to reiterate that the final states labeled n consist of a superposition of quanta of molecular and lattice modes, and for near resonance, the condition

$$\sum_r v_r \nu_r \approx \Delta E/h \qquad (19)$$

must hold, where v_r is the quantum number for the rth normal mode having frequency ν_r, and ΔE is the electronic energy difference between initial and final states. In general, a number of directly coupled final states meeting the criterion of Eq. (19) exists. This number increases substantially with increasing ΔE. *Under most conditions, those β_n which depend upon high-frequency modes associated with geometry changes of the molecule and the local environment are the most important*.[8]

We state above that the introduction of the environment contributes a large number of additional final states. Assume that there are $(N-1)$ such states which in zero-order are nearly degenerate with one of the directly coupled final states, and further assume that these $(N-1)$ zero-order states are coupled to the directly coupled state and to each other by a matrix element $\alpha \gg \beta_n$ [Fig. 1(a)]. The N final states then form a band of width approximately equal to α [Fig. 1(b)]. The various indirectly coupled final states[24] of which we speak here correspond to the electronic final state plus molecular and lattice vibrational additions. Each successive indirectly coupled state contains a different distribution of molecular and lattice vibrational quantum numbers. The parameter α, as can be seen from the schematic energy level diagram in Fig. 1(a), is envisioned as coupling together zero-order final states which differ by one (or a small number) of molecular vibrational quanta. This kind of coupling among the final states preserves the expected stepwise nature of the transfer of internal energy to lattice energy through the molecular vibrations. It is apparent

[22] M. Born and J. R. Oppenheimer, *Ann. Physik* **84**, 457 (1927).
[23] D. R. Bates, A. Fundaminsky, and H. S. W. Massey, *Phil. Trans. Roy. Soc.* (London) **A243**, 93 (1950).
[24] This somewhat artificial division of final states is made for convenience, a point which is made more clear in the next section.

FIG. 1 (a) Schematic energy level diagram illustrating the coupling parameters α and β_n. The figure shows how the directly coupled final state ψ_0'' interacts weakly with the initial state ψ_0' but strongly with the set of indirectly coupled final states ψ_0^I, ψ_0^{II}, $\cdots \psi_0^{N-1}$. For simplicity, only a single molecular mode and a single lattice mode are shown. In general a variety of such modes is involved. When there are many lattice modes, a number of final states having the same molecular vibrational energy as ψ_0^I may exist. There may also be many ψ_0^{II}, etc. The parameter α used in the text of the paper represents an average over all these final states. (b) This figure schematically represents the coupling between the initial state and the final state band. It is the integration over all final states in this band which yields $w_n(t)$. Summation over all the directly coupled final states labeled n is required in order to obtain the total radiationless transition probability $W(t)$. The scale in this figure has been greatly magnified compared with that in Fig. 1(a) since $\alpha \approx 1$ cm^{-1} while generally $\Delta E > 1000$ cm^{-1}.

that the quantity $\hbar \alpha^{-1}$ is of the order of the lifetime of a zero-order indirectly coupled final state, i.e., it is of the order of the vibrational relaxation time τ_{vib} associated with a molecular vibrational level in the solid environment. Estimates of τ_{vib} can be made from absorption linewidths.[3] In general an entire spectrum of α's exist, since each one depends upon the specific nature of the two final states which it couples together. For simplicity of discussion, however, in this paper we assume that there exists some average $\alpha = \hbar \tau_{vib}^{-1}$ which can be applied to all the final states. It is this average α with which we deal in the remainder of the paper.

One would expect the matrix element connecting the

initial state with any one of the states in the final state band to be reduced on the average, because of normalization, to $N^{-\frac{1}{2}}\beta_n$. Oscillation of $\psi'^2(\mathbf{x}, t)$ back and forth between $\psi'^2(\mathbf{x})$ and final states *at* resonance therefore occurs at an exceedingly low frequency for large N by virtue of the smallness of $N^{-\frac{1}{2}}\beta_n$. When there is a preponderance of final states, the few states *at* resonance can make a measurable contribution to the radiationless process only at times very much longer than the average lifetime of the initial state and therefore can be neglected. *Thus, members of a final state band, which are not too close to and yet not too far from resonance, make the greatest contribution to the transition probability.* This is fortunate since the perturbation result given by Eq. (17) can then be used. Irreversibility is built into the radiationless process when N is large since, because of the smallness of $N^{-\frac{1}{2}}\beta_n$ compared with α, there is a vanishingly small probability that the system will return to the initial state. In most physical systems N is indeed large because indirectly coupled final states for the transition exist not only in the crystal itself, but also in the crystal holder, the immediate environment, and the outside world.

Summation or integration of Eq. (17) over all indirectly coupled final states and further summation over all the directly coupled final states each with its own β_n gives the total transition probability. The integration may be easily carried out for an idealized, but intuitively reasonable, set of indirectly coupled final states, namely, a uniformly spaced, quasi-continuous set of N states each of which is coupled to the initial state by a matrix element of order $N^{-\frac{1}{2}}\beta_n$. Later it will be seen clearly that the limit $\tau_{\mathrm{el}} \gg \tau_{\mathrm{vib}}$ is implicitly contained in the statement "the N indirectly coupled final states are strongly coupled to each other, and the resulting matrix element to any one of these N states thereby becomes approximately $N^{-\frac{1}{2}}\beta_n$." Inserting the environmentally modified matrix elements into Eq. (17) yields for the integrated transition probability associated with the nth directly coupled final state,

$$w_n(t) \approx \int_{-\alpha/2}^{+\alpha/2} \frac{4\beta_n^2}{N\Gamma^2}\rho(\Gamma)\,\sin^2\tfrac{1}{2}\Gamma t/\hbar\,d\Gamma. \qquad (20)$$

One expects the density of final states $\rho(\Gamma)$ to be of the order of N/α. The limits of integration extend approximately from $-\alpha/2$ to $+\alpha/2$, since states further removed from resonance with the initial state cannot strongly interact, through the manifold of indirectly coupled final states, with the initial state. A change of variable in Eq. (20) yields

$$w_n(t) = \frac{4\beta_n^2 t}{\hbar\alpha}\int_0^{\alpha t/4\hbar} \frac{\sin^2 x}{x^2}\,dx. \qquad (21)$$

The transition probability $w_n(t)$ is seen to vary linearly with the time for $t \gg 4\hbar\alpha^{-1}$, that is, for times very much longer than the vibrational relaxation time. In this

case the limit of integration becomes essentially infinity, and $w_n(t)$ may be evaluated immediately, giving

$$w_n(t)/t = (2\pi\beta_n^2/\alpha\hbar) \ \sec^{-1}.\tag{22}$$

This is the result given in an earlier paper.[8],[25] As indicated there, it still must be summed over all directly coupled final states n, each with its own Franck–Condon factor,[26] to obtain the over-all transition probability

$$W(t)/t = (2\pi/\alpha\hbar)\sum_n \beta_n^2 = (2\pi\beta_{el}^2/\alpha\hbar)\sum_n \langle\phi_n''\mid\phi_0'\rangle^2.\tag{23}$$

The mathematical importance of the physical limit $\tau_{el}\gg\tau_{vib}$ is illustrated in the derivation of Eq. (22). The over-all vibrational factor $\sum_n \langle\phi_n''\mid\phi_0'\rangle^2$, which we will henceforth denote as $\langle\phi_n''\mid\phi_0'\rangle_{tot}^2$, is discussed in a moment. For simplicity, we have assumed in deriving Eq. (23) that α does not depend upon n. As stated earlier, this is certainly an approximation. The inverse dependence on α of the over-all transition probability in Eq. (23) is itself, at first sight, surprising. This kind of dependence arises since the density of final states, $\rho(\Gamma)$ in Eq. (20), decreases with increasing α. It is important, however, to point out here that the inverse dependence of $w_n(t)$ upon α will be largely lost when the summation over n is carried out, since the number of terms possible in the summation increases approximately linearly with increasing final state bandwidth. Thus there are no specific solvent effects, other than those arising from perturbations of β_{el}, which can be easily predicted from Eq. (23). One does expect relatively slow radiationless transitions in very light atom environments (H_2 and D_2) simply because of the dearth of final states. This expectation is borne out by the recent observation[27] of fluorescence emission from *upper* vibrational levels of the excited electronic state of benzene "dissolved" in solid H_2.

In Eq. (22) and in the expression for $W(t)/t$ the transition probability per unit time is a constant in time, and when a large number of molecules are de-

[25] This result is analogous to that obtained from a continuum model for the final states. The conditions for the validity of Eq. (22) when applied to the present problem are, we feel, more firmly spelled out than they are in previous discussions of this subject. In addition, instead of the somewhat arbitrary normalization of continuum states, we have normalized in terms of a final state band which is directly related to an experimentally available quantity, the vibrational relaxation time.

[26] The summation over all the directly coupled final states, each with its own Franck–Condon factor, is peculiar to the molecular electronic relaxation problem. Because of the large variation of the molecular-lattice Franck–Condon factors among the directly coupled final states, the matrix elements β_n cannot be treated as constants. The usual process of integrating over all final states with the matrix elements assumed identical therefore fails for the molecular problem. For the atomic relaxation problem, a single term of the form of Eq. (22) might suffice providing the purely lattice Franck–Condon factors do not vary widely among the available final states.

[27] R. P. Frosch and G. W. Robinson (unpublished work).

caying from an excited state, the rate of disappearance of the excited states becomes first order in the number x of excited molecules. The rate equation is

$$-(dx/dt) = kx,\qquad(24)$$

where $k = W(t)/t$. This leads to exponential decay with a *half-life*,[28]

$$t_{\frac{1}{2}} = k^{-1}\ln 2.\qquad(25)$$

Times for which $t \gg k^{-1}$ or $t \ll k^{-1}$ are usually experimentally unattainable. In the first limit, there is the difficulty of detection of the small number of excited states remaining at long times; and in the second limit, the fraction of molecules decaying within any interval of time very much smaller than the lifetime is small. Nonexponential decay resulting from the breakdown of first-order perturbation theory, as in the limit in Eq. (16), is not expected to be of importance providing there are a large number of final states.[29] For example, if there are $N_m^{(n)}$ states which are very, very close to resonance, then

$$W_m(t)/t \approx \sum_n (N_m^{(n)}/N)\beta_n^2\hbar^{-2}t.\qquad(26)$$

This is negligible relative to k providing t is not too large compared with k^{-1} and N is large compared with $N_m^{(n)}$. As stated earlier, the limit of large N will be important for most physical situations. In the case where the lattice levels are widely spaced, deviations from Eq. (22) might occur, and in a first approximation, the apparent radiationless half-life becomes time dependent and decreases as the time increases

The need for the limit of large N in the derivation of Eq. (22) is pertinent in another respect. *This limit automatically excludes the treatment by the present theory of processes involving electronic resonance* ($\Delta E = 0$). For the case where $\Delta E = 0$ in zero order, no purely vibrational relaxation process in the final state can occur. The coupling to the lattice is associated with electronic relaxation from the degenerate pair of vibrationless electronic states under discussion to still lower electronic states (for example, the ground state). This kind of coupling is normally much weaker than that between degenerate states because of the small vibrational factors associated with large ΔE. Thus many transitions back and forth between the degenerate initial and final states can occur during the lifetime of these states. The result given by Eq. (23) is, of course, useless when this is the case. It follows that the limit of large N in conjunction with the limit $\tau_{\mathrm{vib}} \ll \tau_{\mathrm{el}}$

---

[28] Very often the so-called lifetime or mean life is the quantity used by experimentalists. This quantity is given the symbol τ and is equal to k^{-1}.

[29] If there are two *identical* molecules A and B, weakly coupled together in a solid solution at $0°K$, one molecule being electronically excited and the other in its ground state, there is only a single final state for the radiationless transition $A†B \rightarrow AB†$. In this case Eq. (22) does not apply, but for short times Eq. (16) is applicable. For longer times the excitation oscillates between the two molecules according to Eq. (4).

necessitates that $\Delta E \gg \alpha \gg \hbar \tau_{\mathrm{el}}^{-1}$ for Eq. (23) to have validity. The limits of strong and weak coupling for radiationless transitions are discussed in more detail in Paper II.

Directly Coupled Final States Far from Resonance

For very large ΔE, the Franck–Condon factors in the matrix elements for directly coupled states near resonance cause β_n to be exceedingly small. One might wonder, then, if it were possible for directly coupled states which are far from resonance, but which have $\beta_n \approx \beta_{\mathrm{el}}$, to contribute measurably to $W(t)$. According to Eq. (17), a maximum in $w(t)$ occurs at $\Gamma = 0$. Subsidiary maxima occur at $\Gamma = (p + \frac{1}{2})\hbar t^{-1}$, where $p = 1, 2 \cdots$. For $t \approx k^{-1}$, that is, for times of physical interest, the contribution to $w(t)$ from the subsidiary maxima relative to that from the main maximum drops off roughly as $4\hbar^2 k^2 \Gamma^{-2}$. The relative contributions to $W(t)$ depend upon this factor multiplied by the relative Franck–Condon factors for the far states F, where $\Gamma \approx \Delta E$, and the resonance states R. One has

$$W^F(t)/W^R(t) = 4(\langle \phi_F'' \mid \phi_0' \rangle_{\mathrm{tot}}{}^2 / \langle \phi_R'' \mid \phi_0' \rangle_{\mathrm{tot}}{}^2)$$
$$\times \hbar^2 k^2 \Delta E^{-2}. \quad (27)$$

In the case of the perprotonated cyclic polyenes, for example, $\langle \phi_R'' \mid \phi_0' \rangle_{\mathrm{tot}}{}^2$ may be estimated from the following empirical expression,[3]

$$\langle \phi_R'' \mid \phi_0' \rangle_{\mathrm{tot}}{}^2 \approx \exp(-0.25 \Delta E^{0.4}) \quad (28)$$

in terms of the electronic energy separation ΔE in cm^{-1} units. Using Eq. (23) for k, and assuming $\langle \phi_F'' \mid \phi_0' \rangle_{\mathrm{tot}}{}^2$ is of the order of unity for $\Gamma \approx \Delta E$, Eq. (27) combined with Eq. (28) gives

$$W^F(t)/W^R(t) = (16\pi^2 \beta_{\mathrm{el}}{}^4/\alpha^2 \Delta E^2) \exp(-0.25 \Delta E^{0.4}),$$
$$\Delta E \gg \alpha \quad (29)$$

for the perprotonated cyclic polyenes. The contribution from the directly coupled states far from resonance is thus negligible when ΔE is of the order of electronic energies and when $\beta_{\mathrm{el}} \ll \Delta E$. This result is expected because of energy conservation. It is the rationale for the statement expressed by Eq. (19).

Vibrational Factors

Providing the resolution of the total eigenfunction in Eq. (18) can be carried out, β_n is related to β_{el} through Franck–Condon factors. Symbolically,

$$\beta_n = \beta_{\mathrm{el}} \langle \phi_n'' \mid \phi_0' \rangle, \quad (30)$$

where the bracketed expression represents the vibrational overlap factor. We have assumed the temperature to be sufficiently low so that the initial state is the zeroth vibrational level. Since the final vibrational level labeled ϕ_n'' consists in general of a superposition of many quanta of a large number of vibrational modes,

$$\langle\phi_n'' \mid \phi_0'\rangle=\prod_r \langle\phi_{v_r}(q_r'') \mid \phi_0(q_r')\rangle, \qquad (31)$$

providing the oscillations are harmonic, and the appropriate linear combinations are used for ϕ_{v_r} when the vibrations are degenerate. In Eq. (31) v_r is the quantum number for the rth normal mode and q_r is the rth normal coordinate; the product is over all molecular and lattice normal modes which contribute to the final level ϕ_n''. For the final states to be in near resonance with the initial state, the criterion given by Eq. (19) must be met. Normalization requires

$$\sum_n \beta_n^2 = \beta_{\mathrm{el}}^2 \qquad (32)$$

over all final states n, but because of energy conservation in nonradiative transitions, only states near resonance give important contributions to k.

For tractable quantitative calculations the assumptions concerning resolution of the total eigenfunction and harmonic oscillations are desirable. The validity of the harmonic oscillator approximation is discussed in the next subsection. The validity of Eq. (18) depends upon the neglect[22,23] of terms in the total vibronic Hamiltonian which have to do with the dependence of the zero-order electronic eigenfunctions upon nuclear coordinates. Such terms can mix zero-order vibronic states and, for example, are responsible for vibronic coupling discussed briefly in Sec. 3. These terms, when they arise from nontotally symmetric vibrations in a polyatomic molecule, will be responsible for multiplicity allowed radiationless transitions between electronic states not having the same symmetry, and they may modify multiplicity forbidden transitions.[3] It is not the intent of the theory to neglect such terms, and, as a matter of fact, they may become dominant when the first-order terms are small. Fortunately, experience has shown that only a small fraction of the $3N-6$ vibrational coordinates are usually very important in vibronic mixing. The treatment of these individual terms then becomes straightforward.[13]

Breakdown of the Born–Oppenheimer approximation may also be responsible for the introduction of correction terms to the vibrational overlap integrals since, in general, the vibronic zero-order states are mixed through vibronic coupling with other states. Such effects may be important at the high vibrational quantum numbers necessary in the case where ΔE is large. For low-lying electronic states, however, the density of electronic zero-order states is sufficiently small that one expects this kind of vibronic interaction to be relatively rare. Coupling of states which have quite different zero-order energies is expected to be small because, in the language of perturbation theory, the energy denominators are large. In addition, interactions, where large differences exist in the initial and final vibrational quantum numbers, are expected to be

weak because of the Franck–Condon effect. It is expected therefore that in the absence of electronic degeneracies, or near degeneracies, these effects will not greatly influence the calculation of vibrational factors for radiationless transitions.

Anharmonicity

Vibrational amplitudes and anharmonicities in large polyatomic molecules, where many atoms are involved in the normal vibrations, are smaller per quantum than amplitudes and anharmonicities in small molecules. As an example, one can consider the case of the $a_{1g}C$—C stretching mode in benzene. In the excited electronic state of the 2600-Å transition seven quanta of this vibration have been observed.[30] By plotting ΔG values against quantum number, one finds that the first anharmonicity constant $\omega_e x_e$ is only 0.5 cm^{-1}, and there is no indication that there is a measurable contribution from the next higher term $\omega_e y_e$. The energy levels of an oscillator whose Hamiltonian contains the anharmonic correction $\alpha x^3 + \beta x^4$ is given by[31]

$$E_n = \hbar\omega(n+\tfrac{1}{2}) - \tfrac{15}{4}(\alpha^2/\hbar\omega)(\hbar/\mu\omega)^3(n^2+n+\tfrac{11}{30})$$

$$+\tfrac{3}{2}\beta(\hbar/\mu\omega)^2(n^2+n+\tfrac{1}{2}), \quad (33)$$

where ω is the angular frequency and μ is the reduced mass for the vibration. The quartic term mixes $n\pm4$, $n\pm2$ levels with the nth level, while the cubic term mixes $n\pm3$, $n\pm1$ levels with the nth level. The energy correction from the cubic term is of the second order. One may assume for simplicity that $\omega_e x_e$ arises solely from the cubic term, in which case,

$$(\hbar\omega)^{-1}\langle n-1 \mid \alpha x^3 \mid n \rangle \approx \{\tfrac{9}{16}[(\omega_e x_e)/\omega_e]n^3\}^{\frac{1}{2}}, \quad (34)$$

$$(3\hbar\omega)^{-1}\langle n-3 \mid \alpha x^3 \mid n \rangle$$

$$= \{\tfrac{1}{216}[(\omega_e x_e)/\omega_e]n(n-1)(n-2)\}^{\frac{1}{2}}. \quad (35)$$

Equations (34) and (35) give the first-order coefficients of the $n\pm1$ and $n\pm3$ eigenfunctions in the corrected nth eigenfunction. The ratio $\omega_e x_e/\omega_e$ is the ratio of the first anharmonic correction to the unperturbed frequency, and for the benzene example this ratio is about 0.0005. Remembering that the squared coefficient is the quantity of physical importance, it is apparent that anharmonic corrections to the eigenfunctions can not be neglected for $n\gtrsim10$ in this particular instance. This is probably an upper limit to the effect of anharmonicities because benzene is relatively small compared with most of the molecules important in the present discussion of radiationless transitions. In addition, anharmonicities in the solid are expected to

[30] F. M. Garforth and C. K. Ingold, J. Chem. Soc. (London) 1948, 417.

[31] Reference 18, p. 136; β here is not to be confused with that used in the rest of the paper.

be smaller than those in the free molecule because of environmental repulsive interactions at large vibrational amplitudes. (If such repulsive interactions become too great an inverse anharmonicity results.) Only in those transitions for which ΔE is large is the question of anharmonicity expected to be an important one. $T_1 \rightarrow S_0$ transitions are generally in this category. Even here, to fill the electronic energy gap, one seldom is forced to use quantum numbers greater than 10 for any single normal mode. For low-frequency vibrations, where the anharmonicity per quantum is much greater than that in the above example, quantum numbers much smaller than 10 give the most important contribution to $W(t)$. One should recognize, however, that, since overlap integrals on the "tail" of the Franck–Condon envelope decrease approximately exponentially with increasing quantum number, a little mixing through anharmonicity of the nth level with lower levels can give a rather large boost to the magnitude of the overlap products in Eq. (31).

6. SIMPLE MODEL FOR RADIATIONLESS TRANSITIONS IN AN ENVIRONMENT

Even though the treatment in the last section seems intuitively reasonable, it would be more satisfying if a model for radiationless transitions were found which could be treated more rigorously. In an idealized case there would be a single initial state ψ_0' and a single directly coupled final state ψ_0'' in resonance with the initial state. Let ψ_0' and ψ_0'' be mixed through the matrix element β_n. Assume now that in the solid there exist $N-1$ other final states $\psi_0^{I}, \psi_0^{II} \cdots$ which are coupled to each other and to ψ_0'' by mechanical coupling in the crystal. These indirectly coupled final states may have less molecular vibrational energy and more lattice energy [Fig. 1(a)] or they may have the same amount of molecular and lattice energy, with the lattice energy distributed among different modes. In general, these final states are multiply coupled together. As a first approximation, however, we may assume that the molecular vibrational relaxation process follows the same selection rules as do radiative vibrational transitions. In this case each molecular-lattice vibrational level is coupled only to adjacent levels where the quantum numbers for the molecular modes are at most raised or lowered by one. For simplicity we take all the matrix elements mixing these final states to be equal. Call them α. Thus $\hbar \alpha^{-1}$ is of the order of the vibrational relaxation time per quantum of molecular vibration. Since we are interested in electronic radiationless transitions which are slow compared with vibrational relaxation times, we assume the inequality $\beta_n \ll \alpha$.

We now choose a representation which is diagonal in the absence of the β_n and α coupling terms, and as a further simplifying assumption we take the initial zero-order state and all the N final zero-order states to be degenerate with one another. The $(N+1)$-order

Hamiltonian matrix A for such a problem is

$$A = \begin{bmatrix} E & \beta_n & & & & \\ \beta_n & E & \alpha & & & \\ & \alpha & E & \alpha & & \\ & & \alpha & E & \cdot & \\ & & & \cdot & \cdot & \cdot \\ & & & & \cdot & \cdot \end{bmatrix} N+1.$$

If $\beta_n = 0$, the matrix A is diagonalized by the symmetrical orthogonal matrix T whose elements are,[32]

$$T_{11} = 1,$$

$$T_{1,s+1} = T_{s+1,1} = 0,$$

and

$$T_{s+1,t+1} = [2/(N+1)]^{\frac{1}{2}} \sin[st\pi/(N+1)], \quad (36)$$

for s, $t = 1$, $2 \cdots N$. The perturbation α removes the degeneracy of the N zero-order final states ψ_0'', ψ_0^I, $\psi_0^{II} \cdots$, the new eigenvalues becoming

$$E_1 = E,$$

$$E_{s+1} = E + 2\alpha \cos[s\pi/(N+1)], \quad s = 1, 2 \cdots N. \quad (37)$$

The transformation

$$A' = T^{-1}AT \quad (38)$$

diagonalizes A when $\beta_n \neq 0$ except for the occurrence of the element β_n with diminished coefficients

$$T_{1,s+1} = (2/N+1)^{\frac{1}{2}} \sin[s\pi/(N+1)],$$

$$s = 1, 2 \cdots N, \quad (39)$$

along the first row and column of A'. Since $\beta_n \ll \alpha$, a first-order perturbation calculation can be used to find the time dependency of the nonstationary state ψ_0'. Using β_n with its diminished coefficients for the matrix elements and the eigenvalues of Eq. (37) for calculating the energy denominators, one obtains, according to Eq. (17), the transition probability to any one of the final states r,

$$w_r(t) = \frac{2\beta_n^2 \sin^2 r\pi/N+1}{(N+1)\alpha^2 \cos^2 r\pi/N+1} \sin^2[(\alpha t/\hbar) \cos r\pi/N+1]. \quad (40)$$

We neglect higher-order contributions from states for which r has values

$$\tfrac{1}{2}(N+1) - (\beta_n/\alpha)(N+1)^{\frac{1}{2}} \lesssim r \lesssim \tfrac{1}{2}(N+1) + (\beta_n/\alpha)$$

$$\times (N+1)^{\frac{1}{2}}. \quad (41)$$

This remaining degeneracy with the initial state will be

[32] C. A. Coulson, Proc. Roy. Soc. (London) A169, 413 (1939); W. E. Moffitt and C. A. Coulson, Trans. Faraday Soc. 44, 81 (1948).

removed by the small elements of order $(2/N+1)^{\frac{1}{2}}\beta_n$. Summation of $w_r(t)$ over all r yields the total transition probability $w_n(t)$ for the process associated with β_n. The fraction of states near resonance decreases as $N^{-\frac{1}{2}}$, and for large N the contribution to $w_n(t)$ from the few states near resonance will be appreciable only at times very much longer than the time scale of physical interest.

It is convenient to change the index r to r', such that

$$r=r'+\tfrac{1}{2}(N+1), \quad -\tfrac{1}{2}(N-1)\leq r'\leq\tfrac{1}{2}(N-1),$$

making

$$w_{r'}(t)=\frac{2\beta_n^2 \cos^2[r'\pi/(N+1)]}{(N+1)\alpha^2 \sin^2[r'\pi/(N+1)]}$$

$$\times\sin^2\{(\alpha t/\hbar)\sin[r'\pi/(N+1)]\}. \quad (42)$$

There are two limiting regions of interest, that for which $r'\approx\pm\tfrac{1}{2}(N-1)$ and that for which $r'\approx 0$. In region I, one can obtain $w_{r'}(t)$ by expansion of $\sin x$ and $\cos x$ about the points $x=-\pi/2$ or $x=+\pi/2$, yielding

$$w_{r'}{}^{\mathrm{I}}(t)\approx\frac{2\beta_n^2\pi^2\{[|r'|/(N+1)]-\tfrac{1}{2}\}^2}{(N+1)\alpha^2}\sin^2(\alpha t/\hbar). \quad (43)$$

In the region near $r'\approx 0$ one obtains by expansion about $x=0$,

$$w_{r'}{}^{\mathrm{II}}(t)\approx[2\beta_n^2(N+1)/\pi^2 r'^2\alpha^2]\sin^2[\pi r'\alpha t/\hbar(N+1)].$$

$$(44)$$

It is readily seen that region I gives an ever-diminishing contribution to $w_{r'}(t)$ as N becomes large. Such contributions are from that portion of the final state band which is very far from resonance. If the contribution from region I is neglected, it remains to carry out a sum of $w_{r'}(t)$ over the states in region II to obtain $w_n(t)$. We carry out in detail the summation for odd N. The result for even N is identical but involves a slightly different series. Since $w_{r'}{}^{\mathrm{II}}$ is symmetric about the origin, one has for odd N

$$\sum_{r'=-n'/2}^{+n'/2} w_{r'}{}^{\mathrm{II}}(t)=\frac{2\beta_n^2 t^2}{\hbar^2(N+1)}+2\sum_{r'=1}^{+n'/2}\frac{2\beta_n^2(N+1)}{\pi^2 r'^2\alpha^2}$$

$$\times\sin^2[\pi r'\alpha t/\hbar(N+1)]. \quad (45)$$

Since most of the contribution to the sum in Eq. (45) arises from that part of the final state band relatively near the origin, the limit $n'/2$ may be taken to be ∞ without giving rise to any significant error, and the summation may be carried out immediately.[33] The result is,

$$w_n(t)=[2\beta_n^2 t^2/\hbar^2(N+1)]+[2\beta_n^2(N+1)/\alpha^2]$$

$$\times\{\tfrac{1}{6}-B_2[\alpha t/\hbar(N+1)]\}, \quad (46)$$

[33] See, for example, R. Courant, *Differential and Integral Calculus* (Blackie and Son, Ltd., London, 1937), 2nd ed. Vol. I, p. 446.

where $B_2(u)$, the second Bernoulli polynomial, is defined by

$$B_2(u) = u^2 - u + \tfrac{1}{6}. \tag{47}$$

Collection of terms leads to the final result for the transition probability $w_n(t)$,

$$w_n(t)/t = (2\beta_n^2/\alpha\hbar)\ \sec^{-1}. \tag{48}$$

Perhaps a more illuminating way of evaluating the transition probability $w_n(t)$ from Eq. (42) is by assuming reasonably large N, making the transformation

$$x = (\alpha t/\hbar)\ \sin[r'\pi/(N+1)], \tag{49}$$

and integrating, in which case,

$$w_n(t) \approx (2\beta_n^2 t/\pi\alpha\hbar) \int_{-\alpha t/\hbar}^{+\alpha t/\hbar} [1 - (x^2\hbar^2/\alpha^2 t^2)]^{\frac{1}{2}}(\sin^2 x/x^2)\,dx. \tag{50}$$

The nonlinear time dependence of $w_n(t)$ at short times is illustrated by this equation. At times for which $t \approx k^{-1}$ the result given by Eq. (48) is obtained as expected.

7. DISCUSSION

Equation (22) differs from the analogous Eq. (48) by a factor of π. This factor arises because the density of states throughout the final state band is assumed constant in the first instance, but varies in the second in such a way that the major contribution to the $w_n(t)$ comes from that part of the band where the density of states is reduced by the factor π. The real density of final states probably does not correspond to either of these idealized situations, and thus the theoretical result always must be considered to contain an unknown factor of the order of unity. Furthermore, we have assumed a strict degeneracy between initial state and directly coupled final state in both calculations. Deviations of the order of α from exact resonance will simply modify by a small factor the density of final states, while those processes involving directly coupled final states farther from resonance than α will contribute little to the over-all transition probability.

As stated earlier in the paper, it is important to remember that while the individual $w_n(t)$ are inversely proportional to α, the number of important directly coupled states in the n sum is proportional to α, and the detailed α dependence will be largely lost in the over-all transition probability $W(t)$. The actual magnitude of α, however, is important since it sets the time scale upon which the electronic relaxation process takes place.

The major importance of Eq. (48) lies in the fact that one can now make reliable predictions about the dependence on the electronic matrix element β_{el} and the dependence on the associated vibrational factors of molecular radiationless transition probabilities in solid media. In the case where there is a single directly coupled final state and the vibrational factor is of the

order of unity, it can be seen that even a 0.01 cm^{-1} interaction corresponds to a rate constant of about 4×10^7 sec^{-1}. This calculation assumes that $\alpha = 1$ cm^{-1} which is a reasonable value for the lattice coupling parameter.[3] Spin–orbit coupling between excited singlet and triplet states is expected to have matrix elements of the order of 0.01 cm^{-1} or greater, so that for closely spaced electronic states, where ΔE is small and the vibrational factors are near unity it is easy to see how a multiplicity-forbidden radiationless process can favorably compete with multiplicity-allowed radiative transitions. Thus the rapid rate of intersystem crossing which has been a matter of speculation for some years is explained by the theory.

It has been well known for some time that, while intersystem crossing is fast, the apparently analogous process of triplet quenching (lowest triplet to ground singlet radiationless transition) is sufficiently slow in solid media that very long-lived ($\tau \approx 10$ sec) triplet→ ground-state light emission can be observed. This phenomenon is also explained by the theory since, as the electronic energy difference ΔE becomes large, the vibrational overlap integrals become small and $W(t)$ is accordingly reduced for such processes. Therefore it is the Franck–Condon principle applied to radiationless transitions which accounts for the slowness of triplet state quenching in solid media.[8] Other experimental evidence in qualitative support of this contention concerns the effect of deuterium substitution on the rate of triplet quenching[3,8,34] and the increased im-

[34] M. R. Wright, R. P. Frosch, and G. W. Robinson, J. Chem. Phys. 33, 934 (1960).

portance of the quenching process as the triplet state energy approaches that of the ground state.[3] Accurate quantum yield experiments are needed to test further the predictions of this part of the theory.[35] One also expects that quenching of the *lowest singlet state* will become important for small ΔE.

When ΔE is small and the vibrational factors are large, it can be shown that deuterium substitution does not substantially alter the vibrational overlap integrals. Thus isotopic substitution is not expected to modify intersystem crossing or internal conversion processes occurring among closely spaced electronic excited states. As a matter of fact, even in the quenching of excited states, the deuterium effect is expected to become less important as ΔE becomes smaller.

In conclusion it is important to point out that the present theory can also be applied to the important "excitation transfer" process $A^{\dagger}B \rightarrow AB^{\dagger}$, where the daggers signify electronic excitation, providing A and B are not identical molecules.[3] This limitation is imposed since our theory is valid only if the inequality $\Delta E \gg \alpha \gg \hbar \tau_{el}^{-1}$ holds. Again, deuterium effects are not expected except in those processes where a large amount of electronic energy is converted into vibrational energy of the system.

[35] Two recent experimental results, one reported by J. H. van der Waals[36] and the other by E. C. Lim,[37] give qualitative support for the theory.

[36] M. S. de Groot and J. H. van der Waals, Mol. Phys. **4**, 189 (1961).

[37] E. C. Lim, J. Chem. Phys. **36**, 3497 (1962); absolute quantum yield measurements of the fluorescence and phosphorescence of C_6H_6.

C. Electronic Excitation Transfer and Relaxation*

G. W. ROBINSON† AND R. P. FROSCH‡

Gates and Crellin Laboratories of Chemistry,§ California Institute of Technology, Pasadena, California

One purpose of this paper is to point out that so-called intermolecular resonance transfer, intermolecular nonresonance transfer, and intramolecular electronic relaxation in solid media are simply all special cases of radiationless transitions between nonstationary states of the entire system of molecules plus environment. Intermolecular resonance transfer is also a special case of the pure crystal exciton problem. The theoretical results from a previous paper are applied to radiationless transitions in π-electron systems, and the importance of the Franck–Condon factors is emphasized. One role which the vibrational factors play in these processes is illustrated by the large isotope effects which can arise when the radiationless transition converts a large amount of electronic energy into vibrational energy of the system. Quantitative calculations are made of the radiationless transition probability for $^1B_{2u} \rightarrow ^3E_{1u}(S_1 \rightarrow T_2)$ and $^1B_{2u} \rightarrow ^3B_{1u}(S_1 \rightarrow T_1)$ "intersystem crossing" in C_6H_6. It is further shown that the $^3B_{1u} \rightarrow ^1A_{1g}(T_1 \rightarrow S_0)$ and $^1B_{2u} \rightarrow ^1A_{1g}(S_1 \rightarrow S_0)$ processes and other similar processes are slow because of the small vibrational factors which accompany the large energy gap between initial and final electronic states. Calculations cannot rule out the relative importance of the $S_1 \rightarrow S_0$ radiationless transition compared with fluorescence and singlet–triplet nonradiative processes. An empirical method by which the Franck–Condon factors may be ascertained from the electronic-energy gaps in π-electron molecules is presented, and the results are used to estimate radiationless transition probabilities for a number of systems. The enhancement of multiplicity forbidden radiationless transitions by a heavy-atom environment is treated, and, in the case where the environment is a solid rare gas, a third-order mechanism accounts for the observed effect. Temperature effects and other kinds of environmental effects upon nonradiative transitions are also dealt with. It is shown that the use of high-energy excitation may increase, but never decrease, Q_P/Q_F, the relative quantum yields of phosphorescence to fluorescence. Radiationless transitions for the interesting case of azulene and the enhancement by a heavy-atom environment of the triplet–triplet emission spectrum of this molecule are discussed. Many needed experiments are suggested throughout the paper.

CONTENTS

This paper is divided into sixteen sections whose headings are as follows:

I. INTRODUCTION

THE absorption of light by a molecule in a dense medium may lead to a number of different consequences. All the electronic energy may be converted into heat; it may be partially converted into heat, and the remainder of the energy may be radiated or be used in a photochemical reaction, or the electronic energy may be transferred to other nearby molecules, with or without the conversion of part of the energy into heat. These molecules can themselves then undergo processes peculiar to a molecule in an electronic excited state. Such mechanisms are of great importance in problems concerned with photochemistry and radiation damage in the solid or liquid state. It is the purpose of this paper to give a semiquantitative discussion of the rates at which such mechanisms occur and to point out clearly the similarities in, and differences among, the various types of radiationless transitions which can occur in a dense medium.

The nonradiative process which converts electronic

energy into heat is analogous to vibrational relaxation and may therefore be termed *electronic relaxation*. This process is often loosely called "energy transfer." It may also be termed "nonresonance excitation transfer" for those intermolecular processes where electronic excitation is transferred between unlike donor and acceptor molecules. The excess electronic energy in this case is changed into vibrational energy of the acceptor and the surroundings. Nonresonance[1] excitation transfer and the intramolecular electronic relaxation phenomena, called internal conversion and intersystem crossing,[2,3] will be shown in this paper to be equivalent types of radiationless transitions between degenerate, nonstationary states of the over-all system. Certain aspects of the electronic relaxation problem have been discussed previously by Förster,[4,5] by Dexter,[6] and by Simon.[7] There will consequently be some overlap between parts of these papers and the present paper.

The "resonance excitation transfer" process where electronic excitation is transferred between like molecules in a dilute solid solution is a further example of an electronic radiationless transition. This process will be shown to have an entirely different time dependency than the nonresonance process. Since the resonance process is fundamentally identical to that met in the pure crystal exciton problem, little is said about it in this paper. The reader is referred to the papers by Peierls,[8] by Frenkel,[9,10] by Franck and Teller,[11] by Davydov,[12] by Simpson and Peterson,[13] and to the review article by McClure.[14]

II. SYSTEM

Since we are talking about dense media, the systems under discussion consist of molecules of interest (the guest or the solute) plus the surrounding medium (the host or the solvent). It is usually convenient to define a set of zero-order states of the *whole system* which are eigenstates of a certain incomplete Hamiltonian H_0. The difference H' between the complete and incomplete Hamiltonians constitutes perturbation terms

[1] The terms resonance and nonresonance in this paper refer to *electronic energies only*. For all the radiationless transitions discussed, the final states are always in close resonance with the initial states when vibrations are included.

[2] M. Kasha, Chem. Revs. **41**, 401 (1947).

[3] M. Kasha, Discussions Faraday Soc. No. **9**, 14 (1950).

[4] Th. Förster, Discussions Faraday Soc. **27**, 7 (1959).

[5] Th. Förster, *Comparative Effects of Radiation* edited by M. Burton, J. S. Kirby-Smith, and J. L. Magee (John Wiley & Sons, Inc., New York, 1960), p. 300.

[6] D. L. Dexter, J. Chem. Phys. **21**, 836 (1953).

[7] Z. Simon, Rev. phys. (Acadamie de la Republique Populaire Roumain). **6**, 105 (1961).

[8] R. P. Peierls, Ann. Physik **13**, 905 (1932).

[9] J. Frenkel, Phys. Rev. **37**, 17 (1931); **37** 1276 (1931).

[10] J. Frenkel, Physik. Z. Sowjetunion **9**, 158 (1936).

[11] J. Franck and E. Teller, J. Chem. Phys. **6**, 861 (1938).

[12] A. S. Davydov, Zhur. Eksptl. i Teoret. Fiz. **18**, 210 (1948).

[13] W. T. Simpson and D. L. Peterson, *J. Chem. Phys.* **26**, 588 (1957).

[14] D. S. McClure, *Solid State Physics*, edited by F. Seitz and D. Turnbull (Academic Press Inc., New York, 1959), Vol. 8, p. 1.

which cause the zero-order states to be nonstationary.[14] A measuring device capable of distinguishing between the nonstationary zero-order states, and rapid compared with the frequency of the oscillatory time factors in the squared moduli of the nonstationary eigenfunctions, is able to follow decay and buildup of the "initial" and "final" states of the system. *In this paper the terms initial state and final state always imply nonstationary states of the system.* It is important to distinguish between *resonance interactions* where the *electronic* energy difference[16] ΔE between the zero-order states is much smaller than the matrix element of the perturbation mixing these states, and *nonresonance interactions* where ΔE is much larger than this matrix element. These are well-defined mathematical limits in the theory of radiationless transitions, and each limit results in an entirely different expression for the transition probability. This and other important mathematical limits are discussed in Sec. VI of this paper.

One example[15] of electronic relaxation concerns intramolecular multiplicity forbidden transitions of the type $S_1 \rightarrow T_1$ and $T_1 \rightarrow S_0$, where S_0 is the ground state, assumed to be singlet, and S_1 and T_1 are the first excited singlet and triplet states of the molecule under consideration. If the system is highly dilute so that resonance interactions between different solute molecules directly or through low-lying virtual states of the solvent can be neglected,[17] then the electronic excitation is localized in the vicinity of the solute. For weak solvent–solute interactions, the initial and final electronic states of the whole system are then to a good approximation two different electronic states of the free solute molecule. The criterion for energy conservation can be met since a change in vibrational energy may occur in the transition.

Another prototype example of energy transfer concerns the transfer of excitation between two different molecules in a solid medium. The initial and final states for the process are again nonstationary states of the whole system. The initial state may consist of an electronically excited molecule A and a molecule B in its ground electronic state. The final state is that where B is excited and A is not excited. If the initial and final states do not have the same electronic energy, energy conservation again may be attained through a change in vibrational energy of the system.

In the simplest kind of system the major role of the solvent in the radiationless transition is to act as a

[15] G. W. Robinson and R. P. Frosch, Paper I in this series, J. Chem. Phys. 37, 1962 (1962).

[16] In Paper I, the terms *electronic energy difference* and *energy gap* were used to mean entirely different things. In this paper the terms are used synonymously and are given the symbol ΔE.

[17] To see what happens in the case where this neglect is not valid, one should consult a forthcoming paper by H. Sternlicht, G. C. Nieman, and G. W. Robinson, J. Chem. Phys. (to be published), and footnote 36 of this paper.

collection of phonon oscillators, coupled to the molecular vibrations, into which energy in the form of lattice vibrations (heat) may ultimately flow. In more complicated systems, the solvent not only serves the above function but also modifies, relative to that in the free solute molecule, the perturbation mixing initial and final zero-order states of the system. A good example is the effect of a heavy-atom environment on multiplicity forbidden radiationless transitions. The magnitude of this effect, it will be shown, depends upon the availability of solvent electronic states, the electrostatic interaction between solute and solvent, as well as the strength of the spin–orbit coupling in the solvent. In general the differentiation between electronic states associated with the solute and those associated with the whole system becomes less precise as the zero-order electronic energy levels of the solvent approach those of the solute.

III. PERTURBATION

Those parts of the total Hamiltonian which are to be included in the perturbation H' are by no means arbitrary but depend upon the experiment of interest.[16] Any term in H' which is so large that no designed experiment can follow the time factors associated with it must be included as part of the zero-order Hamiltonian. On the other hand, small terms in H' can be associated with physically detectable time variations of the zero-order eigenfunctions. *It is important to realize that H_0 and H' refer to the entire system of molecules plus surroundings.* The Hamiltonian H_0+H' therefore contains terms originally present in the free molecules possibly modified by the surroundings, terms belonging to the surroundings possibly modified by the presence of the molecules, and terms representing coupling among the molecules and their surroundings. Providing they are sufficiently small, terms in any of the above three categories can be associated with experimentally observable radiationless transitions.

While Gouterman[18] in a recent paper has put strong emphasis on the importance of lattice vibrations in one class of molecular radiationless transitions, we believe that lattice vibrations will, except in special cases, only slightly modify the pertinent perturbation terms which are already present in the free-molecule Hamiltonian. Our point of view relative to the intramolecular electronic relaxation problem has already been discussed in Paper I. For radiationless processes involving more than one molecule we also feel no need to consider the effects of lattice vibrations on H'. Our view simply assumes as a first approximation the factorization of the total system eigenfunction into an electronic part, a molecular vibrational part, and a part associated with lattice vibrations. In addition to

[18] M. Gouterman, J. Chem. Phys. **36**, 2846 (1962)

purely electronic contributions to the perturbation Hamiltonian, terms representing the coupling between electronic and vibrational motions must also be present. The opinion held by us takes the purely electronic terms in H' or at most *molecular* vibronic coupling terms as giving the most important contributions to the matrix element associated with electronic radiationless transitions. We do not, of course, neglect the degeneracies created by the lattice levels, the mechanical coupling between the lattice modes and the molecular vibrations, nor the effect of lattice vibrations on the Franck–Condon factors in the interaction matrix elements. As stated in Paper I, however, we believe that for radiationless transitions associated with polyatomic molecules the molecular vibrational contributions greatly dominate the role played by the phonons in the Franck–Condon factors.

IV. TRANSITION PROBABILITY

The radiationless transition probability is easily calculated in two special cases, that where *a resonance interaction between an electronic initial state and an electronic final state occurs*, and that where *an initial state of the system is coupled weakly to a very large number of final states in near resonance with the initial state.*

In the first case (case 1, Sec. VI) it is well known[19] that for an initial condition where the system is in the initial state ψ' at $t=0$, the time variation is described by the expression,

$$(\cos^2\beta t/\hbar)\psi'^2 + (\sin^2\beta t/\hbar)\psi''^2. \qquad (1)$$

In Eq. (1), β is the matrix element of the perturbation between initial and final states. Specifically,

$$\beta = \int \psi'' H'\psi' d\tau \equiv \langle \psi'' \mid H' \mid \psi' \rangle. \qquad (2)$$

It is clear that a measuring process which is rapid compared with a time scale $t \approx \hbar\beta^{-1}$ and capable of distinguishing between ψ' and ψ'' would be able to follow the time variation of the eigenfunctions. Thus, for resonance interactions, a decay of the initial state occurs in a time interval $t = h/4\beta$, and a subsequent buildup of the initial state again occurs after another interval of $t = h/4\beta$, providing there is no mechanism which quenches ψ' or ψ''. An example of this type of energy transfer process occurs in the case where two identical guest molecules are present in the host. The initial state is that where the first molecule is electronically excited and the other is in its ground state. A transition to the final state, where the second molecule is excited and the first is in its ground state, occurs in an average time $t_{\mathrm{avg}} = h/4\beta$.

[19] L. Pauling and E. B. Wilson, Jr., *Introduction to Quantum Mechanics* (McGraw-Hill Book Company, Inc., New York, 1935), pp. 322–325.

The other situation where the radiationless-transition probability may be computed exactly is that where there is a very large number of final states which are coupled to the initial state in an elementary way. A simple but realistic model for this radiationless process was treated rigorously in Paper I. It was shown there that two limits exist; namely, that where $\Delta E \gg \alpha \gg \beta$ and that where $\Delta E \gg \beta \gg \alpha$. Here β is the matrix element mixing initial and final vibronic states, and α is an average coupling energy between the lattice modes and the molecular vibrational modes. The limit $\Delta E \gg \alpha \gg \beta$ is the limit of physical interest for relatively slow radiationless transitions such as most $S_1 \rightarrow S_0$, $S_1 \rightarrow T_1$ and $T_1 \rightarrow S_0$ intramolecular transitions (case 3, Sec. VI) and for many transitions between two different molecules in a solid where the purely electronic initial and final states are not in resonance (case 2, Sec. VI). A special solution to the radiationless-transition problem in the limit $\Delta E \gg \alpha \gg \beta$ is given by,[1b]

$$w(t) = \frac{2\beta^2}{(N+1)\alpha^2} \sum_{r=1}^{N} \tan^2\left[\frac{r\pi}{N+1}\right] \sin^2\left[\frac{\alpha t}{\hbar}\cos\frac{r\pi}{N+1}\right], \quad (3)$$

where N is the number of states in the final state band defined by α, and r labels these states. In the physically important case where N is very large

$$w(t)/t \approx 2\beta^2/\alpha\hbar. \quad (4)$$

The result is very similar to that obtained from a continuum model[6,20,21,22] for the final states, but the derivation is more illuminating for our purposes since the criteria for its validity, $\beta \ll \alpha$ and N large, are more firmly spelled out. In addition, the usual fuzziness introduced by the normalization of continuum states is not present.

Since $\hbar\alpha^{-1} \approx \tau_{\text{vib}}$, where τ_{vib} is the vibrational relaxation time for loss of a single vibrational quantum, Eq. (4) may be written,

$$w(t)/t \approx 2\beta^2\hbar^{-2}\tau_{\text{vib}}. \quad (5)$$

Equation (5) is useful since τ_{vib} is related to linewidths (Sec. IX) which are experimentally obtainable quantities. Here, however, one must beware of experimental line broadening caused by extraneous effects. Extraneous line broadening shows up on the zeroth vibrational level as well as upon the higher levels and is not related to the vibrational relaxation time.

When more than one *directly coupled final state* is involved, $w(t)/t$ must be summed over all such final

[20] W. Pauli, *Handbuch der Physik*, edited by S. Flügge (Springer-Verlag, Berlin, 1933), 2nd ed., Vol. XXIV, p. 160.

[21] D. R. Bates, in *Quantum Theory Vol. I—Elements*, edited by D. R. Bates (Academic Press Inc., New York, 1961), pp. 264–268.

[22] L. I. Schiff, *Quantum Mechanics* (McGraw Hill Book Company, Inc., New York, 1955), 2nd ed., Chap. VIII.

tronic-energy gap, since the energy difference must be accounted for by excitation of a large amount of vibrational energy in the final states. Under such conditions the effect of anharmonicities on energy-transfer phenomena indeed exists but is probably not of dominant importance.[18]

For polyatomic molecules, the vibrational overlap integral $\langle \phi'' \mid \phi' \rangle$ in Eq. (8) is a fairly complicated function when there is a large energy gap. When the initial electronic state is in its lowest vibrational state the integral becomes

$$\langle \phi'' \mid \phi' \rangle = \prod_r \langle \phi_{v_r}(q_r'') \mid \phi_0(q_r') \rangle. \tag{9}$$

This is a low-temperature result important in most experiments. In Eq. (9), v_r is the quantum number for the rth normal mode and q_r is the rth normal coordinate referred to the entire system. The product is over all *molecular* and *lattice* normal modes which contribute to the directly coupled final state. In general a large number of directly coupled final states are possible, and the number increases with increasing ΔE. Thus the decrease of β for large ΔE, because of diminished Franck–Condon factors, is partially compensated for by the increased degeneracy of directly coupled final states. It is the summation over such directly coupled states which defines $W(t)$ in terms of the individual quantities $w(t)$. Since it is the square of the overlap integral which enters the expression for the transition probability and since these vibrational parts of $W(t)$ are assumed to factor from the electronic part, a sum of squares of the overlap integrals over all directly coupled states enters into all the equations. We designate this over-all vibrational factor as $\langle \phi'' \cdot \phi' \rangle_{\text{tot}}^2$. The counting of the directly coupled final states, each with its own vibrational factor, presents the most serious problem in any *a priori* calculation of nonresonance molecular radiationless transitions. Perhaps an empirical approach to the evaluation of the Franck–Condon factors will, in the end, be the best. A preliminary discussion is given in Sec. XI of this paper. In any case, more knowledge concerning the change of vibrational coordinates and frequencies upon electronic excitation would be of immense help in the quantitative evaluation of these factors.

VI. STRONG AND WEAK COUPLING AND THE MASTER EQUATIONS

In Sec. IV it is stated that Eqs. (4) and (5) are valid only in the well-defined mathematical limit $\Delta E \gg \alpha \gg \beta$. This is the limit where the electronic transition time τ_{el} for a nonresonance process is slow compared with the vibrational relaxation time τ_{vib}. Thus it is not only the convenience of dealing with a Boltzmann distribution of vibrational levels in the initial state which causes this limit to be important.

The other important nonresonance limit $\Delta E\gg\beta\gg\alpha$ is also of interest since here the vibrational relaxation process determines the over-all electronic relaxation time. Transitions back and forth between the initial state ψ' and the final state ψ'' take place rapidly compared with the vibrational relaxation time. The transfer of molecular electronic excitation energy to the lattice then depends upon the rate at which vibrational energy is redistributed among the molecular and lattice vibrational levels associated with the electronic states represented by the appropriate linear combinations of ψ' and ψ''. An interesting consequence of this limit occurs in regions where there is a moderately high density of electronic states. This subject will be discussed in Sec. XIV of this paper.

For the case of resonance interactions, $\Delta E\ll\beta$, there is no vibrational relaxation process in the final state. This limit is precisely that met in the crystal exciton problem and itself has two sublimits; namely, that where β is of an order much smaller than the Franck–Condon bandwidth between initial and final states, and that where β is much larger than the Franck–Condon bandwidth. These limits are the well-known Simpson–Peterson (SP)[13] limits of weak and strong coupling, respectively. A subsidiary limit exists when β is less than lattice vibrational energies.[11] There is no fundamental difference between intermolecular interactions in pure crystals and interactions between identical solute molecules in a solid solution. Therefore, the theory of Simpson and Peterson in the strong, intermediate, or weak coupling limits is perfectly applicable to the intermolecular resonance excitation transfer problem. For resonance transfer between solute molecules in a dilute mixed crystal, the weak coupling limit is probably always appropriate. For this reason the SP weak coupling limit is of greatest interest in this paper. Even in the case where the two molecules are not alike and ΔE is not zero, the theory in the resonance limit is applicable providing $\Delta E\ll\beta$.

Franck and Teller[11] have given a beautiful qualitative description of the meaning of the limits met in the resonance interaction problem. A paper stressing the importance of various limits has also been presented recently by Förster.[5] This paper apparently does not directly consider the nonresonance case where ΔE, the electronic-energy gap, is large compared with β and α (Förster's $|u|$ and ϵ', respectively), even though this is the limit with which the earlier papers of Förster dealt. In reference 5 Förster defines a case c where the electronic interaction is smaller than lattice coupling energies ($\beta\ll\alpha$ in our notation), and cites it as an example of a system where the nonradiative transition follows an equation like our Eq. (4). It is important to stress that this can be true for transfer between vibrationless, electronically degenerate states only in the case where the density of available final

states is high, i.e., when there is some important quenching process associated with the *zeroth vibrational level* of the electronic excited state of the acceptor. In many problems where electronic energy is transferred among identical molecules in a mixed or pure crystal the lifetime of this zeroth vibrational level is long compared with the transfer time. For such cases the usual Förster equation, which is basically equivalent to our Eq. (4), does not apply, and an equation like our Eq. (10) must be used.

It suffices to say that intermediate cases yield complicated time dependencies for the initial to final state transition. Fortunately, there are a large number of interesting experimental systems which illustrate the limiting cases. Interest in the intermediate cases will grow more rapidly after simple cases are better understood. *It is important to realize that all these problems which deal with radiationless transitions between states of the over-all system require the same fundamental theoretical approach treated in different mathematical limits.*

The transition probability expressions inclusive of the vibrational factors for three important weak-coupling cases are given below.

1. Intermolecular Resonance Transfer

$\psi_A{}^\dagger\psi_B \rightarrow \psi_A\psi_B{}^\dagger$, $\Delta E \ll \beta$, SP weak coupling.

$$t_{avg}{}^{-1} = 4h^{-1}\langle\phi_A{}^\dagger \mid \phi_A\rangle\langle\phi_B{}^\dagger \mid \phi_B\rangle\beta_{el}, \qquad (10)$$

where

$$\beta_{el} = \langle\Theta_A{}^\dagger\Theta_B \mid H' \mid \Theta_A\Theta_B{}^\dagger\rangle,$$

and (†) distinguishes between zero-order electronic states. In the usual case, A and B are identical molecules, the † state is an electronic excited state, the †'-less state is the ground electronic state, and for low temperatures all the vibrational eigenfunctions refer to the zeroth vibrational state in each electronic state. The magnitude of the electronic matrix element β_{el} depends strongly on the "allowedness" of the transitions $\psi_A \rightarrow \psi_A{}^\dagger$ and $\psi_B \rightarrow \psi_B{}^\dagger$. For many electronic states of interest, higher-order contributions to β_{el} may dominate the usual dipole term (see Sec. VIII). The value of β_{el} decreases rapidly with increasing separation of molecules A and B so that the SP weak coupling case is always valid in sufficiently dilute solid solution. It is noteworthy that, even though there has been no change of vibrational energy, the Franck–Condon factors do not in general reduce to unity since the potential surfaces are different for the two electronic states. For most molecules the overlap integrals are of the order of 0.2 to 1.0, making the over-all vibrational factors 0.04 to 1.0.

2. Intermolecular Nonresonance Transfer

$\psi_A{}^\dagger\psi_B \rightarrow \psi_A\psi_B{}^\dagger$, $\Delta E \gg \alpha \gg \beta$.

$$w(t)/t = 2\hbar^{-2}\tau_{vib}[\langle\phi_A{}^\dagger \mid \phi_A\rangle\langle\phi_B{}^\dagger \mid \phi_B\rangle]^2\beta^2{}_{el}. \quad (11)$$

This is the case treated by the Förster theory (see

Sec. VIII). Equation (11) follows from Eq. (5) if one takes the initial state of the system to be $\psi_A{}^\dagger \psi_B$ and the final state to be $\psi_A \psi_B{}^\dagger$. In Eq. (11) β_{el} has precisely the same form as it has in Eq. (10) but now enters as a square rather than a first power. Since this is the intermolecular nonresonance case, A and B must correspond to two different molecules having different electronic energies. They must have the same *vibronic* energies, however, because energy must be conserved in nonradiative transitions. At low enough temperatures the initial state is the zeroth vibrational state of $A^\dagger$ and of B, but the final state corresponds in general to excited vibrational levels of both A and $B^\dagger$. The individual vibrational factors here are usually smaller[5] than in the previous case not only because of the 4th power dependence upon overlap integral but also because ΔE is nonzero. The summation over all $w(t)/t$ compared with only a single-term contribution in Eq. (10) may partially compensate for this, however. The vibrational factors in Eq. (11) are not simple to determine because a sum must be carried out over all directly coupled final states, and an entire set of such states, each with its own vibrational factor, exists. Each of these states involves different vibrational excitations of A and $B^\dagger$ and lattice modes in such a way that total energy is conserved. It should be stressed that even though β_{el} itself may be much larger than α, the small vibrational factors appearing in Eq. (11) reduce the over-all matrix elements β. The inequality $\Delta E \gg \alpha \gg \beta$ therefore is valid for many systems of physical interest. An experimental example of case 2 is any "sensitized" fluorescence or phosphorescence phenomenon providing $\Delta E \gg \alpha \gg \beta$. If the inequality $\alpha \gg \beta$ does not hold, then, as mentioned previously, excitation "oscillates back and forth" between $\psi_A{}^\dagger \psi_B$ and $\psi_A \psi_B{}^\dagger$ until a vibrational relaxation process occurs. In this situation vibrational relaxation becomes rate determining, and Eq. (11) does not apply.

3. Intramolecular Nonresonance Transfer

$\psi_A{}^\dagger \to \psi_A$, $\Delta E \gg \alpha \gg \beta$.

$$w(t)/t = 2\hbar^{-2}\tau_{\mathrm{vib}}[\langle \phi_A{}^\dagger \mid \phi_A \rangle]^2 \beta_{el}{}^2, \qquad (12)$$

where

$$\beta_{el} = \langle \Theta_A{}^\dagger \mid H' \mid \Theta_A \rangle.$$

This is the case dealt with in the first paper of this series. Here, the vibrational eigenfunction in the initial (†) state refers to the zeroth vibrational state, while that in the final state corresponds to vibrational excitation equal approximately to ΔE. A sum over $w(t)$ yields $W(t)$ so that an equation for $W(t)$ similar to Eq. (12) holds providing $\langle \phi_A{}^\dagger \mid \phi_A \rangle_{\mathrm{tot}}{}^2$ is used for the vibrational factor. Experimental examples of case 3 are $S_1 \to T_1$, $S_1 \to S_0$, and $T_1 \to S_0$ radiationless transitions. The actual crossing of potential-energy surfaces

belonging to the initial and final electronic states is a special case where the vibrational factor becomes very large; i.e., of the order of unity. It is important to note that a large, discontinuous increase in transition probability near a "cross-over" region between nondissociative states may not occur since the Franck–Condon factor does not necessarily change in this way. The change actually may be a very gradual one in such regions. In regions where the density of electronic states is sparse, it is not likely that potential surface crossing in the vicinity of the lowest vibrational level of the initial electronic state is of very common occurrence anyway. It should be realized that classical crossing of potential-energy surfaces is not necessary for rapid radiationless transitions to occur, since the vibrational eigenfunctions are not bound by the potential surfaces, and quantum mechanical penetration between potential surfaces can take place. This effect is expected to be especially prominent when the molecule contains light atoms.

In all cases it is well to remember that the Franck–Condon factors contain contributions from the lattice as well as from the molecule. It is well known that certain vibrational factors may be obtained directly from the Franck–Condon envelopes for radiative transitions, since these factors appear unchanged in the expressions for the radiative transition probabilities. In the first case above when both initial and final state vibrational eigenfunctions refer to the zeroth state, the factors $[\langle \phi_A^\dagger | \phi_A \rangle]^2$ and $[\langle \phi_B^\dagger | \phi_B \rangle]^2$ may be determined from the intensity of the $(0,0)$ band relative to the total electronic intensity for the emission or absorption processes, $\psi_A^\dagger \leftrightarrow \psi_A$ and $\psi_B^\dagger \leftrightarrow \psi_B$. In Case 2, the excess electronic energy ΔE may be distributed in different ways over vibrational quanta of the states ψ_A and $\psi_B^\dagger$. For the case where ψ_A is the ground state of A and ψ_B is the ground state of B, Förster[28] has used an integral over the product of emission $\psi_A^\dagger \leftrightarrow \psi_A$ and absorption $\psi_B^\dagger \leftrightarrow \psi_B$ band envelopes as a measure of the vibrational factors. For those cases where the overlap integral is large, this approximation is probably a good one. On the other hand, for slow radiationless transitions an extrapolation into the high quantum number "tail" of the Franck–Condon envelope is dangerous since the falloff of Franck–Condon factors is different for different modes of vibration. For example, the dominant contribution to the breadth of the Franck–Condon envelope for π–π^* transitions in π-electron systems arises from the C—C modes. On the tail of the envelope, however, where the vibrational quantum numbers are much larger than those which correspond to the Franck–Condon maxima, calculations[29] show that C—H modes dominate the effect of the C—C modes.

[28] Th. Förster, Ann. Physik 2, 55 (1948).
[29] R. P. Frosch, unpublished results.

The Franck–Condon factors in Eqs. (11) and (12) can lead to a large isotope effect providing the electronic-energy gap ΔE is sufficiently large. An isotope effect on "intermolecular" excitation transfer has not been reported, but for the "intramolecular" case a large effect upon the $T_1 \rightarrow S_0$ radiationless transition in π-electron systems occurs. This is evidenced since the over-all lifetime of the triplet state is measurably shorter in perprotonated benzene,[30,31] naphthalene,[32,33] and anthracene[34] than in the respective perdeuterated molecules. The presence of the radiationless transition is consistent with quantum yield measurements which have been carried out in the case of benzene[35] and naphthalene.[33,35] For large energy gaps the dominant contribution to the vibrational factor comes from high-frequency modes associated with normal coordinate and frequency differences in the initial and final electronic states. For the same energy gap, low-frequency vibrations correspond to very high quantum numbers and thus yield small overlap integrals.[31]

When the energy gap is relatively small, such as in most intramolecular transitions of the type $S_1 \rightarrow T_1$ and in all intermolecular excitation transfers which have been studied, a relatively small isotope effect is expected since the magnitude of the vibrational factor near the Franck–Condon maximum does not have a strong mass dependence.

VIII. COMPARISON WITH FORSTER'S THEORY OF ENERGY TRANSFER

Förster's expression[4,28] for excitation transfer is applicable only for our case 2 of Sec. VI and only then when the interaction is dipole–dipole. A very pertinent paper on this subject, where the dipole–dipole theory is clearly derived and extended to the interesting case where one or both of the transition dipoles vanish, has been presented by Dexter.[6] Dexter's paper is primarily concerned with atomic systems but applies equally well to molecular systems if the integrals over the continuous energy variables in, for example, his Eq. (5) are replaced by vibrational overlap integrals. A summation over the directly coupled final states, similar to what Dexter calls a "sum over all possible transitions," must be carried out. Our Eq. (4) $w(t)/t \approx 2\beta^2\alpha^{-1}\hbar^{-1}$, is related to Dexter's Eq. (1)

$$P_{sa} = 2\pi\hbar^{-1}\rho_E \left| \int \psi_I{}^* H_1 \psi_F d\tau \right|^2,$$

[30] M. R. Wright, R. P. Frosch, and G. W. Robinson, J. Chem. Phys. **33**, 934 (1960).

[31] G. W. Robinson, J. Mol. Spectroscopy **6**, 58 (1961).

[32] C. A. Hutchison and B. W. Mangum, J. Chem. Phys. **32**, 1261 (1960).

[33] M. S. de Groot and J. H. van der Waals, Mol. Phys., **4**, 189 (1961).

[34] J. H. van der Waals (unpublished).

[35] E. H. Gilmore, G. E. Gibson, and D. S. McClure, J. Chem. Phys. **20**, 829 (1952); J. Chem. Phys. **23**, 399 (1955); E. C. Lim, J. Chem. Phys. **36**, 3497 (1962).

through our normalization procedure. We do not go into detail here since this was done in Paper I.[15] However, *the relationship between the above two equations* is made clear when the following points are considered. For N final states coupled together by a molecular-lattice coupling matrix element α, the final states form an energy band of approximate width α. Providing vibrational relaxation is the important mechanism for broadening of the final-state levels, the density of final states ρ_E is then roughly equal to N/α. The interaction matrix element, because of normalization, divides itself among all the N final states with a coefficient roughly equal to N^{-1} so that N vanishes in the final expression. Therefore, except for a factor of π, the two equations become identical. The reason that the transition probability $w(t)$ in Eq. (5) decreases for short vibrational relaxation times follows, since a short time corresponds to a wide final-state energy band where the density of states is small. As mentioned at the end of Sec. IV and in Paper I, this sort of dependence will be largely lost in the expression for $W(t)/t$.

Since Dexter in his Eqs. (6)–(16) shows how Förster's expression follows from the basic transition probability expression, it will not be done here. It should be remembered, however, that the dipole–dipole theory is of practical importance in only a limited number of cases. This has been pointed out many times before by Förster[4,5] and others, but experimentalists still *attempt to fit data to this theory* when it is totally inapplicable. A number of other considerations should also be borne in mind when using Förster's equation. In the first place, the interaction may take place directly, or it may take place indirectly through the virtual electronic states of the solvent. For high-lying solvent states a factor which corrects for the field in a dielectric medium[6] may account approximately for the indirect interaction. On the other hand, when the solvent electronic states are low-lying, the effective matrix element for the interaction between solute molecules through these solvent states may be orders of magnitude *larger* than that for interaction through a vacuum.[36] Thus, Förster's formula sets only a lower limit to the transition probability in such solids. If the interaction takes place at too small a distance then the matrix element β becomes larger than α and the basic theory becomes inapplicable. At large distances retardation effects which change the R dependence become important. For excited states involving a change in multiplicity, exchange

interactions,[6,37] charge transfer interactions,[38] or second-order perturbation contributions, all of which have a different R dependence than the dipole–dipole interaction, are of dominant importance. Even when there is no multiplicity change, the low-lying transitions in many classes of polyatomic molecules are of a forbidden type, $f<0.1$. In this case, as for many cases of resonance interactions in pure crystals, higher terms in the multipole expansion[39] or second-order perturbation contributions may dominate the dipole–dipole interaction, and an R^{-6} dependency is not expected. *It is just these lowest states of a molecule which are often the ones of greatest interest in the energy-transfer process.* The statistical nature of the distribution of solute molecules in a solid solution sometimes causes the very concept of R to become fuzzy, and certainly an average R is inappropriate. This last consideration is especially important when the solute molecules have a greater affinity towards one another than they do toward the solvent, in which case, in the solidification process, the statistical distribution may be distorted in favor of short intermolecular distances.

IX. QUANTITATIVE CALCULATIONS

The two main barriers to be surmounted in undertaking quantitative calculations of radiationless transition probabilities are the calculation of the electronic matrix element and the calculation of the Franck–Condon factors. In very few cases are both of these quantities available. Resonance interactions in the SP strong coupling limit present a good case for quantitative calculations since the details of the vibrational eigenfunctions are not important. Many such calculations have been performed for pure crystals,[14] not only in this limit but also in the more complicated case where the coupling is weak.[39] *It is worth pointing out, however, that even for very weak, higher-order coupling, excitation transfer transitions can occur in a time which is extremely short compared with excited-state radiative lifetimes.* A 0.001 cm^{-1} (2×10^{-19} ergs) interaction, for example, according to Eq. (10) leads to a transition time of about 10^{-8} sec. Nearest-neighbor interactions which cause singlet excitation migration are nearly always much greater than 1 cm^{-1} under the weakest kinds of coupling.[40] Nearest-neighbor interactions which

[37] R. E. Merrifield, J. Chem. Phys. **23**, 402 (1955); G. C. Nieman and G. W. Robinson, J. Chem. Phys. **37**, 2150 (1962).

[38] H. Sternlicht and H. M. McConnell, J. Chem. Phys. **35**, 1793 (1961).

[39] D. P. Craig and S. H. Walmsley, Mol. Phys. **4**, 113 (1961), and papers by other authors cited here.

[40] In the benzene crystal, octopole–octopole coupling is the lowest-order, nonvanishing term in the multipole expansion. Nevertheless, exciton interactions are probably of the order of 50 cm^{-1}, corresponding to more than 10^5 transitions per lifetime. D. Fox and O. Schnepp, J. Chem. Phys. **23**, 767 (1955). See also McClure (reference 13). Recent unpublished work by G. C. Nieman and G. W. Robinson, however, has shown that, while the magnitudes of the intermolecular coupling constants are roughly those given in the above papers, the detailed interpretation in this earlier work of the first singlet–singlet crystal spectrum of benzene is in serious error.

cause triplet excitation migration are probably also greater than 0.001 cm^{-1}, and here the long excited-state lifetime (in the solid phase) may cause *the number of radiationless transitions per triplet lifetime to be much larger than the number per singlet lifetime!*

For the nonresonance case $\Delta E \gg \alpha \gg \beta$, it usually happens that neither the matrix element nor the vibrational factors are readily obtainable quantities, but a fair approach to a quantitative calculation can be made for the $S_1 \rightarrow T$ radiationless transitions in C_6H_6. The electronic-energy levels for benzene are depicted in Fig. 1. The dotted levels are calculated by the Pariser–Parr[41,42] method which is probably not very reliable for the triplet states.[43] The $\pm$ superscripts refer to eigenstates formed by symmetric and antisymmetric combinations of configurations which are degenerate in the Hückel approximation. This property is useful later in the paper, but the notation is usually dropped. Radiationless transitions from the zeroth vibrational level of $S_1(^1B_{2u})$ to triplet states may take place by direct interaction with the $^3B_{1u}$ state. Here first-order spin–orbit mixing is formally allowed, but there is a fairly large energy gap. On the other hand, the interaction between $^1B_{2u}$ and triplet states may occur "indirectly" with an e_{2g} vibrational level in the $^3E_{1u}$ state by virtue of vibronic mixing between $^1B_{2u}$ and $^1E_{1u}$, and spin–orbit mixing between $^1E_{1u}$ and $^3E_{1u}$; or through vibronic mixing within the triplet manifold of $^3E_{1u}$ with $^3B_{1u}$ which also requires an e_{2g} vibration. Interaction between $^1B_{2u}$ and $^3B_{2u}$ is indirect, occurring most probably by vibronic mixing of $^3B_{2u}$ and $^3B_{1u}$. This mechanism requires an a_{2g} vibration. Only one fundamental of this symmetry exists in benzene. It involves predominantly a hydrogen motion and is not expected to be very effective in mixing π-electron states. In addition, the $^3B_{2u}$ state plus the appropriate vibration probably lies higher than the $^1B_{2u}$ state and would therefore contribute nothing to *the probability for radiationless transitions from the* $^1B_{2u}$ state at low temperatures. The $^1B_{2u} \rightarrow {}^3B_{2u}$ mechanism will therefore be neglected.

Some π-electron matrix elements of the spin–orbit operator in C_6H_6 have been calculated by Hameka and Oosterhoff[44] and by Clementi.[45] These calculations

[41] R. Pariser, J. Chem. Phys. **24**, 250 (1956), and earlier papers cited there.

[42] The $^1E_{2g}{}^+$ state is included for a later purpose. Its energy has been calculated to be 8.2 eV by Pariser and 7.7 eV by R. G. Parr, D. P. Craig, and I. G. Ross, J. Chem. Phys. **18**, 1561 (1950).

[43] In these calculations certain electron-repulsion integrals are left as empirical parameters. These are then evaluated from the experimental spectrum. Since the spatial eigenfunctions for the triplet states are not expected to be the same as those for the singlets, the values of the integrals cannot be carried over from the singlet states to the triplet states. Better estimates [see, for example, D. R. Kearns, J. Chem. Phys. **36**, 1608 (1962)] imply that the real $E(^3E_{1u}{}^+)$ is probably a few thousand cm^{-1} above 33 800 cm^{-1}. The qualitative aspects of our calculations, however, will not be changed appreciably by a subsequent upward revision of $E(^3E_{1u}{}^+)$ from the Pariser-Parr value used in the paper.

[44] H. F. Hameka and L. J. Oosterhoff, Mol. Phys. **1**, 358 (1958).

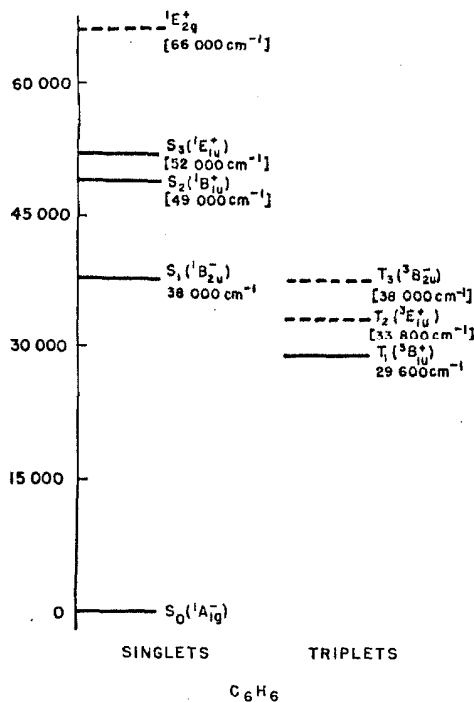[45] E. Clementi, J. Mol. Spectroscopy **6**, 497 (1961).

FIG. 1. Energy-level diagram showing the low-lying singlet and triplet electronic states of benzene. The dashed levels are taken from theoretical calculations.[41] The wavenumbers are for the *electronic origins*. Those values in square brackets are uncertain.

give 5.05×10^{-5} eV (0.41 cm^{-1}) and 4.05×10^{-5} eV (0.33 cm^{-1}) respectively for the ($^1E_{1u}$, $^3E_{1u}$) and ($^1B_{2u}$, $^3B_{1u}$) interactions. The matrix element for the vibronic interaction between $^1B_{2u}$ and $^1E_{1u}$ can be obtained from the known oscillator strengths for radiative transitions involving these states. Use is made of the assumption, which is almost certainly correct, that the major part of the intensity of the $^1B_{2u} \leftrightarrow {}^1A_{1g}$ transition is caused by ($^1B_{2u}$, $^1E_{1u}$) mixing. The oscillator strengths and the vibronic matrix element $\langle {}^1B_{2u} \mid H_{\mathrm{vib}} \mid {}^1E_{1u} \rangle$ are then mutually related by the perturbation expression

$$f_{\mathrm{B}} = f_{\mathrm{E}}(\nu_{\mathrm{B}}/\nu_{\mathrm{E}}) \left(\langle {}^1B_{2u} \mid H_{\mathrm{vib}} \mid {}^1E_{1u} \rangle^2 / \Delta E^2 \right) \qquad (13)$$

where $\Delta E = E(^1E_{1u}) - E(^1B_{2u})$. Using the values $f_{\mathrm{B}} = 0.0014$, $f_{\mathrm{E}} = 0.88$, $\nu_{\mathrm{B}} = 40\,300$ cm^{-1} and $\nu_{\mathrm{E}} = 56\,800$ cm^{-1}, respectively, for the oscillator strengths and *average* wavenumbers [not (0,0) bands] of the $^1B_{2u} \leftarrow {}^1A_{1g}$ and $^1E_{1u} \leftarrow {}^1A_{1g}$ transitions,[46,47] one finds that

$$\langle {}^1B_{2u} \mid H_{\mathrm{vib}} \mid {}^1E_{1u} \rangle = 780 \text{ cm}^{-1}.$$

For the calculation of the radiationless transition probability, the electronic matrix elements β_{el} mixing $^1B_{2u}$ with $^3B_{1u}$ and with $^3E_{1u}$ are required. The first is

[46] H. B. Klevens and J. R. Platt, as quoted by A. C. Albrecht, J. Chem. Phys. **33**, 169 (1960).
[47] V. J. Hammond and W. C. Price, Trans. Faraday Soc. **51**, 605 (1955).

0.33 cm^{-1}, coming directly from the above calculated value of Hameka and Oosterhoff.[44] One contribution to the second may be obtained from second-order perturbation theory,[48]

$$\langle {}^1B_{2u} \mid H' \mid {}^3E_{1u} \rangle$$

$$= \frac{\langle {}^1B_{2u} \mid H_{\mathrm{vib}} \mid {}^1E_{1u} \rangle \langle {}^1E_{1u} \mid H_{\mathrm{s.o.}} \mid {}^3E_{1u} \rangle}{\Delta E}, \quad (14)$$

where ΔE is the same as before. The first factor in the numerator on the RHS is the vibronic matrix element 780 cm^{-1}, and the second factor is, according to Clementi,[45] 0.41 cm^{-1}. The desired matrix element in Eq. (14) is therefore 0.02 cm^{-1}.

A second contribution to the interaction between the $^1B_{2u}$ state and the $^3E_{1u}$ state may arise from ($^1B_{2u}$, $^3B_{1u}$) spin–orbit mixing plus ($^3B_{1u}$, $^3E_{1u}$) vibronic mixing. For ($^3B_{1u}$, $^3E_{1u}$) mixing, the matrix element is unknown. If, however, the same vibronic matrix element as for the singlets is used, this contribution to the indirect ($^1B_{2u}$, $^3E_{1u}$) interaction is 0.03 cm^{-1}. The contributions from the two paths involving $^3E_{1u}$ therefore give $\langle {}^1B_{2u} \mid H' \mid {}^3E_{1u} \rangle \approx 0.05$ cm^{-1}. Other mixing mechanisms may be present which raise this value somewhat.

Using these matrix elements in Eq. (12) and the correct units, the calculated radiationless transition probabilities may be found providing the vibrational relaxation time and the vibrational factors are known. Certain limits on vibrational relaxation times for benzene in solid solution may be set. The fluorescence lifetime of the $^1B_{2u}$ state is about 6.6×10^{-7} sec.[49] In the usual solids, where something is known experimentally about the radiationless transition, the intensity of fluorescence from vibrational levels other than the lowest is so small that it has never been detected. As we will mention in Sec. XVI, in some other solids this is not the case. Let's say then that the vibrational relaxation time in "normal" solvents is at least 100 times shorter than the fluorescence lifetime, i.e., for the relaxation time, one obtains $\tau_{\mathrm{vib}} < 6.6 \times 10^{-9}$ sec. On the other hand absorption linewidths set a lower limit for τ_{vib}. Linewidths for transitions in benzene from the ground state to upper vibrational levels in the $^1B_{2u}$ state are known to be no greater than 1 cm^{-1} in certain solids (e.g., C_6H_6 in solid argon[31]). The linewidth is related to the lifetime of the state through the uncertainty relationship. Assuming the lifetime of

[48] P. A. M. Dirac, *The Principles of Quantum Mechanics* (Oxford University Press, New York, 1947), 3rd ed., pp. 178–180.

[49] Calculated from the oscillator strength $f=0.0014$. This value agrees quite well with the direct experimental value (5.9×10^{-7} sec) of J. W. Donovan and A. B. F. Duncan, J. Chem. Phys. **35**, 1389 (1961). The lifetime calculated from the oscillator strength in the Donovan–Duncan paper is in slight error. Using the values, $f=0.00147$ and $\nu_B=40\,100$ cm^{-1}, Donovan and Duncan have recalculated τ; they obtain 0.634 μsec.

these vibrational levels to be governed by the vibrational relaxation time, one obtains $\tau_{vib} > 0.5 \times 10^{-11}$ sec. Thus, the limits $0.5 \times 10^{-11} < \tau_{vib} < 6.6 \times 10^{-9}$ sec are set in this particular case. But this is not the vibrational relaxation time that we want! We want the vibrational relaxation time in the final electronic state, not in the initial state. The order of magnitude, nevertheless, should be about right for the following reason. It is true that the over-all vibrational relaxation process which involves many individual transitions is much faster in regions where the density of states is high. The τ_{vib} in Eq. (12), as previously emphasized, however, is not related to the over-all process. It is related to the mechanical coupling between final states and, therefore, refers to a single process. It is not expected that the coupling constant α varies by more than a factor of two or three among different electronic states except in those electronic states where solute–solvent interactions become excessively strong. We therefore assume $\tau_{vib} \approx 10^{-11}$ sec.

Using the above as a universal, but tentative, value of τ_{vib} one obtains from Eq. (12),

$$w(t) = (0.71 \times 10^{12}) \beta_{el}^2 \langle \phi'' \mid \phi' \rangle^2, \qquad (15a)$$

or

$$W(t)/t = (0.71 \times 10^{12}) \beta_{el}^2 \langle \phi'' \mid \phi' \rangle_{tot}^2, \qquad (15b)$$

where $w(t)/t$ and $W(t)/t$ have units of sec^{-1} and the unit of β_{el} has been chosen to be cm^{-1}. Following Eq. (15b) and using the appropriate matrix elements from above, the low-temperature radiationless transition probabilities in terms of vibrational factors for the two mixing mechanisms in C_6H_6 are

$$W(t)/t({}^1B_{2u} \rightarrow {}^3E_{1u})$$

$$= (0.18 \times 10^{10}) \langle \phi({}^3E_{1u}) \mid \phi_0({}^1B_{2u}) \rangle_{tot}^2 \text{ sec}^{-1} \quad (16)$$

$$W(t)/t({}^1B_{2u} \rightarrow {}^3B_{1u})$$

$$= (0.77 \times 10^{11}) \langle \phi({}^3B_{1u}) \mid \phi_0({}^1B_{2u}) \rangle_{tot}^2 \text{ sec}^{-1}. \quad (17)$$

The experimental value of k in EPA may be estimated from the fluorescence lifetime of the ${}^1B_{2u}$ state in conjunction with measurements of the relative quantum yields of phosphorescence and fluorescence,[36] providing proper account is taken of the nonradiative process from the triplet state.[31] Use is made of the values[31,36] $\tau_F = 6.6 \times 10^{-7}$ sec, $\tau_P = 26$ sec, and $Q_F/Q_P = 1.0$. To account for the over-all 7-sec triplet lifetime, 9.5 sec must be taken as the ${}^3B_{1u} \rightarrow {}^1A_{1g}$ nonradiative lifetime. Since only $\frac{7}{26}$ of the molecules in the triplet state emit, the fraction of excited molecules reaching the triplet state is 0.79. If the nonradiative process from ${}^1B_{2u}$ competes only with fluorescence emission, then the experimental value of k for $S_1 \rightarrow T$ radiationless transitions is 5.7×10^6 sec^{-1}. This result assumes that the $S_1 \rightarrow S_0$ radiationless process is unimportant.

Agreement between calculated and experimental values of k can be obtained if, for the $^1B_{2u} \rightarrow ^3E_{1u}$ process $\langle \phi'' | \phi_0' \rangle_{tot}^2 \approx 3.2 \times 10^{-3}$. The energy gap is unknown experimentally, but the Pariser–Parr calculation[41] gives about 4200 cm^{-1}. Providing the vibrational factors $\langle \phi'' | \phi_0' \rangle_{tot}^2$ were as high as 7.4×10^{-5}, the $^1B_{2u} \rightarrow ^3B_{1u}$ process could also explain the observed k, but here the electronic energy gap is about 8400 cm^{-1}. We know very little about the vibrational factors and the number of directly coupled final states for these large energy gaps. The maximum of the Franck–Condon envelope for the unperturbed phosphorescence spectrum occurs closer to the origin than that for the $^1B_{2u} \leftrightarrow ^1A_{1g}$ spectrum. The relative intensities of successive a_{1g} C—C vibrational bands are roughly 1: 1.46: 1.12: 0.42: 0.17 for the singlet–singlet transition[50,51] and roughly 1: 1.2: 0.3 for the singlet–triplet transition. This fact indicates the presence of the normal coordinate change necessary for a nonvanishing overlap integral to exist between the $^1B_{2u}$ and $^3B_{1u}$ states. Presumably some difference in these quantities also exists between $^1B_{2u}$ and $^3E_{1u}$ states. In Sec. XI an attempt is made to estimate empirically the vibrational factors. These estimates indicate that the $^1B_{2u} \rightarrow ^3E_{1u}$ mechanism dominates the $^1B_{2u} \rightarrow ^3B_{1u}$ mechanism providing the energy levels and spin–orbit matrix elements used here are reasonably correct. This point of view becomes even more likely when account is taken of the fact that the real $(^1B_{2u}, ^3E_{1u})$ energy gap is probably smaller than the one used in the calculation.

The uncertainties in these order-of-magnitude calculations, however, lie not only in our ignorance of the vibrational factors but also in the calculated values of the spin–orbit matrix elements. Actually, if the observed[31] oscillator strength $f(^3B_{1u} - ^1A_{1g}) = 7.7 \times 10^{-11}$ is to be explained by $\pi-\pi^*$ singlet–triplet mixing the calculated spin–orbit matrix elements may be as much as an order of magnitude too small. However, the apparent discrepancy between calculated and observed oscillator strengths may arise not only because of errors in the calculated spin–orbit matrix elements but also because of the uncertainty in the phosphorescence mechanism. If β_{01}^2 does turn out to be larger than the calculations indicate, correspondingly smaller vibrational factors would be needed to explain k.

X. VERY LARGE ENERGY GAPS—THE $T_1 \rightarrow S_0$ AND THE $S_1 \rightarrow S_0$ RADIATIONLESS TRANSITIONS

In π-electron systems which have a center of symmetry, the first-order spin–orbit matrix element between the ground state and the lower $\pi-\pi^*$ triplet states vanishes because of the (g, u) symmetry rule. The interaction must occur in a higher order. If it is

[50] W. F. Radle and C. A. Beck, J. Chem. Phys. **8**, 507 (1940).
[51] D. P. Craig, J. Chem. Soc. **1950**, 2146.

assumed in this case that $\beta_{el} \approx 0.01$ cm^{-1}, *but again that* $\tau_{vib} \approx 10^{-11}$ sec, then

$$W(t)/t(^3B_{1u} \to {}^1A_{1g})$$

$$= (0.71 \times 10^8) \langle \phi(^1A_{1g}) | \phi_0(^3B_{1u}) \rangle_{tot}^2 \text{ sec}^{-1}. \quad (18)$$

One of the authors[31] has estimated k for the $^3B_{1u} \to {}^1A_{1g}$ radiationless transition to be 0.024 sec^{-1}. The over-all vibrational factor must be 3.4×10^{-10} to be consistent with this experimental value! Using the harmonic oscillator approximation and the vibrational parameters for the $^1B_{2u}$ state (instead of for the $^3B_{1u}$ state where data are unknown), it is found that the maximum *individual vibrational factors* which can be obtained theoretically are around 10^{-17}. Anharmonicity may increase this to 10^{-16}. When the actual parameters for the $^3B_{1u}$ state are used, the overlap integrals are expected to be smaller than those for the $^1B_{2u}$ state, and this correction might more than offset the anharmonicity effect.

The preceding result implies that the number of directly coupled final states must be greater than 10^6. Very crude estimates show this to be easily possible. Considering still the case of C_6H_6, four to nine quanta of the totally symmetric C—H stretching mode, coupled with the appropriate number of totally symmetric C—C stretching quanta necessary to meet the near resonance criterion, give *overlap integrals* of the order of 10^{-9}. Overlap integrals of similar magnitude may be obtained by substituting *even quanta* of antisymmetric C—H and C—C stretching modes for the same number of totally symmetric quanta. In addition, 0, 2 or 4 quantum additions of low-frequency, antisymmetric vibrations may be substituted for the appropriate number of high-frequency quanta without lowering the overlap integral substantially. The contribution to the overlap integral from antisymmetric modes arises from a difference of frequency in the absence of a shift of the normal coordinate origin in the initial and final electronic states.

The degeneracy of the nth quantum level of a g-dimensional oscillator is given by,

$$[(n+g-1)!/n!(g-1)!]. \quad (19)$$

For antisymmetric modes, the actual quantum numbers must be halved to obtain the correct n for Eq. (19). It is then found, for example, that there are $1+18+171 = 190$ ways of distributing the 18 different low frequency, antisymmetric modes among quantum numbers 0, 2 or 4. Using the same methods it can be determined that there are about 60 000 ways of distributing quanta of the 12 high-frequency modes so as to meet the near-resonance criterion and to give overlap integrals of the order of 10^{-9}. Thus, the degeneracy of the directly coupled states (i.e., those states present in the free molecule which are associated with non-
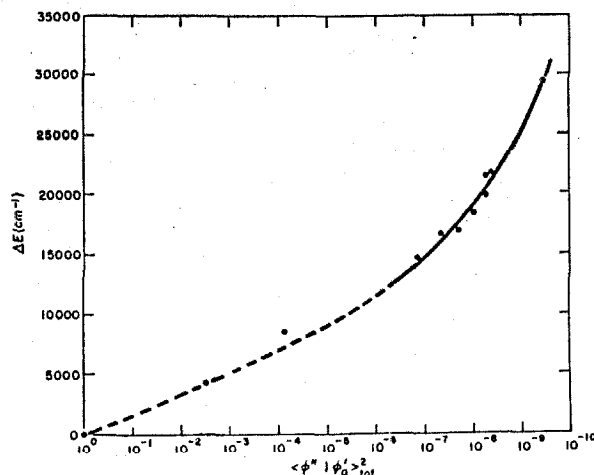
Fig. 2. Empirical vibrational factors plotted against electronic-energy gap for protonated π-electron systems. This curve is subject to change as more is learned about the electronic matrix elements and the quantum yields for the radiationless processes. The experimental points are included to indicate the magnitude of the deviation from the empirical curve. The dotted portion of the curve indicates considerable uncertainty.

negligible overlap integrals) is of the order of 1.14×10^7, a value which is consistent with the required degeneracy factor in Eq. (18). Naturally, lattice vibrations must be included to meet the energy-conservation criterion. Such additions tend to lower all the vibrational factors so that either a final-state degeneracy somewhat larger than 10^7 must actually exist in the system, or the estimated valued of β_{el} or τ_{vib} must be revised upward. Certainly the order-of-magnitude estimates here seem reasonable.

Because of the great importance of the C—H vibrations at quantum numbers which correspond to the "tail" of the Franck–Condon envelope, the deuterium effect is expected to be large when ΔE is large. In the case of benzene, the deuterium effect is probably so large that the radiationless transition can not favorably compete with the radiative phosphorescence transition.[52] For this reason the phosphorescence lifetime of C_6D_6 in the absence of environmental perturbations (heavy atoms, oxygen, etc.) can be taken to be the true radiative lifetime. It is on the basis of the ~26-sec C_6D_6 lifetime that the oscillator strength for the $^3B_{1u} \rightarrow$ $^1A_{1g}$ transition in benzene[30,31,53] is taken to be $f = 7.7 \times 10^{-11}$.

[52] R. P. Frosch and G. W. Robinson, Paper III of this series (to be published).

[53] We have omitted in this calculation a degeneracy factor of 3 suggested by G. N. Lewis and M. Kasha, J. Am. Chem. Soc. 67, 994 (1945). This factor applies to triplets only in the case of allowed transitions. The degeneracy factor to be used for a forbidden transition depends upon the degeneracy factor associated with the allowed transitions from which intensity is "borrowed." In the above calculation, this factor may be as high as 2 but it is certainly not 3. Because of the uncertainty in the exact mechanism through which S–T transitions in π-electron systems gain intensity, we have preferred to leave out the degeneracy factor. For this reason the oscillator strength given above may have to be revised upward by a factor no greater than about 2, nonintegral values being allowed if more than one mechanism is present.

In the case of the $S_1 \rightarrow S_0$ radiationless transition in C_6H_6, the vibrational factor will probably be still smaller than 3.4×10^{-10} since the energy gap is now 38 000 cm^{-1} instead of 29 565 cm^{-1}. If the results of the next section are used, however, β_{el} need be only about 75 cm^{-1} for the $S_1 \rightarrow S_0$ radiationless transition to compete favorably with the $S_1 \rightarrow S_0$ radiative and $S_1 \rightarrow T_1$ or $S_1 \rightarrow T_2$ nonradiative transitions. Since vibronic or interconfigurational matrix elements are very often of this magnitude, the existence of an important $S_1 \rightarrow S_0$ radiationless transition can not be ruled out even when there is a large energy gap. Such an effect, however, is expected to be primarily important in those instances where the energy gap is smaller than it is in benzene.

XI. EMPIRICAL VIBRATIONAL FACTORS FOR PROTONATED π-ELECTRON MOLECULES

It would be extremely useful if the vibrational factors could be estimated by some approximate method. These factors depend upon difference in geometry, differences in vibrational frequencies, size of the molecule, and energy gap between initial and final electronic states. It might be hoped that in many cases energy gap alone will encompass all of these parameters in some complicated fashion. Thus, if vibrational factors for a set of similar molecules are plotted against ΔE, a smooth curve might be obtained from which unknown vibrational factors can be found by interpolation. Perprotonated π-electron molecules form a set whose triplet state lifetimes have been extensively studied. If the purely radiative lifetimes for all these molecules are assumed to be greater than 10 sec, then the measured lifetimes must correspond closely to the nonradiative lifetimes (except for C_6H_6 where $k = 0.024$ sec^{-1}). Good quantum yield measurements (not estimates!) must be carried out to test the validity of this hypothesis. If we tentatively assume it to be true, an empirical determination can be made of vibrational factors between low-lying π-electron states of these molecules. Coronene and triphenylene do not fit this empirical correlation.

Figure 2 shows a semilogarithmic plot of ΔE vs $\langle \phi' | \phi_0' \rangle_{tot}^2$. This vibrational factor is the effective over-all factor needed for the calculation of $W(t)/t = k$ in Eq. (15b). In other words, the vibrational factor given in Fig. 2 is a sum of factors over all directly coupled states. It therefore leads to the rate constant k through the expression,

$$k(\text{sec}^{-1}) = (0.71 \times 10^{12})\beta_{el}^2 \langle \phi'' | \phi_0' \rangle_{tot}^2, \quad (20)$$

where β_{el} is again in cm^{-1} units. For the construction of Fig. 2 we have somewhat arbitrarily assumed $\beta_{el} = 0.01$ cm^{-1} for the lowest-triplet–ground-state interaction in all cases. We have chosen this value on the basis of the fact that "allowed" spin–orbit matrix elements in these systems are of the order of 1.0 cm^{-1}. Matrix elements for symmetry forbidden but vibron-

ically allowed interactions are reduced by a factor equal to $H_{vib}'/\Delta E$, where ΔE is probably of the order of the energy difference between the lowest triplet and the ionization potential. Since $H_{vib}' \approx 100{-}1000$ cm^{-1}, the value of β_{ri} chosen is not unreasonable. Included in Fig. 2 is the point for which $\Delta E=0$, where the vibrational factor is expected to be near unity, and the point for which $\Delta E=4200$ cm^{-1} from the $(^1B_{2u}, {}^3E_{1u})$ interaction in C_6H_6. The point corresponding to the vibrational factor which would be required if the dominant mechanism for radiationless transitions from $^1B_{2u}$ were $^1B_{2u}{\rightarrow}^3B_{1u}$ is also shown in Fig. 2. We have chosen the first mechanism as dominant since it is apparent from Fig. 2 that the slightly smaller matrix elements are in all probability more than offset by larger vibrational factors. Table I gives the data that were used in preparing this figure. The resulting smooth curve, corresponding to a uniform increase of lifetime with energy gap, gives us some confidence in the assumptions which have been made here. A rough analytic expression, $\log\langle\phi''\mid\phi_0\rangle_{tot}^2 = -0.1096\Delta E^{0.4332}$, where ΔE is in cm^{-1} units, can be derived from the curve.

Certainly one important general conclusion can be drawn from these crude kinds of estimates. One expects nonradiative singlet–triplet transitions among excited states to be much faster, because of smaller energy gaps, and probably larger matrix elements, than those which occur between the lowest triplet and the ground state. Thus $S_1{\rightarrow}T_1$ transitions, either directly or through intermediate triplet states, are fast, while $T_1{\rightarrow}S_0$ transitions are generally slow. Deviations from this rule certainly occur, but they are just the deviations which are predicted by the theory. A good example of a deviation is illustrated by the azulene molecule which will be discussed in the next two sections.

XII. SO-CALLED ANOMALOUS $S_2{\rightarrow}S_0$ FLUORESCENCE IN AZULENE

It has been known for some time[54,55] that azulene emits from its second excited singlet state S_2 but not from its lowest singlet state S_1. The experimental electronic energies[56] are $E(S_1)\approx 14\,650$ cm^{-1} and $E(S_2)\approx 28\,050$ cm^{-1}. The energy gap between S_2 and S_1 is almost exactly the same as that between S_1 and the ground state, a rather unusual situation. The oscillator strengths for transitions to the ground state[56] are $f(S_1{\rightarrow}S_0)=0.009$ and $f(S_2{\rightarrow}S_0)=0.08$. The oscillator strength $f(S_2{\rightarrow}S_1)$ must be much smaller than 0.08 since no emission in the $14\,000$ cm^{-1} region has ever been detected although it has been looked for.[54] The computed radiative lifetimes of S_1 and S_2 are 0.8×10^{-6}

[54] M. Beer and H. C. Longuet-Higgins, J. Chem. Phys. **23**, 1390 (1955).

[55] J. W. Sidman and D. S. McClure, J. Chem. Phys. **24**, 757 (1956).

[56] D. E. Mann, J. R. Platt, and H. B. Klevens, J. Chem. Phys. **17**, 481 (1949).

TABLE I. Experimental triplet-state radiationless lifetimes and (T_1, S_0) energy gaps for some protonated cyclic polyenes.[a]

Molecule	$\Delta E(cm^{-1})$	$k^{-1}(sec)$
Anthracene	14 700	<0.1
1,2 Benzanthracene	16 500	0.3
Pyrene	16 800	0.7
1,2–5,6 Dibenzanthracene	18 300	1.4
Crysene	19 800	2.6
Naphthalene	21 300	2.5
Phenanthrene	21 600	3.3
Benzene	29 565	42

[a] The data, except those for benzene, are from D. P. Craig and I. G. Ross, J. Chem. Soc. 1954, 1589. The benzene data are our own. In all cases, except that of benzene, the phosphorescence lifetime has been assumed to be the radiationless lifetime. For C_6H_6, the value of k was obtained from the 26-sec radiative lifetime and the 16-sec over-all lifetime (see reference 31).

sec and 2.4×10^{-8} sec, respectively. The wavefunctions of S_0, S_1, and S_2 form bases for the A_1, B_1 and A_1 irreducible representations respectively of the C_{2v} point group.[57] Direct coupling can occur only between S_0 and S_2, while indirect (probably vibronic) coupling connects the pairs of states (S_0, S_1) and (S_1, S_2). In actuality an MO calculation by Pariser[57a] indicates little mixing is expected between the ground state and the S_2 state. We neglect then the radiationless transition $S_2 \rightarrow S_0$ because of the unfavorably large energy gap for a probable weak interaction. We neglect also the effect of $S \rightarrow T$ transitions, since even though this may not be justified, we are interested in only a rough estimate here. Assume now that the pairs of states (S_0, S_1) and (S_1, S_2) are both mixed by matrix elements $\beta_{el} \approx 100$ cm^{-1}. This is a reasonable value for vibronic coupling. Taking $\langle \phi'' | \phi_0' \rangle_{tot}^2$ from Fig. 2 to be 2×10^{-7} for a 14 000 cm^{-1} energy gap, one obtains $k^{-1} \approx 0.7 \times 10^{-9}$ sec for the reciprocal of the radiationless rate constant for both the $S_2 \rightarrow S_1$ and $S_1 \rightarrow S_0$ processes. This is roughly one-thirtieth the fluorescence lifetime of the S_2 state so that emission can be observed, but with fairly low efficiency. The estimated value of k^{-1}, however, is about three orders of magnitude smaller than the fluorescence lifetime of the S_1 state. Thus the fluorescence intensity from this state is expected to be much less than that from the S_2 state. It should be noted that our result here is wholly dependent upon the longer radiative lifetime of S_1. A knowledge of the details of the interaction and of the vibrational factors[57b] could change these values some-

[57] (a) See, for example, R. Pariser, J. Chem. Phys. 25, 1112 (1956). (b) G. R. Hunt and I. G. Ross, J. Mol. Spectroscopy 9, 50 (1962); Ross, in a private discussion with us, has emphasized the strong possibility of the existence of much larger vibrational factors for the azulene $S_1 \rightarrow S_0$ process than those given in Fig. 2.

what, and other radiationless transitions from the S_1 state could further reduce the intensity of $S_1 \rightarrow S_0$ emission relative to the $S_2 \rightarrow S_0$ emission. A search for the weak $S_1 \rightarrow S_0$ and $S_2 \rightarrow S_1$ fluorescence in the 14 000 cm^{-1} region seems worthwhile, since a measurement of intensities of these emissions compared with that from $S_2 \rightarrow S_0$ would greatly amplify our knowledge about radiationless transitions in this interesting molecule.

XIII. SOME COMMENTS ON THE TRIPLET STATES OF AZULENE

The short radiative and radiationless lifetimes of S_2 and the short radiationless lifetime of S_1 have another consequence. *Any nonradiative singlet–triplet transition would have to be extraordinarily fast in order to compete with these processes.* It is probable that this is one of the underlying reasons why radiative transitions within the triplet manifold have been so difficult to detect in azulene. Other reasons have to do with the expected fast $T_1 \rightarrow S_0$ nonradiative process because of the small energy gap between these states, and fast nonradiative processes within the triplet manifold similar to those just discussed for the singlets. The first kind of process quenches phosphorescence, while the second quenches triplet–triplet emission. There is now some preliminary experimental evidence[58] which supports the contention above that *the triplet states do not get appreciably populated under normal conditions, but under special conditions the rate of the $S \rightarrow T$ radiationless transitions may be enhanced.* Using a heavy-atom solvent (argon, krypton, or xenon) it is possible to quench part of the $S_2 \rightarrow S_0$ fluorescence and to observe a new spectrum near 5000 Å which is very likely due to a $T \rightarrow T$ emission of azulene. The relative intensity of the $T \rightarrow T$ emission compared with the $S_2 \rightarrow S_0$ emission, as expected, increases rapidly with increasing atomic number of the solvent, i.e., from argon to xenon. This is rather good evidence that subtle environmental effects can be used to change quantum yields which depend strongly upon the radiationless process. Rapid quenching of T_1 in azulene and the very unfavorable spectral region may still prevent phosphorescence from being observed even in heavy-atom environments, but this kind of experiment, using perdeuterated azulene would present optimum conditions for the detection of this transition. (The heavy-atom effect may also increase the rate of phosphorescence quenching, but it should increase the rate of triplet population and increase the triplet radiative transition probability to an even greater extent. See Sec. XVI.)

---

[58] P. Leermakers, G. W. Robinson, and G. S. Hammond, unpublished work. Energetic considerations in these experiments tentatively indicate that the T_1 state of azulene must lie no higher than 6000 cm^{-1} above the ground state.

For case 3 of Sec. VI, Eq. (15b) indicates that as the vibrational factor $\langle \phi | \phi' \rangle_{tot}^2$ approaches unity, very rapid radiationless transitions may take place. For over-all matrix elements of the order of 0.1 cm^{-1} or greater, the limit $\beta \ll \alpha$ no longer applies, and, strictly speaking, Eqs. (15) do not give a true mathematical representation of the transition probability. For $\beta \approx \alpha$, the system is partially oscillatory between the initial and final states with periods of the order of the vibrational relaxation time. A very complicated time dependency is expected, intermediate between that given by Eq. (1) and that given by Eq. (12). In this case vibrational relaxation plays a large role in the rate-determining mechanism for the over-all process. For still larger β, the system has time to "oscillate back and forth" many times between "initial" and "final" states during the vibrational relaxation process, and the excitation becomes evenly distributed among all of the interacting electronic states. In the simple case where only two states are interacting, the excitation becomes distributed half and half between the two. This distribution will remain until, after subsequent vibrational relaxation processes, an energy region is reached where again $\beta \ll \alpha$. At this stage, slow radiationless processes occur according to Eq. (12), but from a population distribution of excited states governed by the previous fast transitions. This kind of radiationless process is important when emission is produced with high energy excitation, such as vacuum uv light, x irradiation, high-energy particle radiation, discharge tubes (in gas phase), etc., since the high density of electronic states in energy regions high above the ground state is optimum for the existence of large β_{el} and large vibrational factors. Even in the case where multiplicity forbidden radiationless transitions are considered, the over-all β may be of the order of 1.0 cm^{-1} or greater.

For most polyatomic molecules with an even number of electrons, only the lowest singlet and triplet states are sufficiently well isolated from other states to allow the radiative process to compete with nonradiative processes. In accordance with what was said in the preceding paragraph, high-energy excitation may lead first to a population distribution over a mixture of states of various multiplicities. Subsequent fast radiationless transitions deplete these high singlet, triplet, quintet···states in favor of lower singlets and triplets. The excitation finally becomes distributed between the lowest singlet and triplet according to the statistical weights of the upper states participating in the fast radiationless processes. Further slow ($k^{-1} \approx 10^{-7}$ sec) nonradiative transitions from the lowest singlet to the lowest triplet may now occur during the lifetime of the lowest singlet state. The over-all result is that,

under high-energy excitation the population of the lowest triplet relative to the lowest singlet is always greater than or equal to that obtained under excitation directly into the lowest singlet. The relative quantum yields Q_P/Q_F of phosphorescence to fluorescence from these states therefore should show either no change or an increase, but never a decrease, under high-energy excitation. Some very recent experimental results[59] with chrysene and hexahelicene apparently bear out this contention. Further experiments along these lines seem profitable.

XV. TEMPERATURE EFFECTS

The effect of temperature on relaxation phenomena is well known. Certainly a temperature effect on the over-all vibrational relaxation process in solids is expected, since at low temperatures only absorption of phonons by the lattice can take place. At higher temperatures both absorption and emission of phonons are possible, and the number of relaxation mechanisms is substantially increased. However, for the transfer of large amounts of electronic energy to the environment as in case 2 or case 3 of Sec. VI, no very large temperature effects are expected since neither α nor β varies substantially with temperature. The matrix element β is simply distributed among a few more levels but with a concomitant reduction in magnitude. A substantial change in the vibrational factor is not expected, since such factors normally change fairly slowly even with molecular vibrational excitation, and a substantial amount of molecular vibrational excitation would occur only at temperatures much greater than those usually employed for these studies. The parameter α is already an effective coupling constant among a very large number of molecular and lattice vibrational modes in the final electronic state. Most of these *final* state vibrations are not in their zeroth state even at 4.2°K. Raising the temperature simply redistributes the final states over other quanta, most higher but some lower than those involved at 4.2°K, and the effective α remains essentially unchanged. Even if α should change somewhat, the effect on $W(t)/t$ will be small for the reason stated at the end of Sec. IV.

A few experiments which have been done seem to bear out the fact that the temperature dependence is small. Naphthalene, which has a 2.5-sec triplet-state (radiationless) lifetime both at 4.2°K[60] and 77°K[32,61] is a case in point. Not very many definitive experiments have been carried out, however. It should be pointed out here that when the density of final solvent

[59] M. F. O'Dwyer, M. A. El-Bayoumi, and S. J. Strickler, J. Chem. Phys. 36, 1395 (1962).

[60] See footnote 11 of reference 30. A so-called temperature effect reported in this paper for C_6H_6 is in reality an environmental effect.

[61] D. P. Craig and I. G. Ross, J. Chem. Soc. 1954, 1589.

TABLE II. Parameters[a] for the calculation of third-order heavy-atom effects on radiationless transition probabilities.

	$\Delta E_a \approx \Delta E_b$ (cm^{-1})	$\langle H_{s.o.} \rangle$ (cm^{-1})
Argon	122 000	−665
Krypton	111 000	−2460
Xenon	99 000	−4300

[a] Calculated from $E(^1B_{3u}^-)$ and $E(^1E_{2g}^+)$ and data in Table II of reference 31, then rounded off.

states is small, and Eqs. (11) and (12) do not strictly apply, then large temperature effects may occur. Solid H_2 and D_2 present about the only possible experimental systems where the density of final states is small enough, but temperature variations of the required magnitude may not be realizable with these solvents.

Another case where large temperature effects on excitation transfer are to be expected is that where a small energy barrier exists which prevents migration of excitation at very low temperatures, but is low enough so that an increase of temperature greatly enhances the transition rate. An experimental example of this is the dilute $C_{10}H_8$ in $C_{10}D_8$ system.[62] Here the $C_{10}H_8$ (0,0) band lies 100 cm^{-1} *below* that of $C_{10}D_8$. A great enhancement of the rate of long-range excitation migration between $C_{10}H_8$ centers is observed as kT of the crystal approaches 100 cm^{-1}. *Such an effect is no doubt of importance in the study of certain chemically impure organic crystals at various temperatures above 4.2°K, where in these cases the chemical impurity acts as the shallow excitation trap.*

An increase in temperature sometimes results in a nonnegligible enhancement of the material diffusion of active chemical impurities or physical defects to the excited molecule in a time comparable to its lifetime. Quenching might then take place which will reduce the lifetime of the excited state. When the viscosity of the solvent is reduced, precisely these effects can occur. Quenching by physical defects might be explained qualitatively on the basis of large solvent perturbations on the molecular potential-energy surfaces. An increase in the magnitude of the vibrational factors could then result. The most serious kind of defect quenching is expected to take place in the liquid state where the structure is primarily defect structure. Large time-dependent perturbations caused by local density fluctuations may increase the radiationless transition probability relative to that in the solid. However, one must beware of many of the quoted liquid-state lifetimes since, as Jackson and Livingston[63]

[62] M. A. El-Sayed, M. T. Wauk, and G. W. Robinson, Mol. Phys. 5, 205 (1962).
[63] G. Jackson and R. Livingston, J. Chem. Phys. 35, 2182 (1961).

have pointed out, minute traces of solvent impurity may cause diffusion-controlled quenching of excited states in a time which is fast compared with the actual lifetime in the liquid state. It may be that these traces of impurity and not the local density fluctuations are the major cause of shorter radiationless lifetimes in the liquid state than in the solid state. Good experiments need to be done on clean systems which will tell just how large the effect of "fluctuation quenching" in the liquid state really is.

XIV. ENVIRONMENTAL EFFECTS

Environmental effects caused by diffusion of chemical impurities or physical defects were discussed briefly in the last section. Here only two environmental effects will be discussed—the heavy-atom effect

and the effect of decreasing the density of final lattice states.

Although numerous mechanisms for the heavy-atom effect on *radiative* transitions can be thought of, the authors believe that a second-order process, which depends upon the matrix elements for the solvent–solute electrostatic interaction and the spin–orbit interaction in the solvent, is of dominant importance when simple solvents are used. A brief theoretical description of this effect has been given in an earlier paper.[31] For *nonradiative* multiplicity forbidden transitions, contributions to β_{01} can arise in the third order if both solute states, between which a transition is to take place, can interact with solvent states which are strongly mixed by spin–orbit coupling. Quantitative estimates may be made from the perturbation result[64]

$$\langle \psi'' \mid H' \mid \psi' \rangle = \frac{\langle \psi'' \mid H_{solv}{}^{I} \mid \psi_{solv}{}^{b} \rangle \langle \psi_{solv}{}^{b} \mid H_{s.o.} \mid \psi_{solv}{}^{a} \rangle \langle \psi_{solv}{}^{a} \mid H_{solv}{}^{II} \mid \psi' \rangle}{(\Delta E_b)(\Delta E_a)},$$

(21)

where the energy denominators refer to the energy differences between the states ψ'' and $\psi_{solv}{}^b$, and ψ' and $\psi_{solv}{}^a$, respectively. It should be noted that the initial and final *vibronic* states are degenerate so that $E' = E''$. The matrix element of the spin–orbit interaction in the solvent is the middle factor in the numerator of Eq. 21, while the first and third factors are matrix elements of the solvent–solute electrostatic interaction.

As an example, we may take the $^1B_{2u} \rightarrow {}^3E_{1u}$ radiationless transition of C_6H_6 in rare-gas solvents. Here, the zero-order eigenfunctions are products of C_6H_6 "states" and rare-gas Russell–Saunders "states." For example, the zero-order ground state for a solute–solvent pair is $(^1A_{1g})(^1S_0)$. A reasonable, but by no means unique, set of zero-order states of the system, which could interact to give an enhancement of the radiationless transition probability, is given by the following correlation (see Fig. 1 for C_6H_6 electronic states):

$$\psi' = (^1B_{2u}{}^-)\,(^1S_0),$$

$$\psi'' = (^3E_{1u}{}^+)\,(^1S_0),$$

$$\psi_{solv}{}^a = (^1E_{2g}{}^+)\,(^1P_1),$$

$$\psi_{solv}{}^b = (^1E_{2g}{}^+)\,(^3P_j).$$

The electrostatic matrix element mixing ψ' with $\psi_{solv}{}^a$ may be as large as 10^4 cm^{-1} since the interaction is formally both spin and dipole allowed. The other electrostatic matrix element is probably no larger than 10^2 cm^{-1} since the interaction, even though spin allowed, cannot take place through an electronic dipole in the solute. Using the values in Table 11 with electrostatic matrix elements of 10 000 and 100 cm^{-1} in the first and second case, respectively, one obtains $\beta_{el}(\text{argon}) = 0.045$ cm^{-1}, $\beta_{el}(\text{krypton}) = 0.20$ cm^{-1}, and $\beta_{el}(\text{xenon}) = 0.44$ cm^{-1}. Assuming no solvent depend-

ence on the role played by α and taking $\langle \phi'' \mid \phi_0 \rangle_{tot}{}^2 = 3.2 \times 10^{-3}$ as before, the respective transition probabilities according to Eq. (15b) are 5×10^6 sec^{-1}, 9×10^7 sec^{-1}, and 4×10^8 sec^{-1}, respectively.[65] The results must be added to the unperturbed value 5.7×10^6 sec^{-1}. This assumes, of course, that only the $^1B_{2u} \rightarrow {}^3E_{1u}$, and not the $^1B_{2u} \rightarrow {}^3B_{1u}$ transition is important, and places a heavy burden on the reliability of the estimated theoretical parameters used. The results should be compared with 1.5×10^6 sec^{-1}, the radiative transition probability for fluorescence $^1B_{2u} \rightarrow {}^1A_{1g}$, in order to estimate the fraction of excited C_6H_6 molecules reaching the triplet state in each solvent. These estimates, while crude, do suggest that a relatively large external heavy-atom effect on the nonradiative transition probability can exist when both the solute–solvent electrostatic interactions and the spin–orbit coupling in the solvent are sufficiently large.

Experimental observations using rare-gas solvents are consistent with these estimates. It has been found that the relative quantum yields of phosphorescence to fluorescence are substantially different in environments having a different atomic number. For C_6H_6 in hydrocarbon solvents at $4.2°$K, $Q_F/Q_P \approx 0.6$.[66] The ratio is 0.05 when solid argon at $4.2°$K is used. The ratio is so small in the case of krypton and xenon that no C_6H_6 fluorescence has ever been detected when these solvents are used, even though the phosphorescence has intensity greater than that in methane or argon. Similar results are obtained for $C_{10}H_8$.

---

[64] This expression must be summed over the entire manifold of intermediate zero-order states, discrete and continuous.

[65] Transition probabilities of this same order of magnitude obtained by summation over the entire set of intermediate states would not require such large values of the electrostatic matrix elements as the ones used.

[66] The values have been corrected for the presence of the nonradiative $T_1 \rightarrow S_0$ process. See reference 31.

Because of the required violation of the (g, u) selection rule in the matrix elements, and the larger energy denominators, a smaller heavy–atom effect is expected for the $^3B_{1u} \rightarrow {}^1A_{1g}$ radiationless transition. It is somewhat difficult to separate experimentally the effects of a heavy-atom environment on the radiative and nonradiative transition probabilities, but the apparent high quantum yields of phosphorescence would seem to indicate, tentatively at least, that the enhancement by heavy rare gases of the $^3B_{1u} \rightarrow {}^1A_{1g}$ radiationless transition probability, as expected, is much smaller than the enhancement of, say, the $^1B_{2u} \rightarrow {}^3E_{1u}$ transition probability.

The enhancement of triplet-state population in azulene by a heavy-atom environment (Sec. XIII) provides further experimental evidence for the existence of the heavy-atom effect on nonradiative transitions. The use of this effect in the production of spectra and in the study of energy transfer should be profitable in many problems. We believe that these results, and the earlier ones,[30,31] establish beyond doubt that large

environmental effects upon both radiative and nonradiative transition probabilities can occur providing a suitable electronic mechanism exists.

If it were possible by a suitable choice of environment to modify greatly the density of lattice states or the vibrational relaxation times, one would be able to modify the radiationless transition probability in the nonresonance case according to the results given for cases 2 and 3 of Sec. VI. From Eqs. (11) and (12) one is led to expect that an increase in τ_{vib} would lead to shorter radiationless lifetimes. However, these equations must be summed or integrated over all directly coupled states to obtain the transition probability. It is important to point out again that the dependence of $w(t)/t$ on $\tau_{vib} \approx \hbar \alpha^{-1}$ will be largely lost when this summation is carried out, since the number of terms in the summation increases with increasing α. In the case of small solvent polarizability, the matrix element α and the density of final states may be so small that the theoretical results for cases 2 and 3 may no longer be valid.

III. Appendix

The purpose of this appendix is to show that the form of the interaction between the vibrational modes of the solute and solvent given in Eq. (12) of section IIA is correct. The perturbation Hamiltonian will, of course, be the difference between the Hamiltonians of the isolated solvent and solute and the combined systems. The solute Hamiltonian can be written

$$H_s = \frac{1}{2} \sum_i \frac{p_i^2}{m_i} + \frac{1}{2} \sum_{i,j} \vec{r}_i \cdot \underset{\approx}{k}_{ij}^a \cdot \vec{r}_j , \qquad (A1)$$

where r_i and r_j are the position vectors of the ith and jth atoms of the solute molecule and k_{ij}^a is the tensor form of the interaction between these two atoms when the molecule is in the ath electronic state. Similarly the Hamiltonian of the isolated lattice can be written (1)

$$H_\ell = \frac{1}{2} \sum_{\ell,b} \frac{p_{\ell b}^2}{m_b} + \frac{1}{2} \sum_{\ell,b,\ell',b'} \vec{q}_{\ell b} \cdot \underset{\approx}{G}_{\ell b \ell' b'} \cdot \vec{q}_{\ell' b'} , \qquad (A2)$$

where $q_{\ell b}$ is the vector displacement of the atom occupying the bth site in the ℓth unit cell, and $G_{\ell b \ell' b'}$ is the interaction tensor between the bth atom in the ℓth unit cell and the b'th atom in the ℓ'th unit cell. If solute molecules are now introduced into the lattice, the Hamiltonian for the combined systems is

$$H = H_s + H_\ell - \tfrac{1}{2} \sum_{n,c} \frac{p_{nc}^2}{m_c} - \tfrac{1}{2} \sum_{n,c,\ell',b'} \vec{q}_{nc} \cdot \underset{\approx}{G}_{nc\ell'b'} \cdot \vec{q}_{\ell'b'}$$

$$- \tfrac{1}{2} \sum_{\ell,b,n,c} \vec{q}_{\ell b} \cdot \underset{\approx}{G}_{\ell bnc} \cdot \vec{q}_{nc} + \tfrac{1}{2} \sum_{\ell,b,i} \vec{q}_{\ell b} \cdot \underset{\approx}{K}^a_{\ell bi} \cdot \vec{r}_i$$

$$+ \tfrac{1}{2} \sum_{\ell,b,i} \vec{r}_i \cdot \underset{\approx}{K}^a_{\ell bi} \cdot \vec{q}_{\ell b} - \tfrac{1}{2} \sum_{n,c,i} \vec{q}_{nc} \cdot \underset{\approx}{K}^a_{nci} \cdot \vec{r}_i$$

$$- \tfrac{1}{2} \sum_{n,c,i} \vec{r}_i \underset{\approx}{K}^a_{nci} \cdot \vec{q}_{nc} \quad , \tag{A3}$$

where the summation indices n and c refer to atoms in the original lattice replaced by the solute. Since only interaction between the lattice and solute is of interest the effective perturbation is

$$H_p = \sideset{}{'}\sum_{\ell,b,i} K^{\alpha\beta}_{\ell bi} r^\alpha_i q^\beta_{\ell b} \quad . \tag{A4}$$

where the prime on the summation indicates that the coordinates of atoms replaced by the solute are not included in the summation. The vectors and tensors have been replaced by their Cartesian components. The α's and β's in Eq. (A4) refer to the Cartesian components and not to powers. The Cartesian coordinates of the solute can be expressed in terms of the normal coordinates

$$r_i^\alpha = \sum_j a_{ij}^\alpha R_j \ . \tag{A5}$$

Similarly the lattice Cartesian coordinates can be expressed in terms of the lattice normal coordinates (2)

$$q_{\ell b}^\beta = \sum_k b_{\ell bk} Q_k e^{-i\vec{k}\cdot\vec{\ell}} \ , \tag{A6}$$

where ℓ is still the vector location of a particular unit cell, and k is the wave vector of the phonon with normal coordinate Q_k. Substituting Eqs. (A5) and (A6) in (A4) and combining coefficients we obtain

$$H_p = \sum_{j,k,\ell}{}' \xi_{jk\ell} R_j Q_k e^{-i\vec{k}\cdot\vec{\ell}} \ , \tag{A7}$$

which is the desired result.

References

1. J. M. Ziman, Electrons and Phonons (Oxford University Press, London, 1962), p. 18.

2. Reference 1, pp. 27-31.

IV. Propositions

Proposition 1

A number of unsuccessful attempts have been made to observe the triplet-triplet absorption spectrum of benzene and certain of its derivatives (1, 2, 3). Porter and Windsor (1) used a high-viscosity liquid paraffin as a solvent while looking for the triplet-triplet absorption spectrum of a number of compounds. They observed triplet-triplet absorption in such diverse compounds as napthalene and benzaldehyde but not in benzene.

Craig and Ross (2) searched for the triplet-triplet absorption of a number of compounds dissolved in rigid glasses. They worked in the region 2650 Å to 7500 Å and found no triplet-triplet absorption in either benzene or the related compounds, hexamethylbenzene, diphenyl, diphenylamine, and pyridine.

McClure (3) also studied the triplet-triplet absorption of a number of compounds dissolved in rigid glasses. He used a Hg—Ne lamp for an exciting source that is rich in the mercury 2537 Å line. For a continuous absorption background he used a tungsten ribbon filament lamp. Therefore he would not have been able to observe triplet-triplet absorption below about 3500 Å. Again he found no triplet-triplet absorption of either benzene, aniline, phenol, or benzophenone.

The failure to observe triplet-triplet absorption in benzene may be due to one or both of two reasons. Either the benzene triplet

is not being sufficiently populated, or the right spectral region has not been searched. The theoretical considerations of Pariser (4) indicate that the right spectral region is not being searched. He predicts the energy of six benzene triplets. According to Pariser only T_5 can combine with T_1 through an allowed radiative dipole mechanism. Pariser predicts a 38470 cm^{-1} energy and a 0.807 oscillator strength for the $T_5 \leftarrow T_1$ transition ($^3E_{2g} \leftarrow {}^3B_{1u}$). Unfortunately, the $S_1 \leftarrow S_0$ transition is at the same energy (6), namely 38480 cm^{-1}. Since the $T_5 \leftarrow T_1$ transition is about 580 times as strong as the $S_1 \leftarrow S_0$ transition (6), only about 0.0017 as many T_1 molecules are needed to see the triplet-triplet absorption as ground state molecules are needed to see the singlet-singlet absorption. Experimentally it has been found that a 0.015 cm thick deposit of solid rare gas containing one mole per cent benzene is sufficient to easily observe the $S_1 \leftarrow S_0$ transition of benzene (5). Therefore, if it is possible to excite into the T_1 state most of the benzenes in a 0.06 cm thick solid rare gas deposit only 0.0004 mole per cent in benzene, one could easily observe the triplet-triplet absorption spectrum of benzene without interference from the $S_1 \leftarrow S_0$ transition. It is the purpose of this proposition to show how the above conditions can be achieved by using x-ray excitation of the lattice and therefore how benzene triplet-triplet absorption can be observed.

If a 10% efficiency of photon production is assumed, a typical x-ray tube can put out 2.8×10^{17} 50-kV photons per second. Now suppose that for geometrical reasons only 1% of these photons can be made to impinge on a 0.5 inch diameter rare gas deposit. This means

that only 2.8×10^{15} photons/sec will strike the deposit. Simple calculations indicate that 0.06 cm thick deposits of Ar, Kr, and Xe will absorb 9%, 54%, and 95% of the incident 50-kV x rays, respectively (7, 8). Actually, since most of the x rays will have energies lower than 50 kV, the absorption will be even more efficient than indicated, especially in the case of Ar. Each 50-kV photon is capable in principle of exciting about 10^4 benzenes. If a 10% excitation efficiency is assumed, i.e. each photon excites 10^3 benzenes, then 2.5×10^{17}, 1.5×10^{18}, and 2.7×10^{18} benzenes/sec will be excited in Ar, Kr, and Xe, respectively. In a 0.0004 mole per cent benzene deposit 0.06 cm thick and 1.27 cm in diameter, there are approximately 1.5×10^{19} benzene molecules (9). The rate of change in the number of benzene triplets in the solid is

$$\frac{dT}{dt} = -kT + C ,$$

where T is the number of triplets, k is the rate constant for uni-molecular triplet state decay, and C is the rate of triplet state excitation. Under steady state conditions $T = C/k$. Since the lifetime of C_6D_6 in Ar is longer than the lifetime of C_6H_6 in the same solvent, C_6D_6 is a more favorable solute in Ar than C_6H_6. For C_6D_6 in Ar $k = 0.038$ sec^{-1} (10) and $C = 2.5 \times 10^{17}$ sec^{-1} (from the above calculations). Then at steady state, $T = 6.6 \times 10^{18}$ for C_6D_6 in Ar. In Kr, k for both C_6H_6 and C_6D_6 is 1 sec^{-1}. The resulting steady-state value of T is 1.5×10^{18}. In Xe, $k = 14$ sec^{-1} for both C_6H_6 and C_6D_6 and the steady-state value of T is 1.9×10^{17}.

Obviously the best chance of observing triplet–triplet absorption is to use C_6D_6 in an Ar deposit. With the assumptions made, the calculations indicate that only 44% of the benzenes in the deposit will be excited. This should be a sufficient number to observe the triplet–triplet absorption. Interference from the singlet–singlet absorption will be minimal, since the singlet absorption intensity (assuming the same Franck–Condon envelope for both transitions) will be $(0.0014)(56)/(0.807)(44) = 0.0022$ that of the triplet–triplet absorption. A high-pressure xenon lamp can be used as a continuous background for the absorption spectra. Of course, the spectra should be taken during x irradiation in order to insure maximum triplet state population. The x rays will not interfere with the absorption.

Whenever x irradiation is used, the question of decomposition always arises. Benzene should be decomposed rather slowly by x rays, although its derivatives such as phenol and aniline may decompose rather rapidly. Benzene phosphorescence has been observed from acetylene–rare gas deposits which were excited with x rays (10). Two methods are available for proving that the observed spectrum is due to triplet–triplet absorption and not to some x irradiation product. First of all the absorption should be reversible. It should go away when the x rays are turned off and reappear upon the resumption of x irradiation. Second the absorption should have a lifetime equal to the triplet state lifetime of C_6D_6 in Ar. Both of these tests are easy to make.

The method is applicable not only to benzene but to any species that is stable to x irradiation and has a long-lived excited state. One

possible search would be for the $^4\Sigma^- \leftarrow {}^4\Pi$ transition of NO which has been tentatively identified in the gas phase (11). Unfortunately, the short 93 msec lifetime of the NO quartet state in Ar makes this experiment borderline.

References

1. G. Porter and M. W. Windsor, Proc. Roy. Soc. A245, 238 (1958).

2. D. P. Craig and I. G. Ross, J. Chem. Soc., 1589 (1954).

3. D. S. McClure, J. Chem. Phys. 19, 670 (1951).

4. R. Pariser, J. Chem. Phys. 24, 250 (1956).

5. M. R. Wright, R. P. Frosch, and G. W. Robinson, unpublished work.

6. H. B. Klevens and J. R. Platt as quoted by A. C. Albrecht, J. Chem. Phys. 33, 169 (1960).

7. M. Siegbahn, Spectroskopie der Röntgenstrahlen (Julius Springer, Berlin, 1931), 2nd ed., pp. 470-471.

8. Handbook of Chemistry and Physics (Chemical Rubber Publishing Co., Cleveland, 1956), 38th ed., p. 2430.

9. The number of benzenes actually varies from about 2.1×10^{19} in Ar to 1.3×10^{19} in Xe but the difference is not important for the rough calculation being made here.

10. This thesis.

11. M. Ogawa, Sci. of Light (Tokyo) 3, 39 (1954).

Proposition 2

Robinson and Frosch (1) have derived the following formula for the calculation of radiationless transition rates

$$\frac{1}{\tau} = \frac{2\beta_{e\ell}^2}{\alpha\hbar} <\phi_n''|\phi_0'>_{tot}^2 \quad , \tag{1}$$

where τ is the nonradiative lifetime of the state in question, $\beta_{e\ell}$ is the electronic matrix element mixing initial and final states, α is a measure of the coupling of the solute to the solvent, and $<\phi_n''|\phi_0'>_{tot}^2$ is the effective Franck-Condon factor between initial and final states. The value of $<\phi_n''|\phi_0'>_{tot}^2$ for perprotonated compounds can be estimated from the measured lifetimes of these compounds. A smooth curve is obtained if $<\phi_n''|\phi_0'>_{tot}^2$ is plotted against the electronic energy separation of initial and final states (2). This curve is described by the formula (3)

$$<\phi_n''|\phi_0'>_{tot}^2 \approx \exp(-0.2524\,\Delta E^{0.4332}) \quad , \tag{2}$$

where ΔE is the electronic energy separation expressed in units of cm^{-1}. This result can be used to obtain an empirical estimate of the radiationless lifetimes of perdeuterated molecules when the radiationless lifetime of the corresponding perprotonated molecule is known. Since the hydrogen stretching modes make the most important contribution to the overlap factors, the most important change in the radiationless transition probability will be due to the change in these

stretching modes. Because the frequency of a deuterium mode is about $2^{-1/2}$ times the frequency of the same hydrogen mode, the effective ΔE in Eq. (2) for perdeuterated molecules should be increased by about $2^{1/2}$. Actually the ratio of the hydrogen-stretching frequencies in the perprotonated π-electron systems to those in the perdeuterated π-electron systems is less than $2^{1/2}$ because carbon has a finite mass. For instance, in benzene (4) $\nu_H/\nu_D = 3062/2293 = 1.335$ rather than 1.414. The formulas for the nonradiative lifetimes of perprotonated and perdeuterated species are in this approximation,

$$\tau_H^{-1} = (2\beta_{e\ell}^2/\alpha\hbar)\exp(-0.2524\ \Delta E^{0.4332}) \ , \tag{3a}$$

and

$$\tau_D^{-1} = (2\beta_{e\ell}^2/\alpha\hbar)\exp[-0.2524\ (\gamma\ \Delta E^{0.4332})] \ . \tag{3b}$$

The quantity γ is the effective factor by which ΔE is increased in perdeuterated compounds. Combining Eqs. (3a) and (3b) gives

$$\tau_D = \tau_H \exp[0.2524\ \Delta E^{0.4332}\ (\gamma^{0.4332} - 1)] \ . \tag{4}$$

The reasonable assumption has been made in obtaining Eq. (4) that α and $\beta_{e\ell}$ are the same for both ordinary and perdeutero compounds. The values of τ_D calculated from Eq. (4) for benzene-d_6, napthalene-d_8, and anthracene-d_{10} are given in Table I. They seem quite reasonable. Both $\gamma = 1.414$ and $\gamma = 1.335$ were used in order to show the sensitivity of τ_D to γ. Since a few quanta of lower frequency modes are

also important in the nonradiative decay, the effective value of γ must

be less than 1.335, and the calculated values of τ_D are therefore an

upper limit. Comparison with experiment is difficult because of the

dearth of reliable quantum yield measurements performed with per-

deuterated compounds. Kellogg and Bennett (5) report quantum yield

results and naphthalene-d_8 which give a nonradiative triplet lifetime for

this molecule of 38 sec which is fairly good agreement with Table I.

Unfortunately, however, their results depend on some assumptions

about donor-acceptor systems which have not been fully confirmed.

The agreement for anthracene in Table I is gratifying but may just

be fortuitous because of the uncertainty in the phosphorescence

lifetime of perprotonated naphthalene.

One can also speculate about the effect of partial deuteration.

The effective energy gap will certainly lie between ΔE and $2^{1/2} \Delta E$

but need not be a simple function of the degree of deuteration.

TABLE I.   Calculated radiationless lifetimes of some

perdeuterated molecules.

Molecule	$\Delta E^a (cm^{-1})$	$\tau_H{}^a$ (sec)	$\tau_{Dcalc.}{}^b$ (sec)	$\tau_{Dexptl.}$ (sec)
benzene	29,565	42	770 (1440)	—
naphthalene	21,300	2.5	31 (54)	>16.9[c]
anthracene	14,700	<.1	<.9 (<1.4)	.7[d]

[a]The values of ΔE and τ_H are taken from Table I of reference 2.

[b]The first value given was calculated using an effective energy gap of 1.335 ΔE.   The value in parentheses was obtained using an effective energy gap of 1.414 ΔE.

[c]Reference 6.

[d]From unpublished work of J. H. van der Waals.

References

1. G. W. Robinson and R. P. Frosch, J. Chem. Phys. $\underline{37}$, 1962 (1962).

2. G. W. Robinson and R. P. Frosch, J. Chem. Phys. $\underline{38}$, 1187 (1963).

3. R. P. Frosch and G. W. Robinson, unpublished work.

4. G. Herzberg, Molecular Spectra and Molecular Structure II. Infrared and Raman Spectra of Polyatomic Molecules (D. Van Nostrand and Co., Princeton, N. J., 1945), p. 364.

5. R. E. Kellogg and R. G. Bennett, unpublished work.

6. C. A. Hutchison and B. W. Mangum, J. Chem. Phys. $\underline{32}$, 1261 (1960).

Proposition 3

Pollack and Broida (1) (PB) have reported that solutions of NO

in liquid Kr absorb continuously below some cutoff wavelength which

depends on the NO concentration. Table I (taken from Pollack and

Broida) gives the cutoff wavelength as well as the mole per cent of NO

present in the vapor above the liquid. Pure liquid krypton does not

absorb in this region. Neither does gaseous NO except in very long

paths. However, a 1.5 m path of NO at 700 mm of Hg does have a

continuous absorption with onset near 2600 Å (2). As the pressure is

lowered the continuous absorption starts progressively farther to the

blue. More recently Ferguson and Broida (3) (FB) have interpreted

the results of PB in terms of a Kr—NO charge transfer spectrum with

NO acting as the donor and Kr as the acceptor. The maximum ab-

sorption of a charge transfer complex occurs approximately at energy

$h\nu = I_D - E_A - C$ where I_D is the vertical ionization potential of the

donor, E_A the vertical electron affinity of the acceptor and C the

stabilization (largely due to Coulomb attraction) of the ion pair. For

the NO—Kr complex FB set the ionization potential of NO equal to

9.9 eV and the value of C equal to 4 eV. In order to explain the

spectrum, they then require an electron affinity for Kr of about 1 eV.

The value of the Kr electron affinity required to explain the spectrum
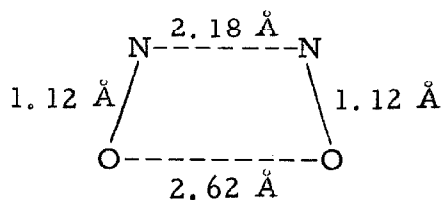
appears to be rather large.

It is the purpose of this proposition to suggest another expla-

nation for the observed spectrum and an experimental means of testing

the alternative explanation. Smith and Johnson (5) have shown that NO

TABLE I

Mole % NO in vapor	Cutoff in liquid $\lambda(\text{Å})$
0.646	2550
0.197	2523
0.0609	2408
0.0177	2224

is present primarily as a diamagnetic species in both pure liquid NO and liquid Kr solutions of NO. The diamagnetic species is believed to be $(NO)_2$. X-ray diffraction studies have shown that NO is dimeric in the solid (6, 7). The dimer is a planar trapezoid with the bond distances shown below.

$$
\begin{array}{c}
N\text{-----}\overset{\text{2. 18 Å}}{\text{-----}}\text{-----}N \\
\text{1. 12 Å} \diagup \qquad\qquad \diagdown \text{1. 12 Å} \\
O\text{-----------}O \\
\text{2. 62 Å}
\end{array}
$$

By assuming that $(NO)_2$'s are the only important diamagnetic species, Smith and Johnson (5) were able to obtain the equilibrium ratio at $116°K$

$$
\frac{[NO]^2}{[(NO)_2]} = 9.222 \times 10^{-3} ,
$$

where the concentrations are expressed as mole fractions. For Pollack and Broida's concentrations which ranged from 0.65 mole % to 0.018 mole % (expressed in terms of the monomer), the calculated degree of dissociation of $(NO)_2$ ranges from .56 to .96. Therefore it is quite possible that what PB saw is the dimer rather than the monomer absorption.

It is very easy to decide whether the absorption is due to the dimer or to the monomer. Suppose one takes the absorption spectrum of a 0.65 mole % solution of NO in liquid Kr using an absorption cell of length ℓ. Then suppose one uses a longer cell with length ℓ' and

concentration c' with 0.65 ℓ = c'ℓ'. If the monomer is the absorbing

species, the absorption should be stronger in the second cell, since

c' < 0.65 mole %, and more of the dimer will be dissociated. On the

other hand, if the dimer is responsible for the observed absorption,

then the absorption should be weaker in the second cell, since there

will be less dimer present.

Jortner and Sokolov (8) have observed similar absorption to

that observed by PB when NO is dissolved in CH_3OH. This also might

be due to dimer formation and should be checked. Oxygen dissolved

in a number of solvents also gives rise to new spectra which are not

present with either oxygen or the solvent alone. In some cases the

spectrum is primarily that of the solvent. The absorption is made

allowed by the presence of dissolved oxygen. For instance, Evans (9)

has observed the singlet-triplet absorption spectrum of benzene when

oxygen or nitric oxide is dissolved in liquid benzene. Jortner and

Sokolov (8) have observed new absorptions between 2000 and 2500 Å

when O_2 is dissolved in methanol, ethanol, acetonitrile, or water

which they attribute to a charge-transfer complex between O_2 and the

solvent. Tsubomura and Mulliken (10) have obtained similar results

with a number of solvents. They also attribute the results to charge-

transfer complexes with the solvent. The above results, although

the interpretations are probably correct should be checked for the

possibility of O_4 absorption by changing the length of the absorption

cell while keeping the amount of dissolved O_2 constant.

If the absorption observed by PB in NO—Kr solutions is due to

$(NO)_2$ as proposed by the author, an explanation must still be sought.

The most obvious explanation is that the absorption is due to the excitation of one of the NO's in the complex to the lowest quartet state of NO. The transition is spin allowed in the complex because the lower state can be either singlet or triplet and the upper state either triplet or quintet. The 0-0 band of the quartet-doublet transition of NO in solid Kr lies at 37856 cm^{-1} (2640 Å), while the cutoff reported by PB for 0.65 mole % NO in liquid Kr is 39200 cm^{-1} (2550 Å). Alternatively the $(NO)_2$ absorption could be the charge-transfer type with $(NO)_2$ being excited to the $(NO)^+(NO)^-$ ion pair.

References

1. G. L. Pollack and H. P. Broida, J. Chem. Phys. 38, 2012 (1963).

2. H. J. Bernstein and G. Herzberg, J. Chem. Phys. 15, 77 (1947).

3. E. E. Ferguson and H. P. Broida, J. Chem. Phys. 40, 3715 (1964).

4. R. S. Mulliken, J. Am. Chem. Soc. 74, 811 (1952).

5. A. L. Smith and H. L. Johnson, J. Am. Chem. Soc. 74, 4696 (1952).

6. W. N. Lipscomb, F. R. Wang, W. R. May, and E. L. Lippert, Acta Cryst. 14, 1100 (1961).

7. W. J. Dulmage, E. A. Meyers, and W. N. Lipscomb, Acta Cryst. 6, 760 (1953).

8. J. Jortner and U. Sokolov, J. Phys. Chem. 65, 1633 (1961).

9. D. F. Evans, J. Chem. Soc. 1351 (1957); ibid., 3885 (1957).

10. H. Tsubomura and R. S. Mulliken, J. Am. Chem. Soc. 82, 5966 (1960).

Proposition 4

Solutions of alkali metals and the alkaline earth metals in liquid ammonia have been extensively studied (1, 2). However, the possibility of obtaining similar solutions of nonmetallic reducing agents in ammonia does not seem to have been considered. It is proposed that compounds like p-phenylenediamine (PPD) and N, N, N', N'-tetramethyl-p-phenylenediamine (TMPD) might dissolve in liquid ammonia to give a solution similar in many ways to the familiar metal-ammonia solutions. Both PPD and TMPD are very soluble in both ether and alcohol (3). PPD is soluble in water and TMPD is slightly soluble in water (3). Since ammonia is intermediate between water and ethyl ether in its properties [μ_{H_2O} = 1.84 Debye, μ_{NH_3} = 1.46 Debye, μ_{ether} = 1.14 Debye (5)], it should certainly dissolve both PPD and TMPD.

Perhaps before discussing the probable properties of PPD and TMPD solutions in ammonia a short discussion about the properties of metal ammonia solutions is worth-while. All of the alkali metals and alkaline earth metals dissolve in liquid ammonia to give a beautiful blue-colored dilute solution. More concentrated solutions are somewhat metallic in appearance. Evaporation of the solution leaves the original metal or, in the case of the alkaline earths, a coordination complex of the metal with ammonia. This complex slowly decomposes with the evolution of ammonia gas leaving the pure metal. The solutions have very high electrical conductivities. For instance, sodium-ammonia solutions at $-33.5°C$ have $\Lambda_o \cong 1016$ cm^2 equiv. $^{-1}$

ohm^{-1} (4). Another unusual property of the solutions is that their volume is greater than the sum of the volumes of the separated solute and solvent (1). The ESR spectrum of potassium in ammonia has been observed (6) indicating the presence of unpaired electrons. The optical spectrum has also been observed. As a rule there are two major absorptions with peaks at about 15000 Å and 6500 Å (2). There is also a weaker continuous absorption with onset at about 5500 Å. The 15000 Å peak is associated with a paramagnetic species, while the 6500 Å peak is associated with a diamagnetic species. Two conflicting models are currently favored to explain the observations. One is the cavitation model of Kaplan and Kittel (7). The model has the following features: 1) The metal atoms are ionized in solution. 2) The electrons are located in cavities in the solution having a volume of two to four ammonia molecules. 3) Electrons in the cavities obey the equilibrium $2\,e^- \rightleftharpoons e_2^= + 0.2$ eV. 4) Electrons in the cavities may be thought of as in M.O. states of the adjacent NH_3 protons. 5) There is a conduction band ~ 1 eV above the cavity states. The model explains the large volume of metal-ammonia solutions, the high conductivity of the solutions and some of their magnetic properties. However, it fails to explain the NMR results of McConnell and Holm (8) who observed an appreciable spin density on both sodium and nitrogen atoms in sodium-ammonia solutions. However, they observed no proton chemical shift relative to pure liquid ammonia indicating that the odd electron does not spend any time in the vicinity of the protons as postulated by Kaplan and Kittel.

The other model has been described by Becker, Lindquist, and Alder (9). They visualize the solutions as containing four distinct species: 1) the monomer, an octahedral metal ammonia complex with the nitrogens pointed toward the metal and the odd electron wandering about among the ammonia protons, 2) a solvated metal cation, 3) a solvated electron, and 4) a dimer consisting of two monomers bound chiefly by exchange forces. The model again fails to explain the lack of a proton chemical shift in the results of McConnell and Holm (8), but does explain the other magnetic measurements and the optical spectra rather well.

It is now possible to speculate on the possible properties of PPD- and TMPD-ammonia solutions based on the properties of metal ammonia solutions. TMPD starts to absorb in a 3-methylpentane glass at about 28000 cm^{-1}; PPD starts to absorb in EPA glass at about 30000 cm^{-1} (10). The absorption spectrum should be drastically changed in liquid ammonia. One would expect the appearance of a band in the infrared corresponding to the 15000 Å absorption of metal-ammonia solutions. One would also expect to look for PPD^+ and $TMPD^+$ absorption. PPD^+ starts to absorb at about 15000 cm^{-1} (10), and $TMPD^*$ should absorb in a nearby region.

The possibility of dimer formation must also be considered. Hausser and Murrell (11) have discussed the formation of dimer of Wurster's blue perchlorate ($TMPD^+ClO_4^-$) in alcohol-ether solutions. Measurements of both the magnetic susceptibility and optical spectrum indicate the formation of dimers. They suggest that the dimer is a

π-complex with the planes of the two molecules situated one above the other. Dimers of the type $(TMPD)_2^+$ should also be observed in liquid ammonia.

Both ESR and optical spectra should be used to study the various possible species in the solution. These are TMPD monomer, $TMPD^+$ monomer, "free electrons," $(TMPD)_2^+$ and $(TMPD)_2^{++}$. Because of the large number of possible species experiments should also be done using equal molar quantities of Wurster's blue perchlorate and TMPD in the same solution to enhance the formation of the $(TMPD)_2^+$ dimer. Wurster's blue perchlorate should also be dissolved alone in liquid ammonia to see the effects of the $(TMPD)_2^{++}$ ion. Some of the above species namely TMPD and probably $(TMPD)_2^{++}$ (12) have singlet ground states, while $TMPD^+$ and $(TMPD)_2^+$ should have doublet ground states. Hopefully it would be possible to observe fine structure in the ESR spectrum and consequently learn the location of the electron in both monomeric $TMPD^+$ and the $(TMPD)_2^+$ dimer. The above suggested experiments should be useful both in a study of π-complexes and also as a compliment to studies of metal-ammonia solutions.

References

1. A good review of the subject up to 1944 is to be found in D. M. Yost and H. Russell, <u>Systematic Inorganic Chemistry of the Fifth-and-Sixth-Group Nonmetallic Elements</u> (Prentice-Hall, Inc., New York, 1944), pp. 136-148.

2. T. P. Das in <u>Advances in Chemical Physics IV</u>, I. Prigogine, ed. (Interscience, New York, 1962), pp. 303-388.

3. <u>Handbook of Chemistry and Physics</u>, D. Hodgman, ed. (Chemical Rubber Publishing Co., Cleveland, Ohio, 1956), p. 1096.

4. C. A. Kraus, J. Am. Chem. Soc. 43, 749 (1921).

5. A. A. Maryott and E. R. Smith, <u>Table of Dielectric Constants and Dipole Moments of Substances in the Gaseous State</u> (U. S. Nat. Bur. Std. Circ. No. 537, 1953).

6. C. A. Hutchison and R. C. Pastor, Rev. Mod. Phys. 25, 285 (1953).

7. J. Kaplan and C. Kittel, J. Chem. Phys. 21, 1429 (1953).

8. H. M. McConnell and C. H. Holm, J. Chem. Phys. 26, 1517 (1957).

9. E. Becker, R. H. Lindquist, and B. J. Alder, J. Chem. Phys. 25, 971 (1956).

10. A. H. Kalantar and A. C. Albrecht, to be published.

11. K. H. Hausser and J. N. Murrell, J. Chem. Phys. 27, 500 (1957).

12. The lowest triplet state of crystalline Wurster's blue perchlorate lies 246 cm^{-1} above the lowest singlet state in the temperature range 20°K to 77°K. The TMPD$^+$ in WB perchlorate at these

temperatures is believed to be located in chains of $(TMPD)_2^{++}$ dimers which are stacked with the molecular planes parallel. D. D. Thomas, H. Keller, and H. M. McConnell, J. Chem. Phys. 39, 2321 (1963).

Proposition 5

The lowest triplet state of acetylene has never been observed in either emission or absorption. Because acetylene is a prototype molecule, theoreticians are particularly interested in both the geometry and the energy of its lowest triplet state. There have been two major problems in obtaining the phosphorescence spectrum of acetylene. First, the molecule is easily photolyzed to give C_2, and second, intersystem crossing from the singlets to the triplets is probably not very efficient (1). The purpose of this proposition is to suggest a way in which the above problems can be overcome unless the lowest triplet itself dissociates which is not likely.

Although the lowest triplet state of acetylene has not been observed, Evans (2) has observed the singlet–triplet absorption of diacetylene under high pressure oxygen. The 0–0 band of diacetylene lies at 27020 cm^{-1}.

Theoretical considerations (3) predict that the lowest triplet state of linear acetylene lies at 47900 cm^{-1}. The lowest triplet state will almost surely be bent, however, and lie much lower in energy. For example, the lowest singlet of linear acetylene is predicted by theory (3) to lie at 64700 cm^{-1}, but the experimental (4) 0–0 band lies at 42198 cm^{-1}. An analysis of the singlet–singlet spectrum indicates that the excited singlet state has a _trans_ configuration. If bending stabilized the triplet state by the same amount (22500 cm^{-1}), the lowest triplet would lie at 25400 cm^{-1}. It therefore seems reasonable to assume that the lowest acetylene triplet state is between 25000 and

30000 cm^{-1}.

Nieman and Robinson (5) have shown that the lowest triplet state of C_6H_6 in a C_6D_6 crystal is at 29660 cm^{-1} (0-0 band). If the acetylene triplet lies below the benzene triplet, it would form a trap in the benzene crystal. It is therefore proposed that benzene be crystallized in the presence of an atmosphere of acetylene for the purpose of growing an acetylene-benzene mixed crystal. If benzene and acetylene do not cocrystallize sufficiently, a spray technique can be used to obtain a suitable mixed crystal (this thesis). Acetylene concentrations between 0.5 and 1.0% should be ideal.

The acetylene phosphorescence would be obtained in the following manner. Energy would be absorbed into the lowest benzene singlet state. The 0-0 band of this transition in the crystal (6) is at 37052 cm^{-1}. Since acetylene begins to absorb weakly (4) at 42198 cm^{-1} it is possible to absorb into the benzene without exciting the acetylene. The benzene singlet can then intersystem cross to the benzene triplet, which will then migrate around until it finds an acetylene trap. The trap will then be excited and the acetylene can emit. The major weakness in this proposition is the requirement that the acetylene triplet lie far enough below the benzene triplet to act as a trap. At $4°K$ a trap depth >200 cm^{-1} would probably be adequate. At $77°K$ a trap depth of 500 or 1000 cm^{-1} might be required. Even if acetylene phosphorescence were not observed from the benzene crystal, a fairly reliable lower limit for the acetylene triplet would have been set.

The appearance of the spectrum will give a clue to the geometry of the triplet state. Appearance of even quanta of the 612 cm^{-1}

trans-bending vibration or of odd quanta, if the transition should be vibronically induced, would indicate a trans triplet state. A similar appearance of even or odd quanta of the 729 cm^{-1} cis-bending vibration would indicate a cis triplet state. Combinations of these bending modes would indicate either a nonplanar excited state or an excited state in which one hydrogen remains colinear with the carbons while the other is bent. Because of the Franck-Condon principle the maximum intensity of the transition will not lie near the 0-0 band if the upper state is bent. Rather the maximum intensity will be shifted to the red. One should therefore concentrate the search for phosphorescence between about 3300 Å and 6000 Å.

The above method is, of course, not limited to acetylene but can be used with any molecule whose lowest triplet lies below that of benzene and which will not react with benzene. Unfortunately many unobserved triplet states such as those of CO_2, H_2O, and NH_3 probably lie above the benzene triplet.

References

1. The probable inefficient intersystem crossing is due to the small number of normal modes of the acetylene molecule. A small number of normal modes means a small number of favorably located final states for a radiationless transition. See sections IIA, IIB, and IIC of this thesis.

2. D. F. Evans, J. Chem. Soc. 1735 (1960).

3. I. G. Ross, Trans. Faraday Soc. 48, 973 (1952).

4. K. K. Innes, J. Chem. Phys. 22, 863 (1954).

5. G. C. Nieman and G. W. Robinson, J. Chem. Phys. 39, 1298 (1963).

6. H. Sponer and E. Teller, Rev. Mod. Phys. 13, 75 (1941).

Proposition 6

A chelate can be formed between nickel, copper, or cobalt and N-N'-disubstituted-1-amino-7-imino-1,3,5-cycloheptatrienes (1) (aminotroponeimines, ATI). The complexes have the general formula $M(ATI)_2$. Chromium gives a product containing three moles of ligand per mole of metal (1). The physical and chemical properties of the nickel chelate have been extensively studied (1,2,3). Eaton, Phillips, and Caldwell (3) (EPC) have demonstrated from temperature dependence studies of the proton resonance shifts in the NMR spectra, of magnetic susceptibility, and of the optical spectra that the nickel chelates exist in two forms, one diamagnetic and one paramagnetic. Steric evidence and the fact that there is an entropy change in passing between the two forms indicates that the two forms have substantially different nuclear configurations. The difference in configuration of the two forms is contrary to the ideas of Ballhausen and Liehr (4) who suggest that low energy paramagnetic complexes of nickel (II) with tetragonal distortion might be obtained by promotion of an electron from the ground state $e_g^4 a_{1g}^2 b_{2g}^2$ configuration which has no net spin to a $e_g^4 a_{1g}^2 b_{2g} b_{1g}$ configuration which has a low energy $^3B_{2g}$ state. Electron correlation effects might make the $^3B_{2g}$ state lower in energy than the $^1A_{1g}$ state obtained from the ground state configuration. In a tetrahedral complex the 3d orbitals split into a t_2 and an e orbital with t_2 higher in energy than e. Therefore the ground state configuration of a tetrahedral complex with eight d electrons would be

$e^4 t_2^4$ which gives a triplet ground state. EPC believe that the paramagnetic form is tetrahedral or distorted tetrahedral, while the diamagnetic form is planar. Unfortunately, no x ray work has been done on the structure of aminotroponeimine-metal complexes.

It is the purpose of this proposition to suggest that further studies be made of the aminotroponeimine complexes. The complex with Pd would be particularly interesting because it might be possible to form a tetrahedral complex with Pd(II) by judicious use of steric hindrance. There apparently are no tetrahedral complexes of Pd(II) known. For example, $NiCl_4^{-2}$ is tetrahedral and paramagnetic (5, 6), but $PdCl_4^{-2}$ and $PtCl_4^{-2}$ are diamagnetic and square planar (5, 7). The Pd(II) complex could probably be obtained in a manner analogous to the way in which the Ni(II) complex is obtained (1). The ligands can be prepared by the series of reactions
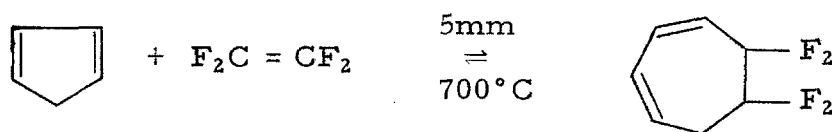

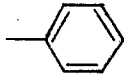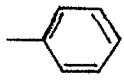The product is then allowed to react with the desired amine.
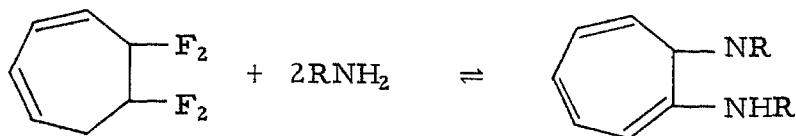
Here R may be H, an allyl, or an aryl radical. The complex can then be made by boiling together one equivalent of $PdCl_2$ with two equivalents of ligand in ethanol containing an excess of aqueous ammonia until reaction is complete. If the ligand does not dissolve well in pure ethanol, benzene or chloroform can be added to achieve complete solubility.

EPC(3) found for R = CH_3 or H that the Ni(II) complex was 99.5% in the diamagnetic form (planar) at 23° C. On the other hand with R = C_2H_5 or higher alkyl groups, the complex was > 99% in the paramagnetic form indicating predominance of the tetrahedral form. When R was an aryl group the complex was found to be 25-75% in the paramagnetic form. The obvious conclusion can be drawn that in the absence of steric hindrance the planar form is more stable. The aryl groups cause less steric hindrance than large alkyl groups because the phenyl rings can rotate into a postion which is perpendicular to the tropolone rings. For the Ni(II) complex reaction

$$\text{diamagnetic} \rightleftharpoons \text{paramagnetic}$$
$$\text{(planar)} \qquad \text{(tetrahedral)}$$
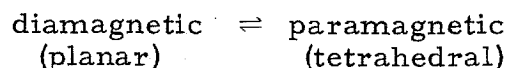
ΔH = 6.16 kcal/mole, and ΔS = 10.3 e.u. for R = CH_3. For

R = C_2H_5, ΔH = 1.25 and ΔS = 9.1. For R = —⟨◯⟩ , ΔH = 3.08 and ΔS = 10.3. Substitution on the tropolone ring had essentially no effect on the results.

It is proposed that an attempt be made to make the amino-troponeiminates of Pd(II) with R = H, C_2H_5, and —⟨ ⟩ . The freezing point depression of the complex should be measured in a suitable solvent, say chloroform, to be sure that the complex has the expected formula, $Pd(ATI)_2$.

Then the temperature dependence of the proton resonance of say H_β in the tropolone ring should be measured. The temperature dependence of the contact shift of the ith proton when thermal equilibrium is established in times shorter than about 10^{-5} sec is (3)

$$\left(\frac{\Delta H}{H}\right)_i = - a_i \frac{\gamma_e}{\gamma_H} \frac{g\beta\ S(S+1)}{2\,SkT\ [\ \exp\ (\Delta F/kT) + 3\ ]}$$

where γ_e and γ_H are the gyromagnetic ratios of the electron and proton, respectively. ΔF is the free energy change for the reaction diamagnetic $\rightleftharpoons$ paramagnetic, a_i is the contact coupling constant and H is the magnetic field. S which is the spin should be equal to one for the Pd(II) complex. If the results for the Ni(II) aminotroponeiminate complexes follow for the Pd(II) complexes, the contact shifts should be greatest in the ethyl complex and least in the complex with R = H. From the NMR spectra one would obtain ΔF for the change from the diamagnetic to the paramagnetic form and also ΔS and ΔH.

Besides the NMR spectra it would be useful to do EPR in order to obtain an idea of the anisotropy and magnitude of the g-factor.

Of course, optical spectra would also be interesting.

Palladium and nickel are not the only complexes with the amino-toponeimines whose magnetic and optical properties should be interesting. The complex with platinum (II) should also be interesting. A study of the Pt(II) complex would provide a measure of the increasing tendency to planar complexes in d^8 configurations as the metal is changed from the first row of transition metal elements to the third row.

Summary

It is proposed that Pd(II) complexes of aminotroponeimines be prepared. Judicious use of steric hindrance should bring the tetrahedral complex fairly close to the planar complex in energy. A tetrahedral structure would be the first example of a Pd(II) tetrahedral complex. The temperature dependence of the NMR contact shifts can be used to obtain the free energy of the

$$\text{planar} \rightleftharpoons \text{tetrahedral}$$
$$\text{(diamagnetic)} \quad \text{(paramagnetic)}$$
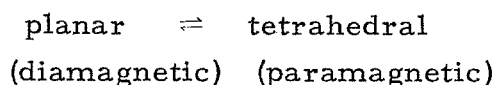
reaction.

References

1. W. R. Brasen, H. E. Holmquist, and R. E. Benson, J. Am. Chem. Soc. <u>83</u>, 3125 (1961).

2. D. R. Eaton, A. D. Josey, W. D. Phillips, and R. E. Benson, J. Chem. Phys. <u>37</u>, 347 (1962).

3. D. R. Eaton, W. D. Phillips, and D. J. Caldwell, J. Am. Chem. Soc. <u>85</u>, 397 (1963).

4. C. J. Ballhausen and A. D. Liehr, J. Am. Chem. Soc. <u>81</u>, 538 (1959).

5. H. B. Gray and C. J. Ballhausen, J. Am. Chem. Soc. <u>85</u>, 260 (1963).

6. N. S. Gill and R. S. Nyholm, J. Chem. Soc., 3997 (1959).

7. V. J. Belova, Chem. Abst. <u>50</u>, 15148 (1956).